Supplementary Information for

Robust Affinity Standards for Cu(I) Biochemistry

Pritha Bagchi[a], M. Thomas Morgan[a], John Bacsa[b], and Christoph J. Fahrni*[a]

[a]*School of Chemistry and Biochemistry and Petit Institute for Bioengineering and Bioscience, Georgia Institute of Technology, 901 Atlantic Drive, Atlanta, GA 30332, USA*
[b]*X-ray Crystallography Center, Department of Chemistry, Emory University, 1515 Dieckey Drive, Atlanta, GA 30322, USA*

Table of Contents

1. Synthesis

Materials and Reagents. Tris(2-chloroethyl)amine hydrochloride (**7**, Aldrich), sodium 3-mercaptosulfonate (TCI), 1,3-diodopropane (Aldrich), 1,3-propanedithiol (Aldrich), 1,3-propanesultone (Aldrich) were commercially available and used without further purification. Thietane (**9**) (7,7-dimethyl-6,8-dioxa-2-thiaspiro[3.5]nonane was prepared following a previously published procedure.[1] NMR: ^{19}F spectra are reported in ppm relative to internal 2,2,2-trifluoroethanol (TFE), which was employed both as a chemical shift standard and integration standard to link the ^{19}F and ^{1}H integrals. The resulting fluorine integration values were between 5.2 and 6 for the PF_6^- signal of all hexafluorophosphates. ^{1}H and ^{13}C spectra acquired in D_2O are referenced to internal sodium 3-trimethylsilylpropionate-2,2,3,3-d_6 (0 ppm) with the exception of those for DHEAMP·2HCl, which were referenced to CH_3OH (3.34 ppm for ^{1}H and 49.50 ppm for ^{13}C) ^{1}H spectra acquired in other solvents are reported in ppm relative to internal TMS, while ^{13}C spectra acquired in other solvents are referenced to the known chemical shift of the solvent peak ($CDCl_3$: 77.0 ppm, $(CD_3)_2SO$: 39.5 ppm).

MCL-1 (1). A solution of tris(2-chloroethyl)amine hydrochloride (2.16 g, 8.97 mmol), sodium 3-mercaptopropanesulfonate 5.28 g, 3.3 equiv. and NaOH (1.58 g, 4.3 equiv.) in methanol (45 mL) plus water (5 mL) was stirred under argon overnight at 60°C. The resulting pasty mixture was diluted to 250 mL in 10:1 methanol-water and heated to boiling. Water was then added slowly until almost all solids had dissolved (required 15 mL). The mixture was filtered while hot, boiled down to 200 mL, diluted back to 300 mL with methanol, and allowed to cool to room temperature under slow stirring. The resulting crystalline slurry was stirred for 2 hours at 0°C, and the colorless product was collected by filtration, washed with cold methanol followed by acetone, and dried under high vacuum to give ligand **1** as a fine powder. Yield 3.75 g (5.95 mmol, 66%). ^{1}H NMR (D_2O, 400 MHz) δ 2.00-2.07 (m, 6H), 2.69-2.75 (m, 12H), 2.77-2.83 (m, 6H), 3.01-3.05 (m, 6H). ^{13}C NMR (D_2O, 100 MHz) δ 27.1, 30.4, 32.8, 52.6, 55.5. Elemental analysis calcd (%) for $C_{15}H_{30}NNa_3O_9S_6$ (629.76): C 28.61, H 4.80, N 2.22; found C 28.27, H 4.70, N 2.17.

[(MCL-1)Cu]Na_3PF_6 (13). Solid $[Cu(CH_3CN)_4]PF_6$ (511 mg, 1.37 mmol) was added to a solution of **1** (864 mg, 1.37 mmol) in H_2O (10 mL). Ethanol (10 mL) was added, and the mixture was stirred in a 60°C bath until all solids dissolved. The resulting green solution was decolorized by adding the minimum amount (<100 mg) of sodium ascorbate, diluted with 40 mL ethanol, boiled down to half its original volume, and diluted slowly with ethanol until slightly turbid. The solution was then removed from the heat source and diluted dropwise with water to the point of clarity. Methanol (15 mL) was added, and the mixture was allowed to cool to room temperature under slow stirring. The resulting crystalline suspension was stirred in an ice bath for 2 hours, and the colorless product was collected by filtration, washed with ethanol, and dried under high vacuum to give a fine powder. Yield 719 mg (858 μmol, 63%). ^{1}H NMR (D_2O, 400 MHz) δ 2.11 (p, J = 7.4 Hz, 6H), 2.79-2.86 (m, 12H), 3.02-3.06 (m, 12H). ^{19}F NMR (D_2O, 376 MHz) δ (TFE) 4.62 (d, J = 708 Hz, 6F). ^{13}C NMR (D_2O, 100 MHz) δ 26.5, 34.5, 36.7, 51.6, 52.2. Elemental analysis calcd (%) for $C_{15}H_{30}CuF_6NNa_3O_9PS_6$ (838.27): C 21.49, H 3.61, N 1.67; found C 21.38, H 3.52, N 1.64.

$[Na_7(Cu(I)(MCL\text{-}1))_2](ClO_4)_3 \cdot 4H_2O$ (13a). Complex **13** (20 mg) was dissolved in water (100 μL) and diluted with ethanol (200 μL.). To this solution was added 500 μL of a solution prepared by dissolving $NaClO_4 \cdot H_2O$ (3.0 g), in ethanol (8 mL) plus water (4 mL). The mixture

was filtered through a 0.2 μm nylon membrane and allowed to stand overnight in a sealed vial, yielding clear, colorless triclinic prisms suitable for X-ray structural analysis.

MCL-2 (2). Tris(3-chloropropyl)amine (2.00 g, 8.11 mmol), sodium 3-mercaptopropane-sulfonate (4.48 g, 3.1 equiv.), and sodium hydroxide (1.01 g, 3.1 equiv.) were stirred in methanol (35 mL) under argon at 60 °C overnight. The resulting pasty mixture was diluted into 150 mL methanol + 10 mL water and heated to boiling. The resulting slightly turbid solution was suction-filtered through a pre-heated glass frit, re-heated to boiling, and allowed to cool to room temperature under slow stirring. The product separated as a colorless crystalline powder, which was collected by filtration, washed with methanol followed by diethyl ether, and dried under vacuum to give ligand **2** as a fine powder. Yield 3.53 g (5.18 mmol, 64%). ^{1}H NMR (D_2O, 400 MHz) δ 1.75-1.83 (m, 6H), 1.99-2.07 (m, 6H), 2.58-2.64 (m, 12H), 2.72 (t, *J* = 7.2 Hz, 6H), 3/00-3.05 (m, 6H). ^{13}C NMR (D_2O, 100 MHz) δ 27.0, 28.0, 31.8, 32.6, 52.6, 54.9. Elemental analysis calcd (%) for $C_{18}H_{36}NNa_3O_9S_6$ (671.84): C 32.18, H 5.40, N 2.08; found C 31.79, H 5.41, N 2.06. For UV spectroscopic measurements, the above material was further purified by treatment with activated carbon followed by recrystallization from ethanol-water.

[(MCL-2)Cu]Na_3PF_6 (**14**, anhydrous). Ligand **2** (679 mg, 1.01 mmol) and $[Cu(CH_3CN)_4]PF_6$ (377 mg, 1.01 mmol) were stirred in methanol (20 mL). The mixture was heated to reflux under argon, and water was added slowly until all colorless solids had dissolved. A small amount of blue solid remained at this point, but dissolved upon addition of 60 μL (1 mmol) of acetic acid. The mixture was concentrated nearly to dryness, and the residue was stirred in boiling isopropanol (50 mL), decolorized with the minimum amount of sodium ascorbate, and diluted dropwise with water until all solids had dissolved. The resulting biphasic liquid was diluted with methanol until monophasic (required 15 mL), and allowed to cool to room temperature under slow stirring. The resulting colorless crystalline powder was collected by filtration, washed with cold isopropanol, and dried under vacuum. Yield 520 mg (0.607 mmol, 58%). ^{1}H NMR (D_2O, 400 MHz) δ 2.07-2.15 (m, 12H), 2.71-2.74 (m, 6H), 2.93-2.98 (m, 12H), 3.02-3.06 (m, 6H). ^{19}F NMR (D_2O, 376 MHz) δ (TFE) 4.64 (d, *J* = 708 Hz, 6F). ^{13}C NMR (D_2O, 100 MHz) δ 25.2, 26.1, 35.8, 36.3, 52.3, 62.8. Elemental analysis calcd (%) for $C_{18}H_{36}CuF_6NNa_3O_9PS_6$ (880.35): C 24.56, H 4.12, N 1.59; found C 24.47, H 4.22, N 1.59.

[(MCL-2)Cu]Na_3PF_6 • 7.5 H_2O (**14a**). Ligand **2** (1.12 g, 1.67 mmol) and $[Cu(CH_3CN)_4]PF_6$ (621 mg, 1.67 mmol) were added to a 50 mL rb flask containing a magnetic stir bar. The flask was sealed and flushed with argon, and water (10 mL) and ethanol (10 mL) were injected. The mixture was stirred until all solids had dissolved and then shaken with air, which resulted in a blue coloration. Triethylamine (100 μL) was added, resulting in a small amount of blue precipitate which was removed by centrifugation. The mixture was heated to boiling, diluted slowly with ethanol (required 35 mL) to the point of permanent turbidity, and allowed to settle while hot. The clear solution was decanted, filtered through a glass frit, and allowed to cool. A mixture of fibrous acicular crystals and irregular hexagonal tablet-shaped granules was deposited. The fibrous crystalline form was separated from the granular crystalline form by swirling and decantation, and a sample of each crystalline form was collected by filtration and dried under argon flow. Both forms yielded ^{1}H and ^{19}F NMR spectra identical to those of anhydrous **14**. The two crystalline slurries were recombined, and the mixture was stirred slowly overnight, resulting in complete conversion to the granular form. This was collected by filtration, washed with cold 4:1 ethanol-water, and dried

by suction in ambient air to give a free-flowing, colorless granular powder consisting of irregular hexagonal tablets. A sample of this material was recrystallized from 3:1 ethanol-water to give larger tablets of identical crystal habit. X-ray diffraction analysis yielded an empirical formula of $C_{36}H_{102}Cu_2F_{12}N_2Na_6O_{33}P_2S_{12}$ (2030.93 g/mol), corresponding to $C_{18}H_{36}CuNNa_3O_9S_6PF_6$ • 7.5 H_2O (1015.46 g/mol) per copper equivalent. Yield 719 mg (0.708 mmol, 42%).

2-Pyridylethylbis(2-methylthioethyl)amine diphosphate (4, PEMEA). Neutral PEMEA was synthesized following a published procedure.[5] For further purification, PEMEA (689 mg, 2.55 mmol) was dissolved in ethanol (10 mL) and a solution of 85% phosphoric acid (734 mg, 2.5 equiv.) in ethanol (5 mL) was added dropwise under stirring. The resulting tan precipitate was collected by filtration and recrystallized from methanol-ethanol under stirring to give a colorless crystalline powder. Titration with KOH using phenolphthalein indicator gave results consistent with the formula PEMEA • 2 H_3PO_4. The phosphate stoichiometry was confirmed via phosphorus NMR with inverse-gated decoupling using hexamethylphosphoramide as an integration standard. Yield 585 mg (1.25 mmol, 49%). Mp 101-102°C. ^{1}H NMR (D_2O + HMPA, 400 MHz) δ 2.14 (s, 6H), 2.95 (t, J = 7.3 Hz, 4H), 3.54-3.58 (m, 6H), 3.69-3.73 (m, 2H), 7.84-7.90 (m, 2H), 8.42 (td, J = 7.9, 1.6 Hz, 1H), 8.68 (ddd, J = 5.7, 1.7, 0.8 Hz, 1H). ^{31}P NMR (D_2O + HMPA, 162 MHz) δ 29.9 (2P).

Tris(3-chloropropyl)amine (**8**).[2] A mixture of 3-amino-1-propanol (20.3 g, 270 mmol), 3-chloro-1-propanol (50 mL, 595 mmol), and Na_2CO_3 (43 g, 405 mmol) in ethanol (120 mL) was magnetically stirred at reflux for 25 h. The mixture was diluted with dichloromethane (300 mL), filtered to remove salts, and concentrated under reduced pressure. The resulting viscous liquid was taken up in acetonitrile (100 mL), refluxed overnight, and allowed to cool. A mixture of thionyl chloride (117 mL, 1.62 mol) and dichloromethane (100 mL) was added slowly to the rapidly stirred reaction mixture via a pressure equalizing addition funnel attached to the top of the reflux condenser. After spontaneous reflux had subsided, the mixture was heated to maintain reflux for 1 h. After cooling, the mixture was quenched with 50 mL methanol, concentrated under reduced pressure, taken up in ethyl acetate (300 mL) + hexanes (300 mL), and washed with 20% NaOH (150 mL, 595 mmol). The organic layer was extracted with a solution of H_2SO_4 (28 g, 284 mmol) in water (300 mL) in 3 portions, and the combined extracts were cooled with ice and neutralized with NaOH. The oily product was extracted with hexanes (2 x 250 mL), and the combined extracts were dried over Na_2SO_4, concentrated to 200 mL, cooled to –20°C, and scratched to induce crystallization. The colorless crystalline product was collected by filtration and dried in air. Yield 43.5 g (176 mmol, 65%). Mp 32-33°C. Lit[2] mp 35°C (EtOH). ^{1}H NMR ($CDCl_3$, 400 MHz) δ 1.90 (p, J = 6.4 Hz, 6H), 2.54 (t, J = 6.5 Hz, 6H), 3.62 (t, J = 6.2 Hz, 6H). ^{13}C NMR ($CDCl_3$, 100 MHz) δ 30.1, 43.1, 50.5.

Diiodide 10. A mixture of thietane **9** (10.70 g, 61.4 mmol),[1] 1,3-diiodopropane (9.11 g, 30.8 mmol), potassium iodide (5.10 g, 30.7 mmol), and powdered potassium carbonate (200 mg, 1.5 mmol) was stirred under argon in a sealed, foil-wrapped flask for 3 days at 65°C followed by 8 days at 45 °C.[3] The mixture was diluted into methanol (120 mL), treated with concentrated aqueous ammonia (20 mL), heated briefly to boiling, and concentrated to a viscous oil. This material was stirred for 2 hours with 1 M aqueous citric acid (100 mL) and cyclohexane (200 mL). The organic layer was separated, dried with $MgSO_4$, concentrated under reduced pressure, and rotated under high vacuum overnight to completely remove cyclohexane, giving the product **10** as a viscous, slightly yellow oil which was used in the next step without further purification. Yield 14.81 g (23.0

mmol, 75%). ^{1}H NMR ($CDCl_3$, 400 MHz) δ 1.41 (s, 6H), 1.42 (s, 6H), 1.92 (p, *J* = 7.1 Hz, 2H), 2.69 (t, J = 7.1 Hz, 4H), 2.70 (s, 4H), 3.40 (s, 4H), 3.72 (d, *J* = 11.8 Hz, 4H), 3.78 (d, *J* = 11.8 Hz, 4H). ^{13}C NMR ($CDCl_3$, 100 MHz) δ 12.8, 23.4, 23.7, 29.6, 32.5, 36.7, 36.8, 66.3, 98.6. EI-MS *m/z* 644 (56, $[M]^+$), 375 (100), 343 (50), 45 (181), 83 (67). EI-HRMS *m/z* calcd for $[M]^+$ $C_{19}H_{34}NI_2O_4S_2$ 643.9988, found 643.9985.

Macrocycle 11. Solutions of diiodide **10** (14.81 g, 24.2 mmol) and 1,3-propanedithiol (2.62 g, 24.2 mmol) in DMF (20 mL total solution volume each) were loaded into all-plastic syringes and added by syringe pump over 48 hours to a stirred suspension of cesium carbonate (23.6 g, 72.5 mmol) in DMF (750 mL) at 80°C (internal temperature) under argon. The hot liquid phase was then decanted from the solid residue and concentrated to dryness. The solids remaining after decantation were stirred in boiling toluene (200 mL), and the liquid phase was decanted and added to the residue remaining after evaporation of the initial liquid phase. The resulting mixture was concentrated to dryness, and the process was repeated. The residue was taken up in DCM (250 mL) and filtered through a 4 cm diameter column containing sequential beds of sand (3 cm), celite (3 cm) and silica gel (4 cm). The column was flushed with an additional 250 mL of DCM, and the combined filtrates were concentrated under reduced pressure. The residue was taken up in boiling acetone (100 mL), diluted slowly with hot hexanes until crystallization initiated, and allowed to cool under slow stirring. The product **11** was collected by filtration, washed with 5% acetone in hexanes, and dried by suction. Yield 7.82 g (65%).[4] ^{1}H NMR ($CDCl_3$, 400 MHz) δ 1.41 (s, 12H), 1.93 (p, *J* = 6.9 Hz, 4H), 2.74 (t, *J* = 6.9 Hz, 8H), 2.79 (s, 8H), 3.71 (s, 8H). ^{13}C NMR ($CDCl_3$, 100 MHz) δ 23.7, 28.7, 32.4, 35.2, 37.9, 66.7, 98.4. EI-MS *m/z* 496 (100, $[M]^+$), 355 (50), 106 (45). EI-HRMS *m/z* calcd for $[M]^+$ $C_{22}H_{40}O_4S_4$ 496.1809, found 496.1813.

Ligand 12 (*tr*MCL-3). Macrocycle **11** (7.58 g, 15.3 mmol) was dissolved in boiling isopropanol (200 mL) and 1 M aqueous HCl (15 mL) was added. The resulting crystalline slurry was boiled down to 150 mL total volume and then allowed to cool to room temperature under slow stirring. The colorless product **12** was collected by filtration, washed with cold isopropanol followed by hexanes, and dried under high vacuum at 120 °C. Yield 6.25 g (98%). Mp 220.5-222°C. ^{1}H NMR (DMSO-D_6, 400 MHz) δ 1.80 (p, *J* = 7.0 Hz, 4H), 2.58 (s, 8H), 2.61 (t, *J* = 7.0 Hz, 8H), 3.30 (d, *J* = 5.1 Hz, 8H), 4.50 (t, *J* = 5.1 Hz, 4H). ^{13}C NMR (DMSO-D_6, 100 MHz) δ 28.9, 31.8, 34.1, 44.6, 62.5. EI-MS *m/z* 416 (100, $[M]^+$), 241 (70), 106 (62). EI-HRMS *m/z* calcd for $[M]^+$ $C_{16}H_{32}O_4S_4$ 416.1183, found 416.1184.

[(12)-Cu(I)]PF_6 (16). Ligand **12** (395 mg, 0.948 mmol) and $Cu(CH_3CN)_4PF_6$ (353 mg, 0.948 mmol) were stirred in pyridine (10 mL) under argon until all solids had dissolved. The mixture was concentrated to a thick paste, diluted with water (10 mL), and concentrated again to a thick paste under a stream of argon in a 50°C bath. The residue was taken up in methanol (15 mL), centrifuged to remove a small amount of pale blue precipitate, concentrated to dryness, and recrystallized from water to give the product as colorless fibrous crystals. Yield 408 mg (69%). ^{1}H NMR (DMSO-D_6, 400 MHz) δ 1.93-2.01 (br. m, 4H), 2.74 (s, 8H), 2.93 (br. t, *J* ≈ 5 Hz, 8H), 3.39 (d, *J* = 5.2 Hz, 8H), 4.88 (t, *J* = 5.2 Hz, 4 H). ^{13}C NMR (DMSO-D_6, 100 MHz) δ 22.8 (br.), 34.6, 37.4, 43.3, 62.3.

MCL-3 (3). Ligand **12** (1.52 g, 3.66 mmol) was added to an oven-dried 100 mL rb flask containing a 25 mm egg-shaped magnetic stir bar. The flask was sealed with a rubber septum and

flushed with argon, and anhydrous DMSO (25 mL) was added. The mixture was stirred until the starting material had completely dissolved, and a solution of n-butyllithium in hexane (2.5 M, 3.07 mL, 2.1 equiv.) was added dropwise under rapid stirring. A white precipitate appeared and subsequently redissolved after addition of each drop, then became persistent once the amount of added n-BuLi exceeded 1.0 molar equiv. The resulting suspension was stirred for 30 minutes under a stream of argon to allow cooling by evaporation of hexane, and 1,3-propanesultone (893 mg, 2.0 equiv.) in anhydrous DMSO (2 mL) was added. The mixture was stirred for 4 hours, after which most of the precipitate had redissolved. A further 2 equiv. of n-BuLi followed by 2 equiv. of 1,3-propanesultone were added as described above, and the mixture was stirred overnight. The reaction vessel was manually agitated to dislodge material deposited on the flask walls, and a further 1.4 equiv. of n-BuLi and 2 equiv. of 1,3-propanesultone were added as described above. After 4 hours, the mixture was almost clear. A final 1.0 equiv. of n-BuLi and 1.0 equiv. 1,3-propanesultone were added, and the mixture became completely clear after stirring overnight. The resulting solution was diluted with ethanol (75 mL), treated with activated carbon to remove colored material leached from the rubber septum, and filtered through Celite. The carbon-Celite pad was washed with 30 mL of ethanol, and the combined filtrate and washings were treated with a solution of sodium iodide in 15 mL ethanol, producing a voluminous white precipitate. The mixture was heated to boiling, diluted slowly with water under rapid stirring until the precipitate completely dissolved (required 20 mL) and allowed to cool to room temperature under slow stirring. The resulting crystalline slurry was cooled to 4 °C, and the slightly colored product was collected by filtration, dissolved in 25 mL water, filtered through cotton to remove a small amount of insoluble material, heated to boiling, and diluted gradually with ethanol (required 75 mL) to the point of permanent turbidity. The mixture was diluted dropwise with water until clear and then allowed to cool under slow stirring. The resulting colorless crystalline powder was collected by filtration and dried overnight at 100°C/0.05 torr to give a fine powder. Yield 2.52 g (2.54 mmol, 69%). ^{1}H NMR (D_2O, 400 MHz) δ1.93-2.05 (m, 12H), 2.75 (s, 8H), 2.76 (t, J = 6.9 Hz, 8H), 2.97-3.01 (m, 8H), 3.44 (s, 8H), 3.62 (t, J = 6.2 Hz, 8H). ^{13}C NMR (D_2O, 100 MHz) δ27.1, 31.2, 34.7, 37.2, 46.5, 50.9, 72.5, 74.6. Elemental analysis calcd (%) for $C_{28}H_{52}Na_4O_{16}S_8$ (993.18): C 33.86, H 5.28, S 25.83; found C 33.45, H 5.51.

[(MCL-3)Cu]Na_4PF_6 (**15**). A solution of $Cu(CH_3CN)_4PF_6$ (221 mg, 0.593 mmol) in acetonitrile (10 mL) was added to a solution of ligand **3** (589 mg, 0.593 mmol) in water (10 mL). The mixture was concentrated to a viscous residue, which was taken up in boiling ethanol (50 mL) and concentrated to dryness. The resulting material was stirred in boiling ethanol (30 mL) and diluted gradually with water until almost all solids had dissolved to give a yellow, slightly turbid solution. This was decolorized with the minimum sufficient amount (< 50 mg) of ascorbic acid, allowed to settle while hot, decanted from the small amount of solid sediment, and allowed to cool under slow stirring to give a colorless crystalline slurry. The product was collected by filtration and dried overnight at 50°C/0.05 torr followed by 1 hour at 100°C/0.05 torr to give a fine powder. Yield 539 mg (0.449 mmol, 76%). ^{1}H NMR (D_2O, 400 MHz) δ1.99-2.06 (m, 8H), 2.07-2.11 (m, 4H), 2.89 (s, 8H), 2.97-3.01 (m, 16H), 3.55 (s, 8H), 3.65 (t, J = 6.2 Hz, 8H). ^{13}C NMR (D_2O, 100 MHz) δ25.6, 27.1, 38.0, 40.7, 45.4, 50.9, 72.5, 74.7. ^{19}F NMR (D_2O, 376 MHz) δ (TFE) 4.66 (d, J = 708 Hz, 6F). Elemental analysis calcd (%) for $C_{28}H_{52}CuF_6Na_4O_{16}PS_8$•$2H_2O$ (1237.69): C 27.17, H 4.56, S 20.72; found C 27.20, H 4.51, S 20.76.

N,N-Bis(2-hydroxyethyl)amino)methyl-pyridine dihydrochloride (**17**, DHEAMP•2HCl, H_2Pmide•2HCl). The neutral ligand was prepared from 8.00 g (48.8 mmol) of 2-

(chloromethyl)pyridine hydrochloride according to the procedure described by Wu et al.,[6] which gave a dark red oil. The crude material was dissolved in ethanol (100 mL), treated with concentrated HCl (4.0 mL, 49 mmol), and concentrated under reduced pressure. The partially solidified residue was recrystallized from ethanol under stirring to give a crystalline powder, which was collected by filtration and dried under argon. Titration against standard KOH was consistent with the dihydrochloride. Yield 2.62 g (11.3 mmol, 23%). ^{1}H NMR (D_2O + 1% CH_3OH, 400 MHz) δ 3.50-3.53 (m, 4H), 3.97-3.99 (m, 4H), 4.92 (s, 2H), 8.01 (ddd, J = 7.8, 5.6, 1.1 Hz, 1H), 8.15 (dt, J = 8.0, 0.9 Hz, 1H), 8.52 (td, J = 7.9, 1.7 Hz, 1H), 8.86 (ddd, J = 5.6, 1.7, 0.7 Hz, 1H). ^{13}C NMR (D_2O + 1% CH_3OH, 100 MHz) δ 55.6, 55.8, 56.0, 128.3, 129.7, 145.0, 145.8, 146.2.

^{1}H-NMR (D_2O, 400 MHz)

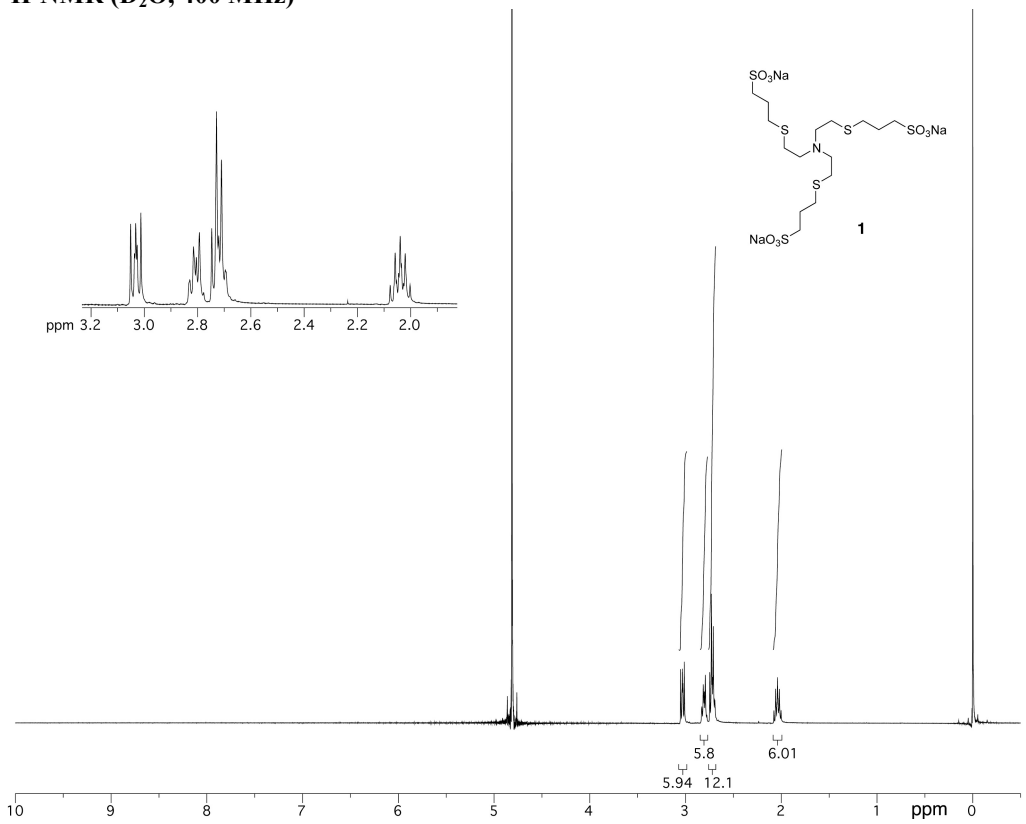

^{13}C-NMR (D_2O, 100 MHz)

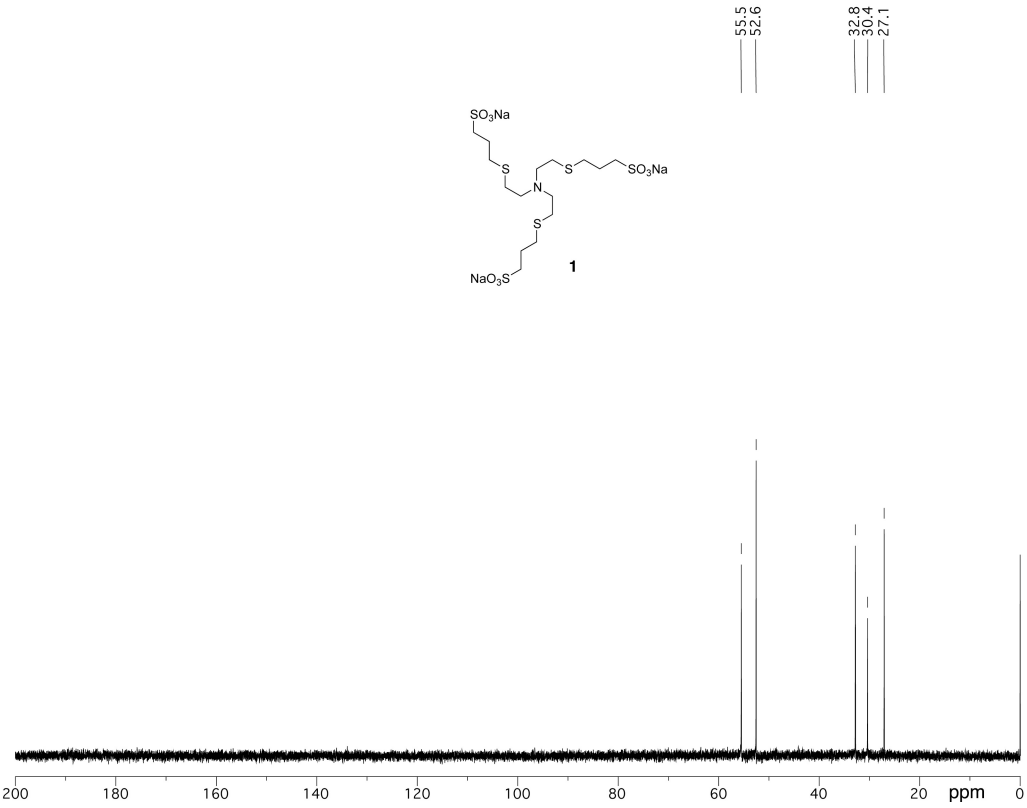

^{1}H-NMR (D_2O, 400 MHz)

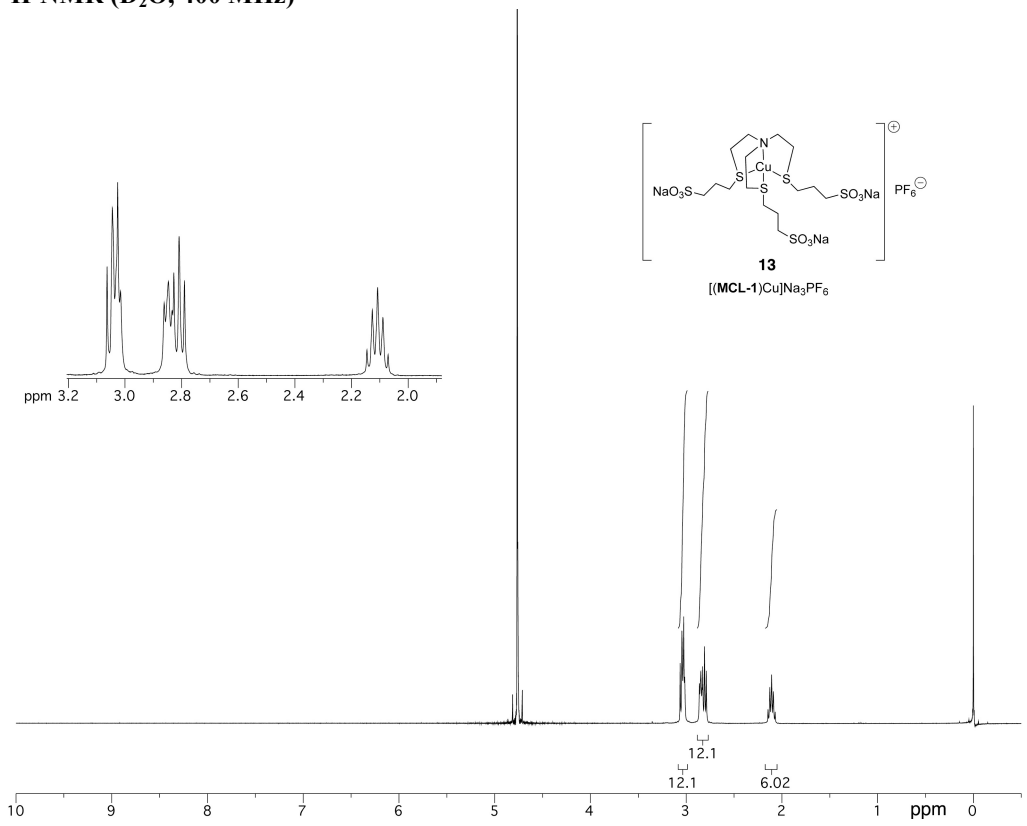

^{13}C-NMR (D_2O, 100 MHz)

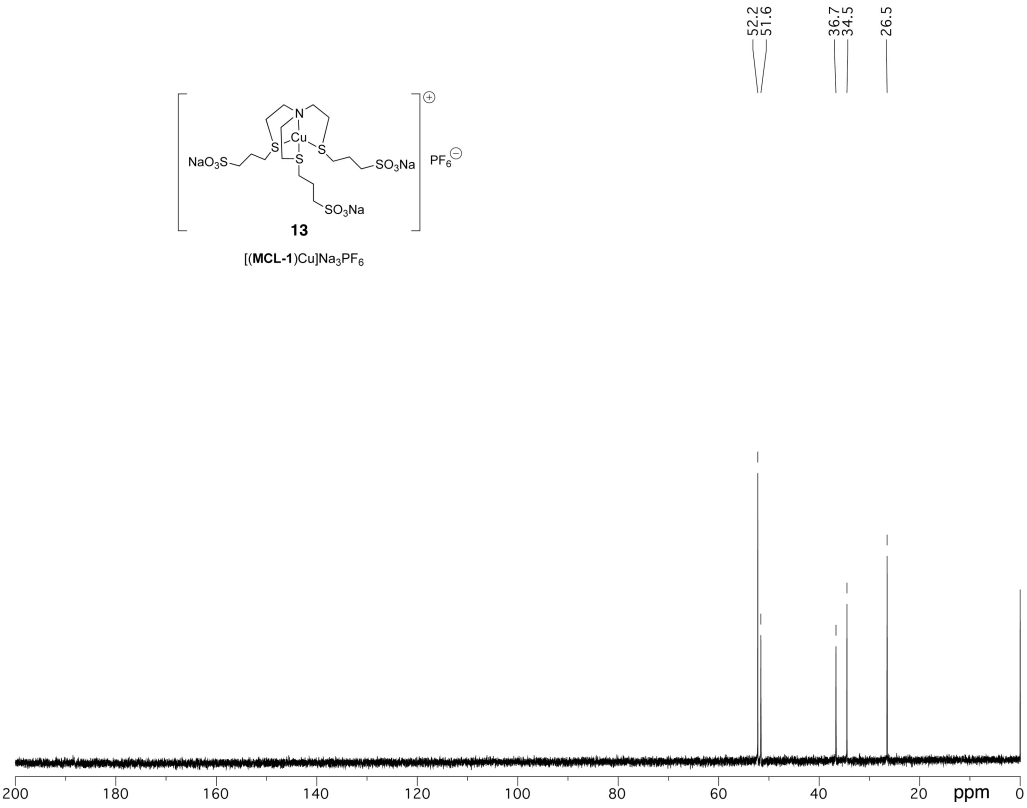

^{1}H-NMR (D_2O, 400 MHz)

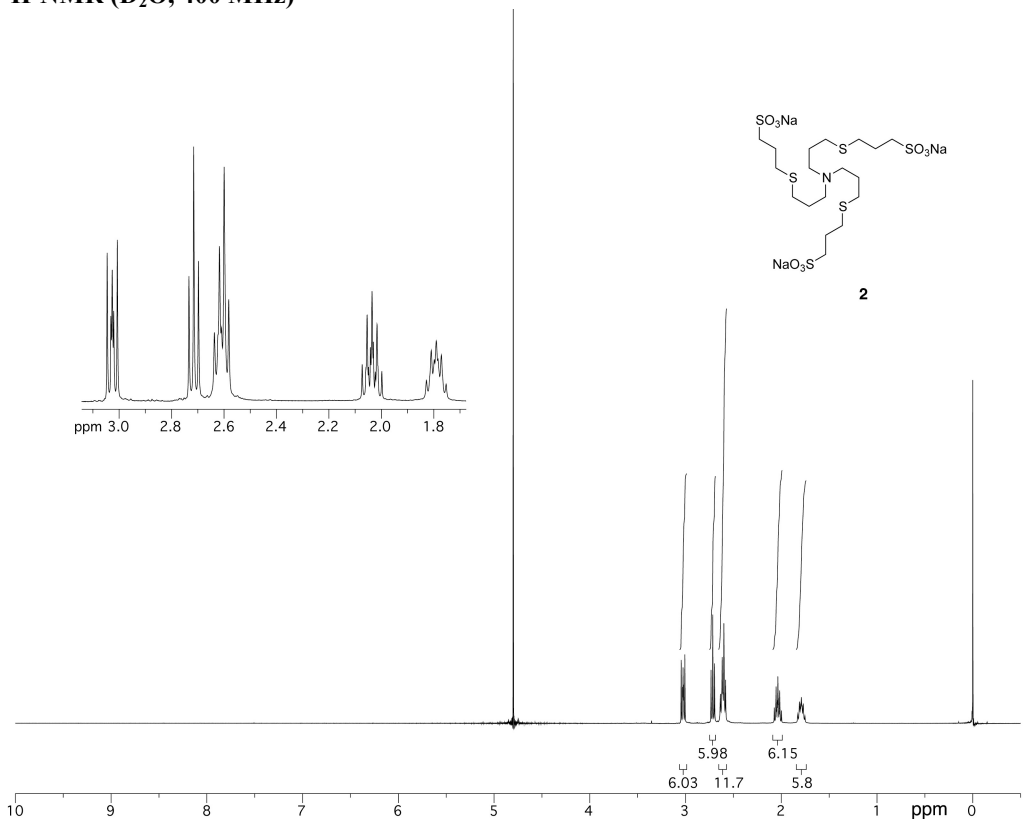

^{13}C-NMR (D_2O, 100 MHz)

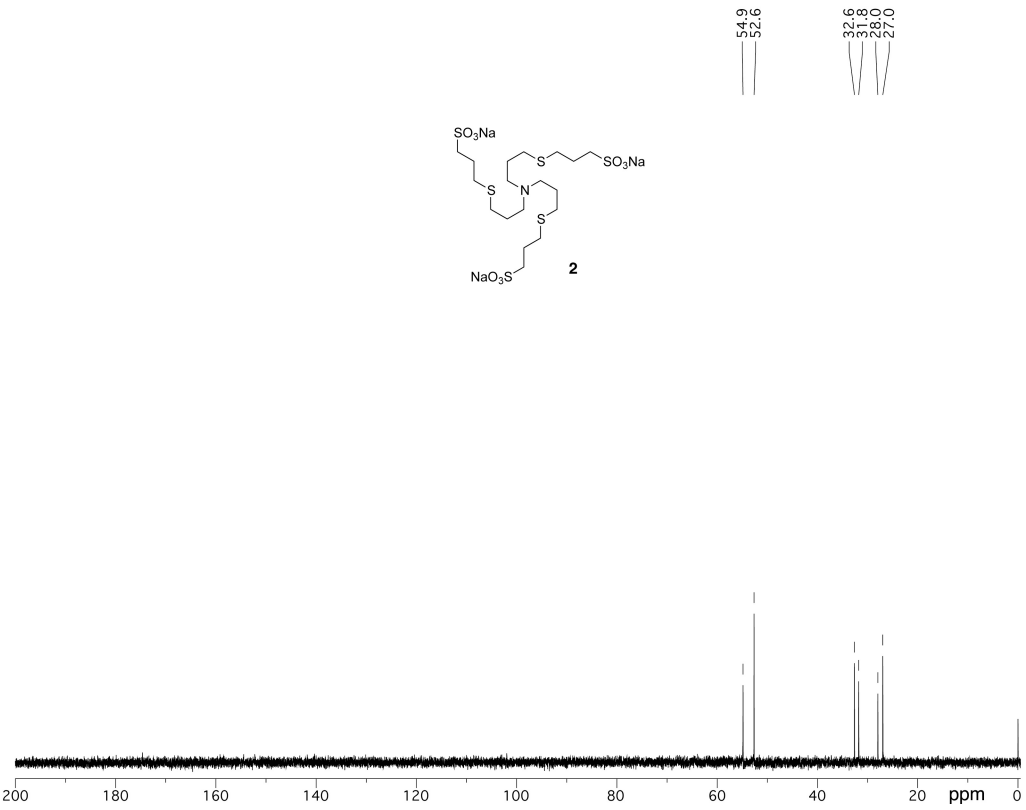

^{1}H-NMR (D_2O, 400 MHz)

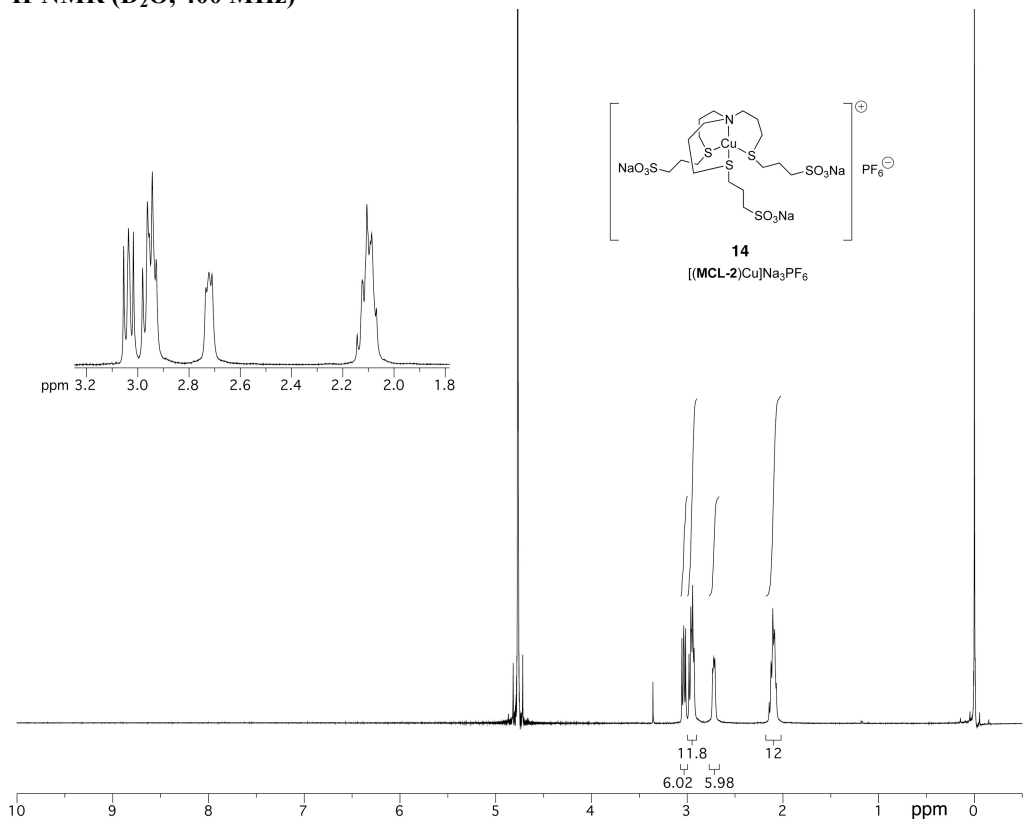

^{13}C-NMR (D_2O, 100 MHz)

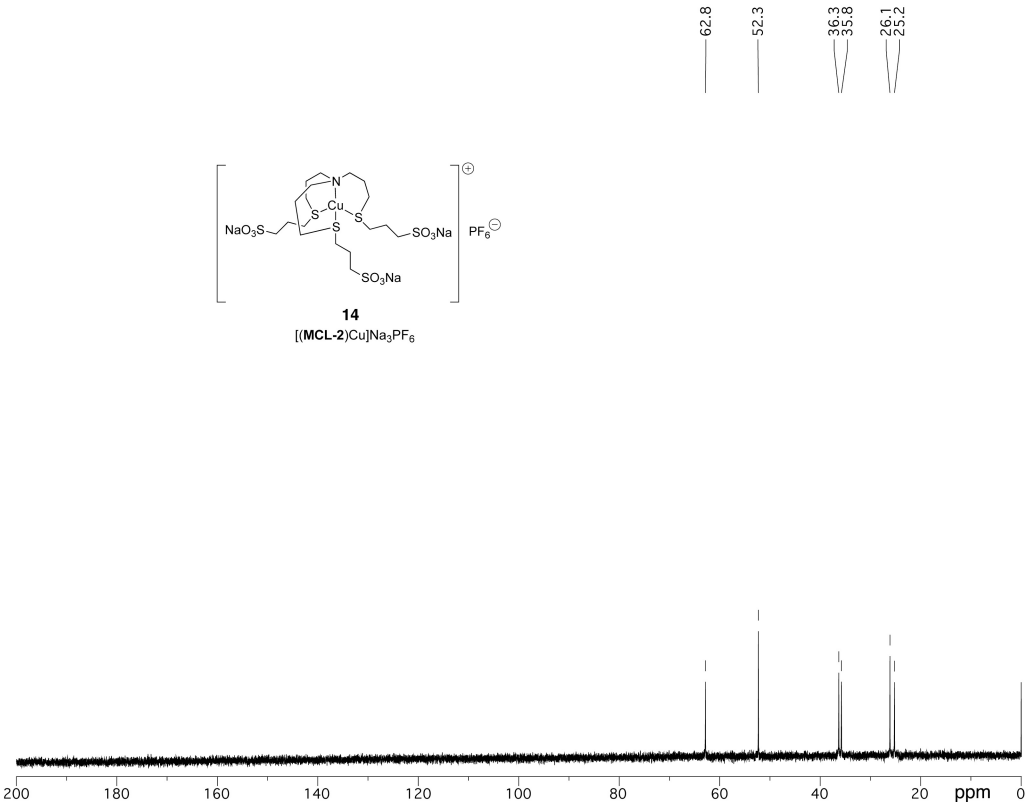

^{1}H-NMR (D_2O, 400 MHz)

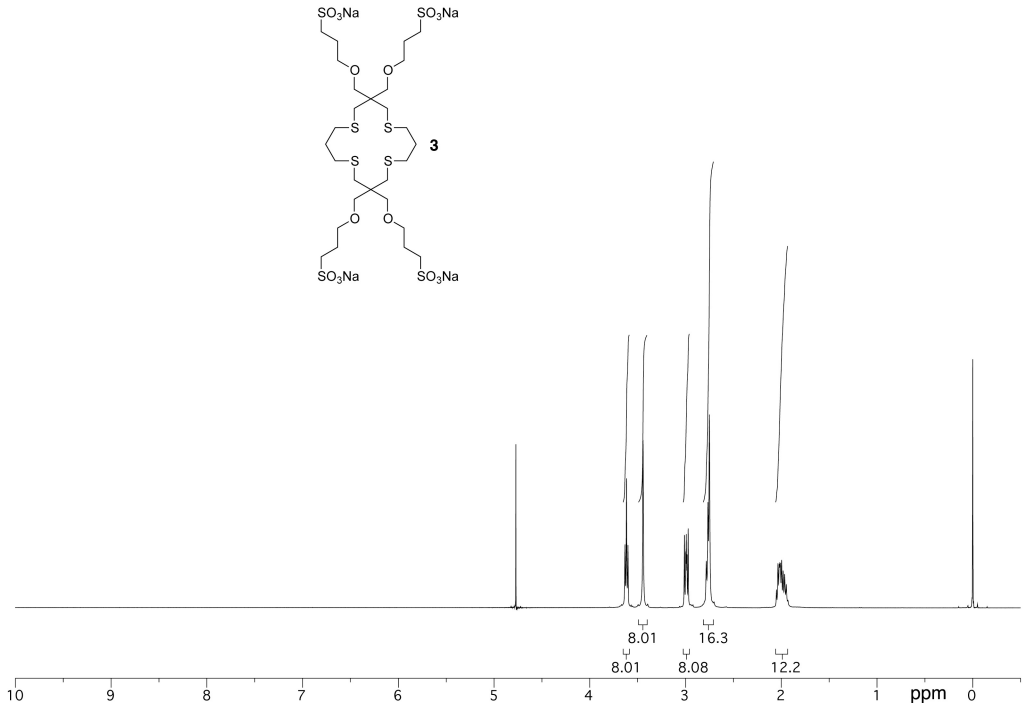

^{13}C-NMR (D_2O, 100 MHz)

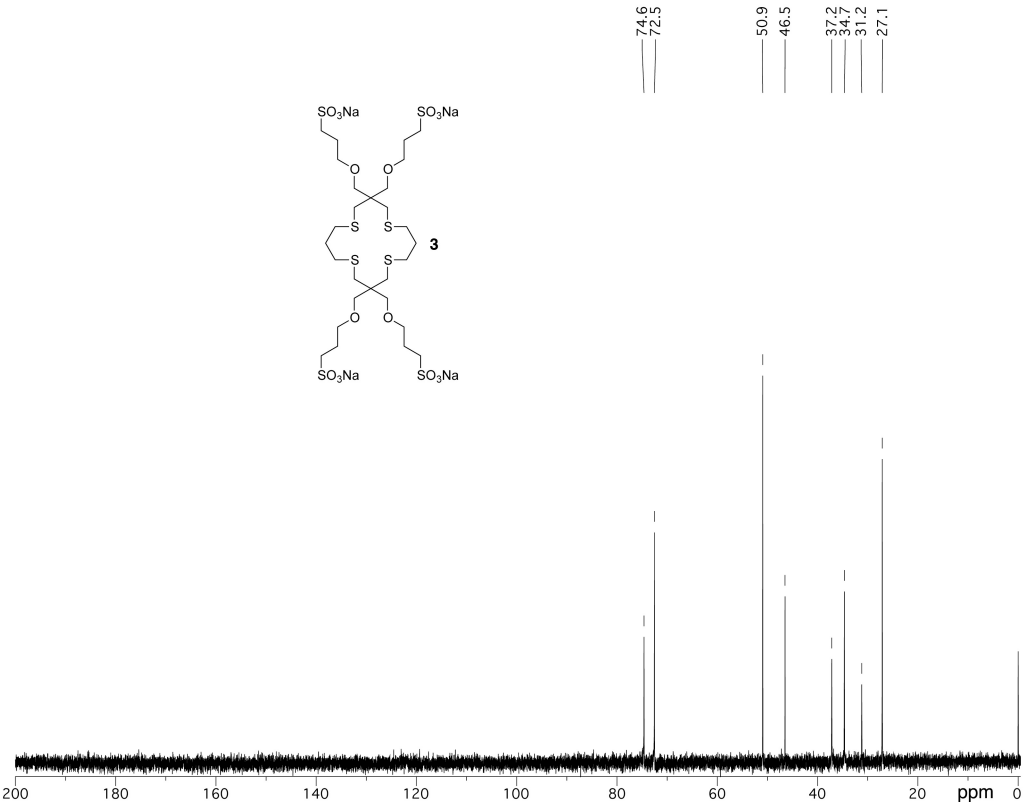

^{1}H-NMR (D_2O, 400 MHz)

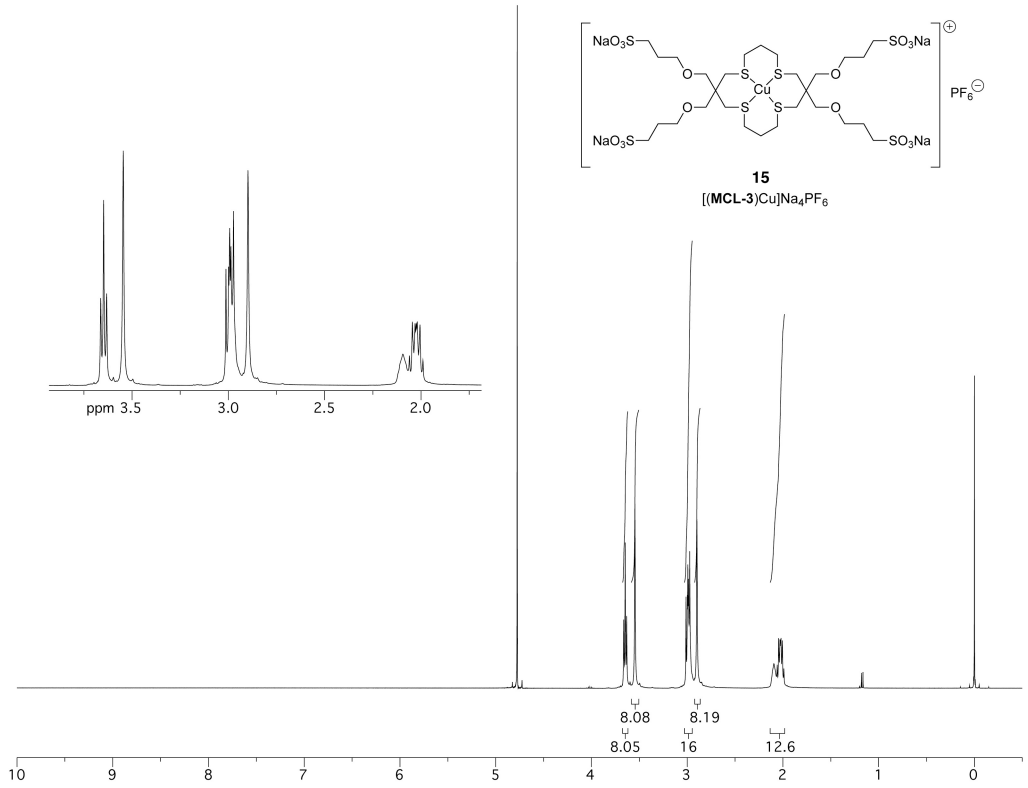

^{13}C-NMR (D_2O, 100 MHz)

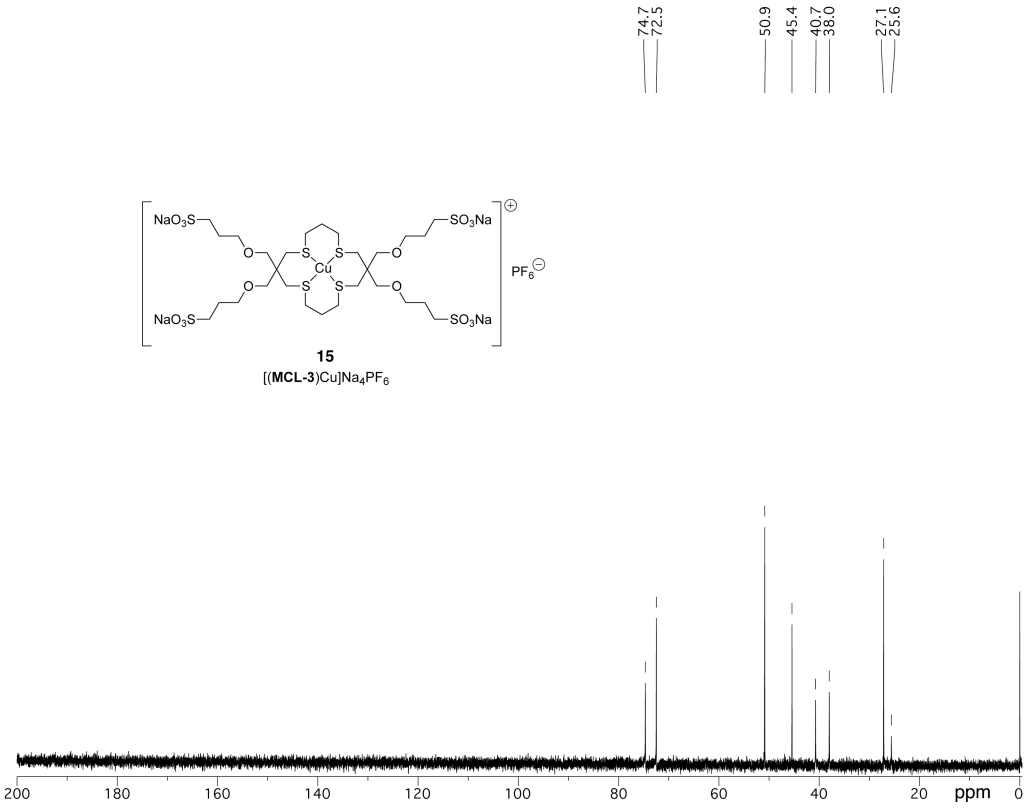

^{1}H-NMR (D_2O, 400 MHz)

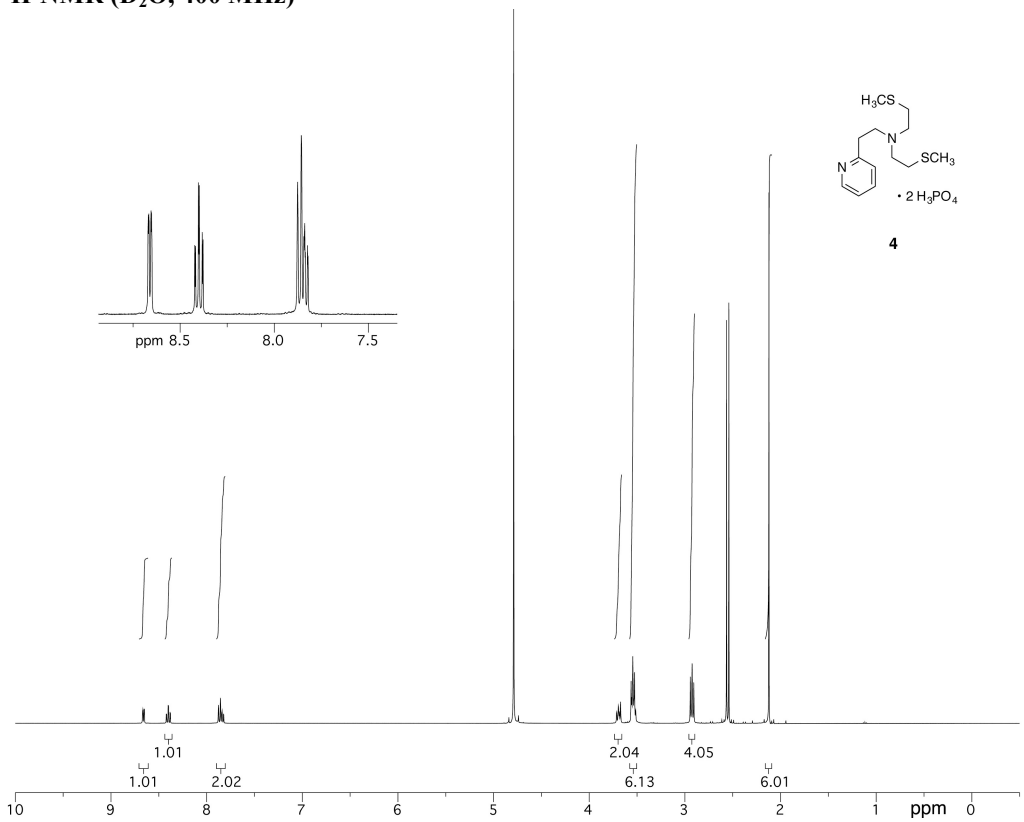

^{31}P-NMR (D_2O, 162 MHz)

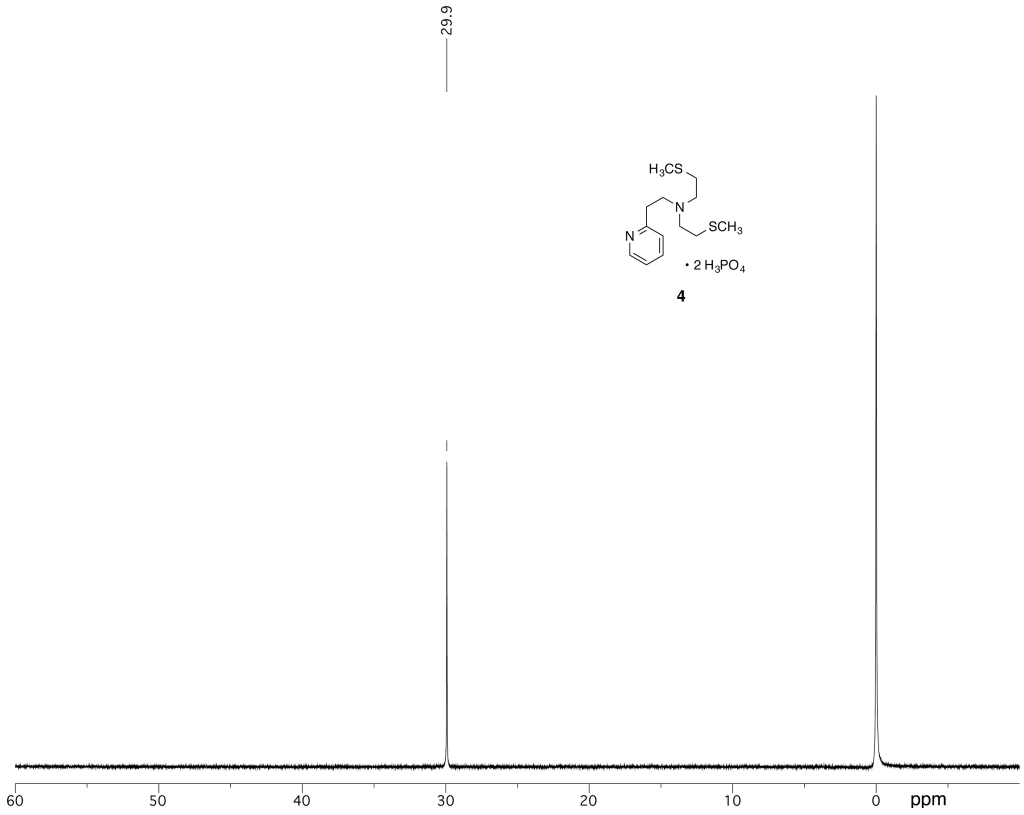

^{1}H-NMR ($CDCl_3$, 400 MHz)

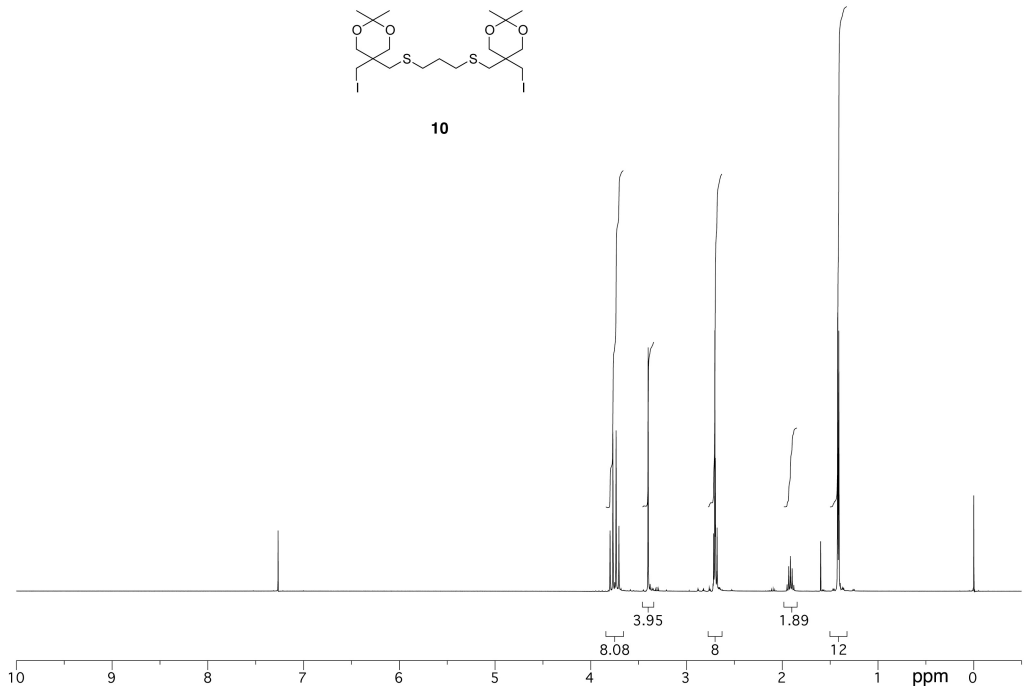

^{13}C-NMR ($CDCl_3$, 100 MHz)

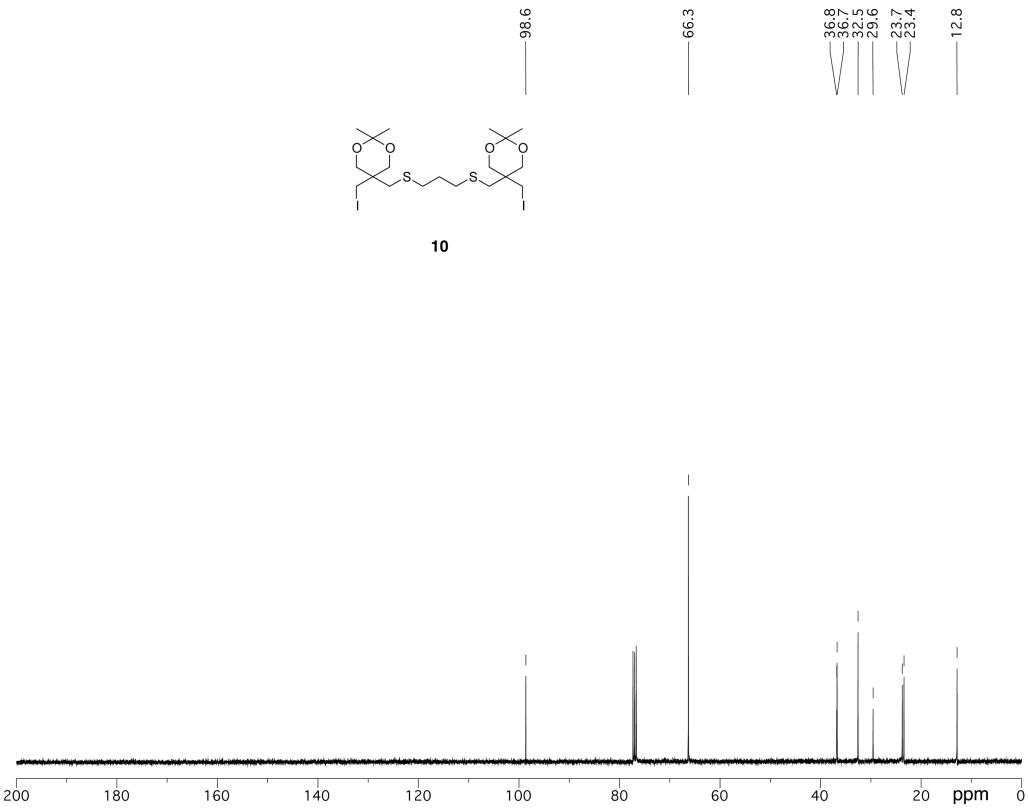

^{1}H-NMR ($CDCl_3$, 400 MHz)

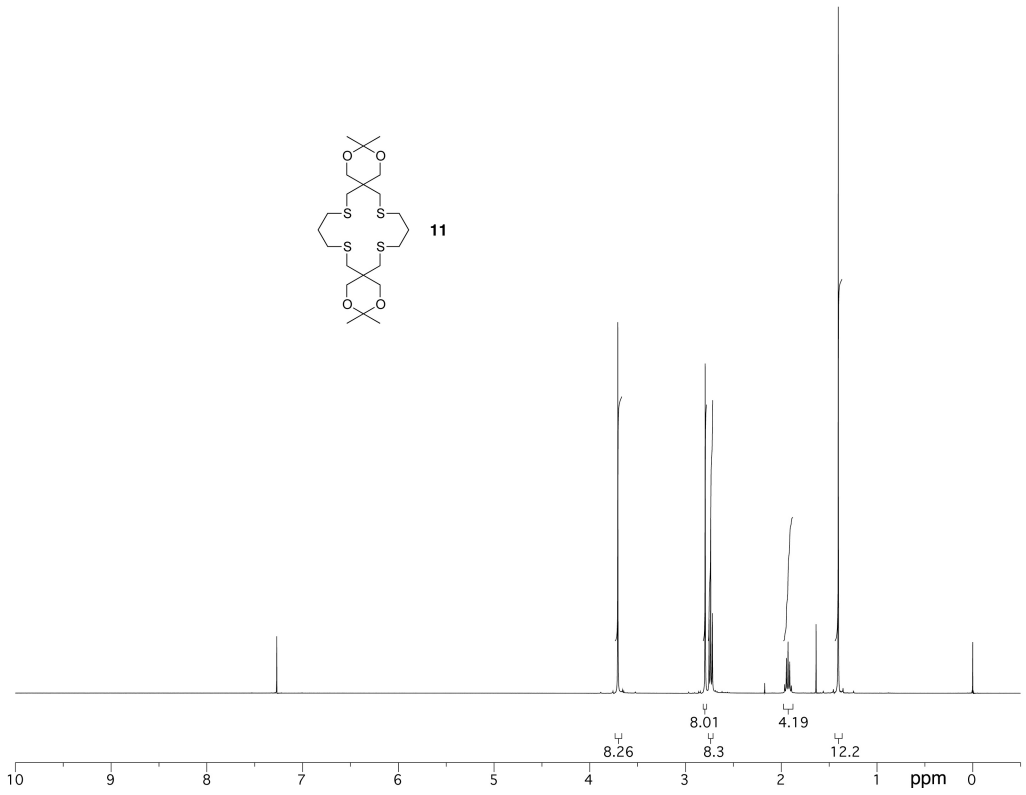

^{13}C-NMR ($CDCl_3$, 100 MHz)

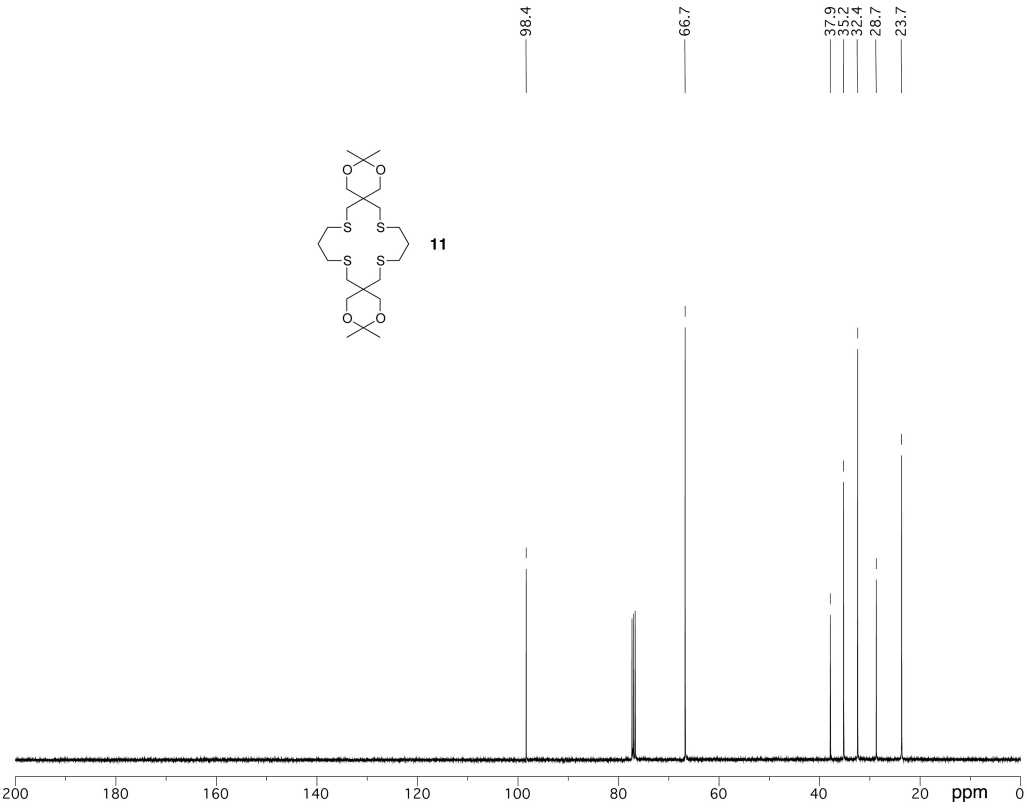

^{1}H-NMR ($CDCl_3$, 400 MHz)

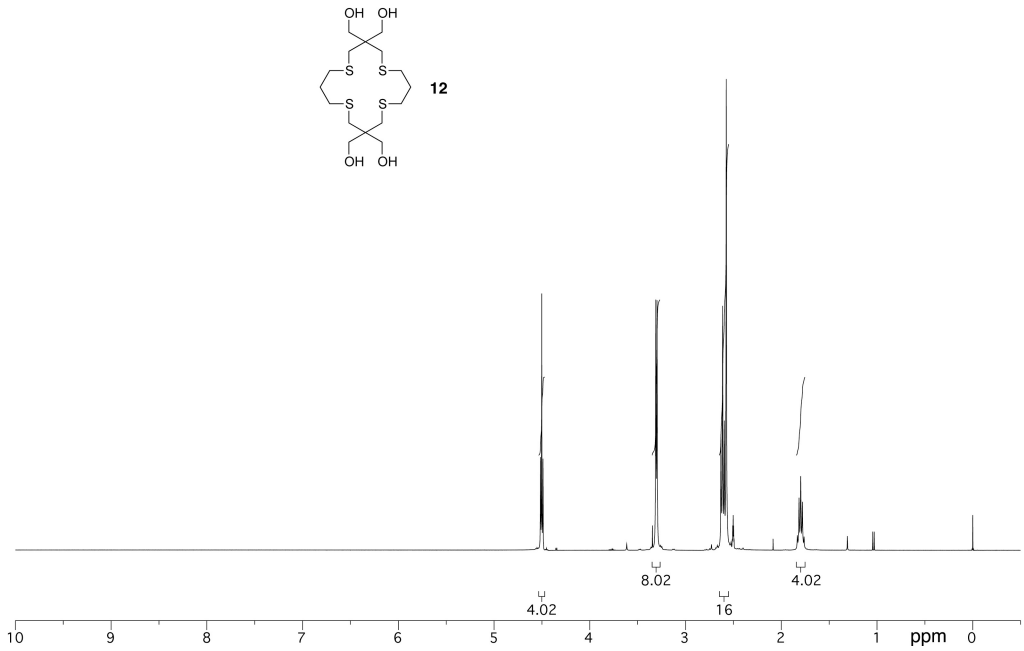

^{13}C-NMR ($CDCl_3$, 100 MHz)

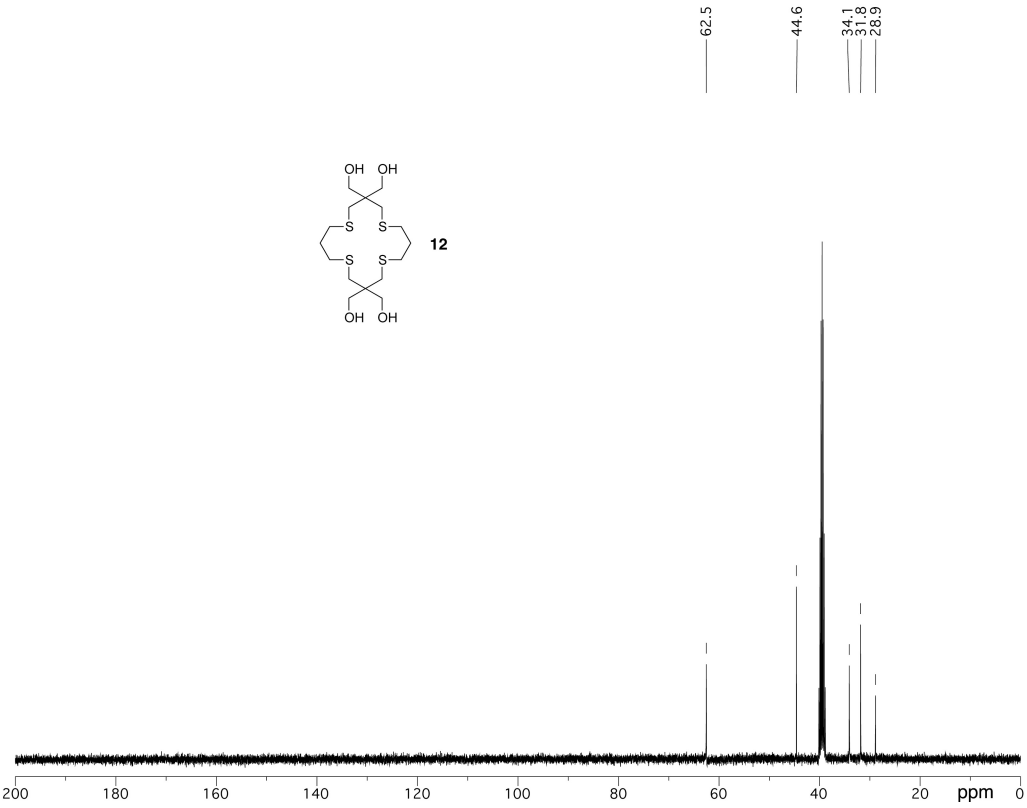

^{1}H-NMR (DMSO-d_6, 400 MHz)

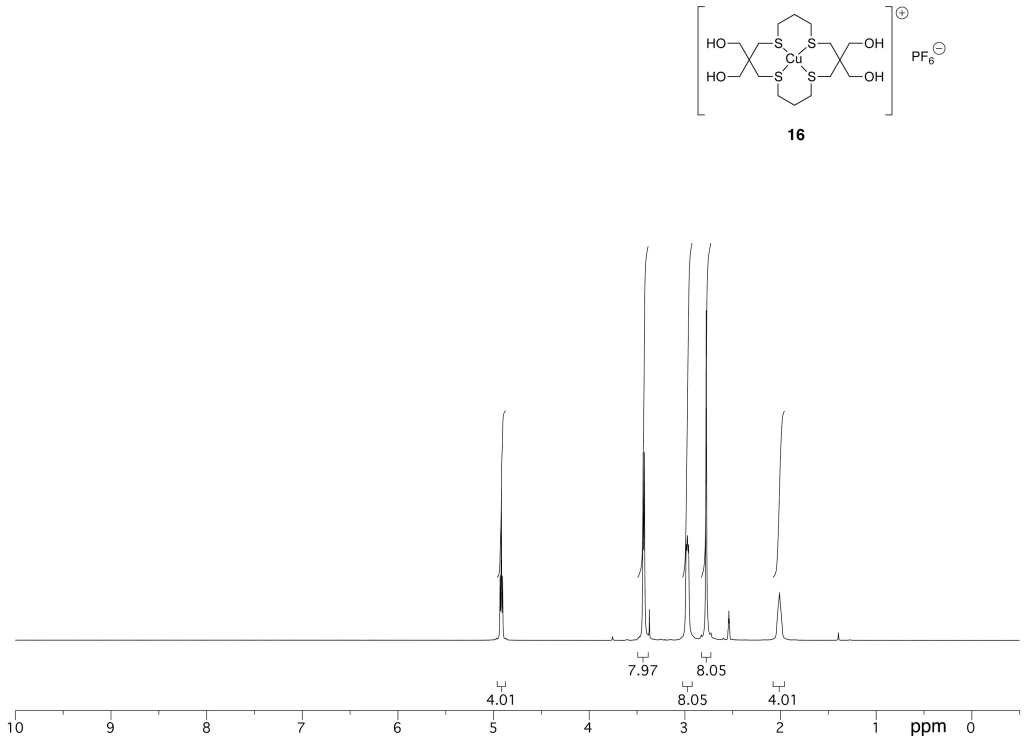

^{13}C-NMR (DMSO-d_6, 100 MHz)

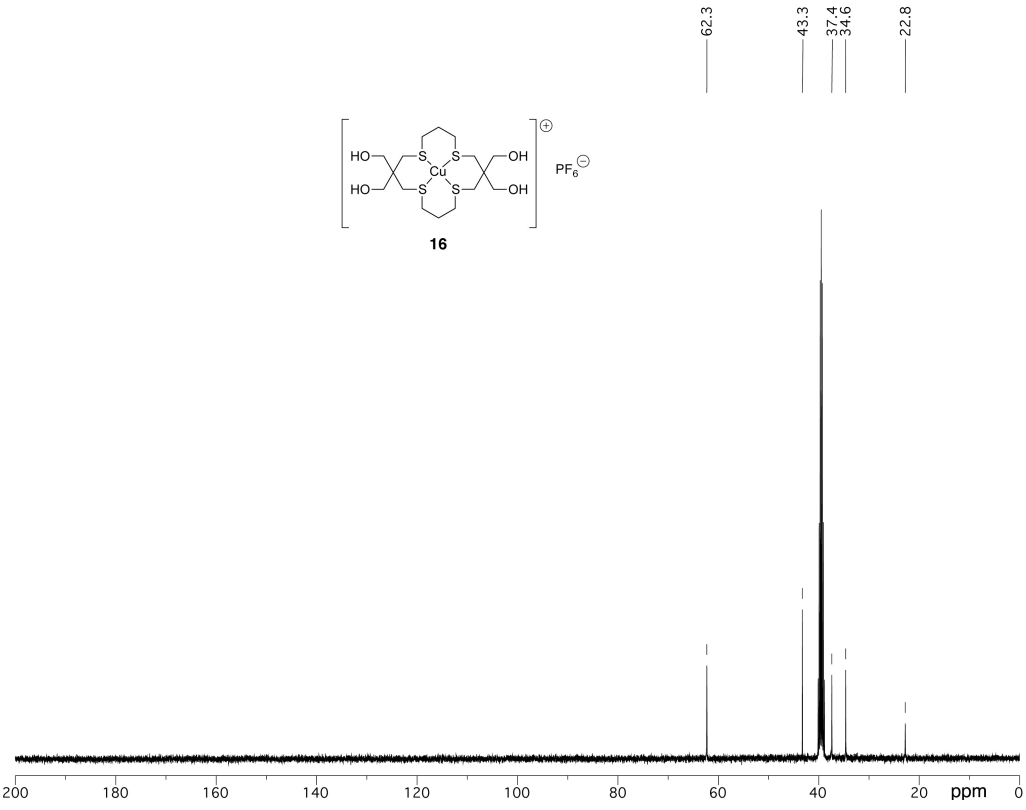

^{1}H-NMR (D_2O, 400 MHz)

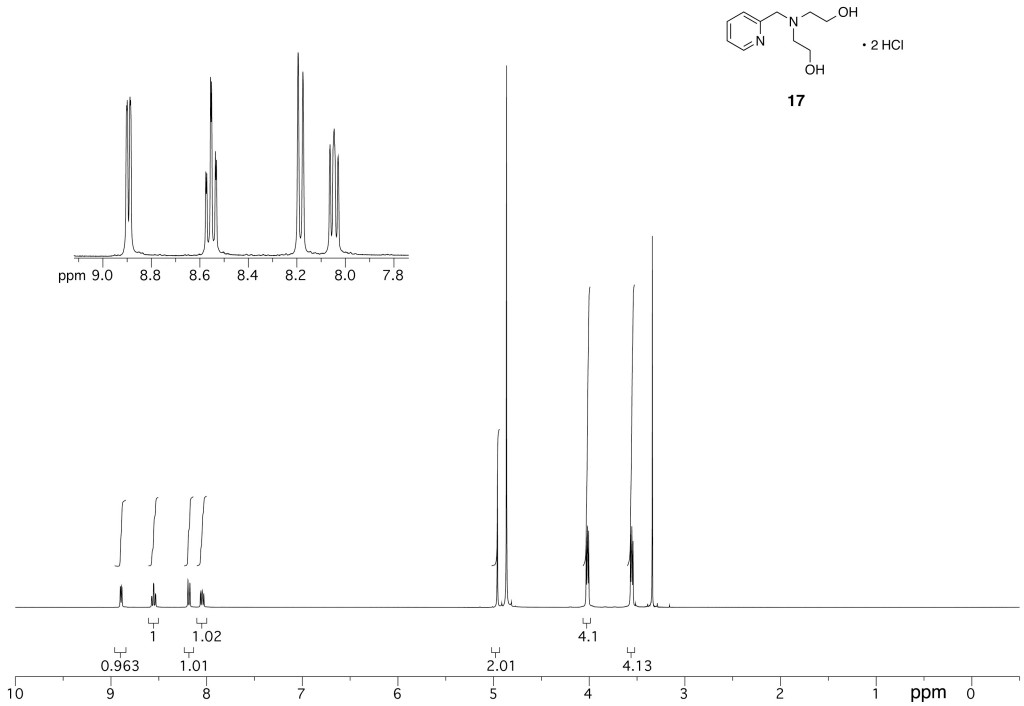

^{13}C-NMR (D_2O, 100 MHz)

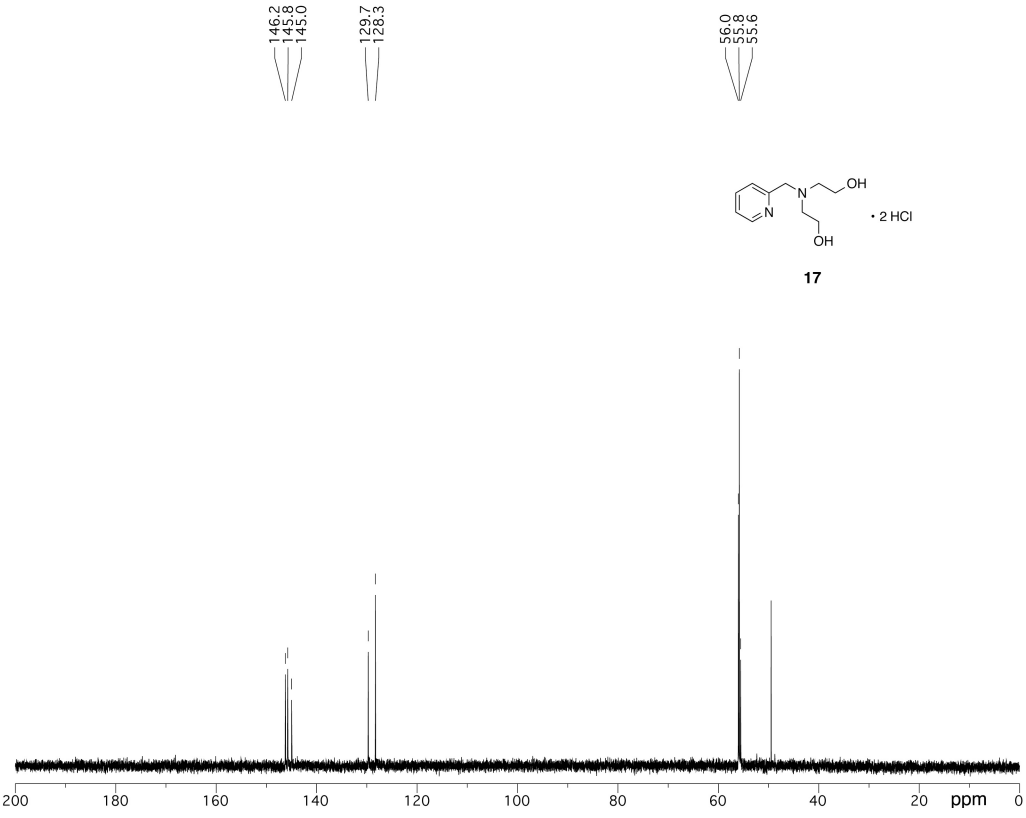

2. Crystallographic Structural Determinations

Table S1: Crystal data and structure refinement of complex **13a** $[Cu(I)\text{-}(MCL\text{-}1)]_2Na_7(ClO_4)_3(H_2O)_4$

Empirical formula	$C_{30}H_{68}Cl_3Cu_2N_2Na_7O_{34}S_{12}$	
Formula weight	1780.08	
Temperature	173(2)	
Wavelength	0.71073	
Crystal system	Triclinic	
Space group	P -1	
Unit cell dimensions	a = 9.8246(15) Å	α = 82.967(2)°
	b = 9.8488(15) Å	β = 84.686(2)°
	c = 18.657(3) Å	γ = 64.474(2)°
Volume	1615.2(4) $Å^3$	
Z	1	
Density (calculated)	1.830 g/cm^3	
Absorption coefficient	1.308 mm^{-1}	
F(000)	912	
Crystal size	0.721 x 0.249 x 0.092 mm	
Theta range for data collection	2.202 to 31.126°	
Index ranges	-14<=h<=14, -14<=k<=14, -27<=l<=27	
Reflections collected	25301	
Independent reflections	10289 [R(int) = 0.0316]	
Completeness to theta = 25.242°	100.0 %	
Absorption correction	numerical	
Max. and min. transmission	1.000 and 0.5883	
Refinement method	Full-matrix least-squares on F^2	
Data / restraints / parameters	10289 / 572 / 574	
Goodness-of-fit on F^2	1.029	
Final R indices [I>2sigma(I)]	R1 = 0.0390, wR2 = 0.1038	
R indices (all data)	R1 = 0.0474, wR2 = 0.1098	
Extinction coefficient	0	
Largest diff. peak and hole	1.026 and –0.603 $e.Å^{-3}$	

Table S2: Atomic coordinates (x 10^4) and equivalent isotropic displacement parameters ($Å^2$x 10^3) for complex **13a** $[Cu(I)\text{-}(MCL\text{-}1)]_2Na_7(ClO_4)_3(H_2O)_4$. U(eq) is defined as one third of the trace of the orthogonalized U^{ij} tensor.

Atom Label	x	y	z	U(eq)
Cu(1)	6651(1)	1120(1)	1824(1)	17(1)
S(1)	8747(1)	1442(1)	1941(1)	18(1)
S(2)	4317(1)	3117(1)	1799(1)	19(1)
S(3)	6560(1)	-1133(1)	1789(1)	18(1)
S(4)	7086(1)	3356(1)	4243(1)	14(1)
S(5)	2455(1)	1625(1)	3965(1)	14(1)
S(6)	8896(1)	-1962(1)	3902(1)	13(1)
N(1)	6864(2)	1408(2)	658(1)	20(1)
C(1)	9324(2)	1319(3)	986(1)	24(1)
C(2)	8023(3)	2001(3)	477(1)	24(1)
C(3)	4535(3)	3763(2)	858(1)	25(1)
C(4)	5383(3)	2485(2)	377(1)	23(1)
C(5)	6479(3)	-960(2)	810(1)	23(1)
C(6)	7361(3)	-118(2)	413(1)	23(1)
C(7)	8134(2)	3438(2)	2049(1)	19(1)
C(8)	7255(2)	3822(2)	2769(1)	18(1)
C(9)	8175(2)	2904(2)	3422(1)	18(1)
C(10)	2994(2)	2282(3)	1747(1)	23(1)
C(11)	2213(2)	2217(3)	2489(1)	22(1)
C(12)	3330(2)	1414(2)	3084(1)	19(1)
C(13)	8298(3)	-2850(2)	1920(1)	23(1)
C(14)	8571(3)	-3220(2)	2728(1)	21(1)
C(15)	9323(2)	-2310(2)	2984(1)	17(1)
Cl(1A)	3097(2)	-2233(2)	1814(1)	24(1)
Cl(1B)	3334(6)	-2371(6)	1917(3)	24(1)
Cl(2)	10040(20)	5030(20)	4(16)	26(1)
Na(1)	6015(1)	946(1)	4739(1)	17(1)
Na(2)	2528(1)	-1884(1)	3827(1)	18(1)
Na(3)	10000	0	5000	14(1)
Na(4)	1665(1)	4761(1)	4732(1)	25(1)

Table S2 continued

O(1)	7867(2)	2157(2)	4801(1)	19(1)
O(2)	5636(2)	3353(2)	4122(1)	20(1)
O(2A)	2856(6)	-1970(6)	2562(2)	68(1)
O(2B)	3390(15)	-1806(16)	2580(5)	68(1)
O(3)	6960(2)	4820(2)	4399(1)	22(1)
O(3A)	3020(5)	-871(4)	1415(2)	42(1)
O(3B)	2822(14)	-1145(12)	1347(6)	42(1)
O(4)	1716(2)	601(2)	4096(1)	19(1)
O(4A)	4590(5)	-3410(7)	1680(4)	53(1)
O(4B)	4836(13)	-3409(18)	1699(10)	53(1)
O(5)	1388(2)	3203(2)	3976(1)	22(1)
O(5A)	1955(4)	-2615(4)	1597(2)	51(1)
O(5B)	2322(9)	-3087(10)	2001(5)	51(1)
O(6)	3694(2)	1189(2)	4451(1)	22(1)
O(7)	9282(2)	-3414(2)	4328(1)	21(1)
O(8)	7280(2)	-971(2)	3953(1)	21(1)
O(9)	9820(2)	-1208(2)	4053(1)	20(1)
O(10)	8986(5)	6543(5)	-183(3)	55(1)
O(11)	10036(6)	4493(5)	736(2)	58(1)
O(12)	9597(6)	4035(6)	-425(3)	64(2)
O(13)	11544(5)	4750(5)	-306(3)	54(1)
O(1W)	4999(2)	-2176(2)	4142(1)	20(1)
O(2W)	3002(2)	5586(2)	3739(1)	28(1)

Table S3: Crystal data and structure refinement of complex **14a** $[Cu(I)\text{-}(MCL\text{-}2)]_2Na_6(PF_6)_2(H_2O)_{15}$

Empirical formula	$C_{36}H_{102}Cu_2F_{12}N_2Na_6O_{33}P_2S_{12}$	
Formula weight	2030.87	
Temperature	173(2)	
Wavelength	0.71073 Å	
Crystal system	Triclinic	
Space group	P -1	
Unit cell dimensions	a = 11.8551(17) Å	α = 91.273(2)°
	b = 11.9311(17) Å	β = 98.023(2)°
	c = 32.214(5) Å	γ = 119.384(2)°
Volume	3909.7(10) $Å^3$	
Z	2	
Density (calculated)	1.725 g/cm^3	
Absorption coefficient	1.047 mm^{-1}	
F(000)	2100	
Crystal size	0.783 x 0.451 x 0.316 mm	
Theta range for data collection	1.284 to 32.106°	
Index ranges	-17<=h<=17, -17<=k<=17, -45<=l<=46	
Reflections collected	50063	
Independent reflections	25380 [R(int) = 0.0266]	
Completeness to theta = 32.106°	99.7 %	
Absorption correction	none	
Max. and min. transmission	0.8602 and 0.6223	
Refinement method	Full-matrix least-squares on F^2	
Data / restraints / parameters	25380 / 54 / 1278	
Goodness-of-fit on F^2	1.022	
Final R indices [I>2sigma(I)]	R1 = 0.0484, wR2 = 0.1242	
R indices (all data)	R1 = 0.0631, wR2 = 0.1339	
Extinction coefficient	n/a	
Largest diff. peak and hole	1.926 and –1.299 $e.Å^{-3}$	

Table S4: Atomic coordinates (x 10^4) and equivalent isotropic displacement parameters ($Å^2$x 10^3) for complex **14a** $[Cu(I)\text{-}(MCL\text{-}2)]_2Na_6(PF_6)_2(H_2O)_{15}$. U(eq) is defined as one third of the trace of the orthogonalized U^{ij} tensor.

Atom Label	x	y	z	U(eq)
Cu(1)	-3220(1)	-1624(1)	233(1)	15(1)
N(1)	-3562(2)	-1847(2)	-437(1)	14(1)
S(1)	-4998(1)	-1427(1)	323(1)	15(1)
S(2)	-3317(1)	-3554(1)	346(1)	15(1)
S(3)	-1206(1)	214(1)	346(1)	15(1)
S(4)	-4964(1)	-3905(1)	1761(1)	15(1)
S(5)	397(1)	-698(1)	1740(1)	15(1)
S(6)	-2878(1)	1435(1)	1726(1)	16(1)
C(1)	-6225(2)	-2861(2)	-24(1)	19(1)
C(2)	-6037(2)	-2677(2)	-483(1)	20(1)
C(3)	-4943(2)	-2855(2)	-615(1)	19(1)
C(4)	-2161(2)	-3423(2)	7(1)	20(1)
C(5)	-2729(2)	-3482(2)	-456(1)	21(1)
C(6)	-2665(2)	-2239(2)	-597(1)	20(1)
C(7)	-1658(2)	1152(2)	-8(1)	20(1)
C(8)	-1967(2)	579(2)	-466(1)	20(1)
C(9)	-3318(2)	-614(2)	-608(1)	19(1)
C(10)	-5494(2)	-1838(2)	832(1)	17(1)
C(11)	-5080(2)	-2746(2)	1042(1)	17(1)
C(12)	-5639(2)	-3111(2)	1447(1)	17(1)
C(13)	-2465(2)	-3550(2)	862(1)	16(1)
C(14)	-1349(2)	-2219(2)	1049(1)	19(1)
C(15)	-645(2)	-2273(2)	1477(1)	17(1)
C(16)	-802(2)	1142(2)	853(1)	17(1)
C(17)	-1991(2)	903(2)	1049(1)	18(1)
C(18)	-1580(2)	1852(2)	1439(1)	17(1)
O(1)	-3574(2)	-2986(2)	1903(1)	24(1)
O(2)	-5169(2)	-5024(1)	1496(1)	20(1)
O(3)	-5689(2)	-4285(2)	2116(1)	22(1)
O(4)	1304(2)	60(2)	1460(1)	23(1)

Table S4 continued

O(5)	1085(2)	-827(2)	2137(1)	21(1)
O(6)	-469(2)	-190(2)	1819(1)	20(1)
O(7)	-3122(2)	240(2)	1911(1)	22(1)
O(8)	-4011(2)	1268(2)	1432(1)	26(1)
O(9)	-2393(2)	2525(2)	2052(1)	27(1)
Cu(1B)	3196(1)	1603(1)	4774(1)	14(1)
N(1B)	3566(2)	1825(2)	5443(1)	15(1)
S(1B)	4991(1)	1462(1)	4659(1)	15(1)
S(2B)	1209(1)	-268(1)	4666(1)	15(1)
S(3B)	3233(1)	3515(1)	4673(1)	15(1)
S(4B)	4730(1)	4063(1)	3289(1)	16(1)
S(5B)	2952(1)	-1343(1)	3288(1)	17(1)
S(6B)	-425(1)	682(1)	3259(1)	17(1)
C(1B)	6219(2)	2890(2)	5008(1)	19(1)
C(2B)	6047(2)	2697(2)	5466(1)	20(1)
C(3B)	4950(2)	2855(2)	5608(1)	19(1)
C(4B)	1712(2)	-1180(2)	5019(1)	19(1)
C(5B)	2019(2)	-608(2)	5476(1)	20(1)
C(6B)	3362(2)	602(2)	5615(1)	19(1)
C(7B)	2088(2)	3348(2)	5022(1)	19(1)
C(8B)	2689(2)	3422(2)	5480(1)	20(1)
C(9B)	2678(2)	2201(2)	5619(1)	19(1)
C(10B)	5450(2)	1919(2)	4147(1)	16(1)
C(11B)	5011(2)	2837(2)	3965(1)	18(1)
C(12B)	5507(2)	3268(2)	3553(1)	19(1)
C(13B)	814(2)	-1201(2)	4160(1)	17(1)
C(14B)	2011(2)	-938(2)	3968(1)	18(1)
C(15B)	1644(2)	-1870(2)	3576(1)	18(1)
C(16B)	2354(2)	3508(2)	4162(1)	17(1)
C(17B)	1262(2)	2171(2)	3969(1)	19(1)
C(18B)	578(2)	2237(2)	3538(1)	19(1)
O(1B)	5300(2)	4521(2)	2912(1)	27(1)
O(2B)	4948(2)	5112(2)	3591(1)	26(1)

Table S4 continued

O(3B)	3339(2)	3098(2)	3175(1)	22(1)
O(4B)	3200(2)	-99(2)	3152(1)	33(1)
O(5B)	2518(2)	-2300(2)	2926(1)	37(1)
O(6B)	4078(2)	-1225(2)	3578(1)	24(1)
O(7B)	-1008(2)	851(2)	2851(1)	23(1)
O(8B)	-1421(2)	-84(2)	3513(1)	23(1)
O(9B)	438(2)	146(2)	3212(1)	21(1)
P(2)	476(1)	5284(1)	5853(1)	20(1)
P(3)	419(1)	5245(1)	833(1)	19(1)
F(1)	926(2)	4409(1)	6131(1)	28(1)
F(2)	-569(2)	4025(2)	5546(1)	39(1)
F(3)	1515(2)	6529(2)	6170(1)	36(1)
F(4)	1567(2)	5537(2)	5572(1)	37(1)
F(5)	-611(2)	5014(2)	6143(1)	35(1)
F(6)	36(2)	6154(2)	5584(1)	39(1)
F(7)	-575(2)	3909(2)	557(1)	44(1)
F(8)	-136(2)	5981(2)	539(1)	40(1)
F(9)	-650(2)	4984(2)	1128(1)	36(1)
F(10)	991(2)	4528(2)	1137(1)	36(1)
F(11)	1506(2)	5522(2)	548(1)	39(1)
F(12)	1418(2)	6597(1)	1118(1)	31(1)
Na(1)	3134(1)	3803(1)	2421(1)	25(1)
Na(2)	3598(1)	6847(1)	2524(1)	34(1)
Na(3)	-2185(1)	-948(1)	2272(1)	23(1)
Na(4)	2247(1)	997(1)	2828(1)	21(1)
Na(5)	3065(1)	-867(1)	2307(1)	21(1)
Na(6)	-2888(1)	-4039(1)	2606(1)	27(1)
O(1W)	3222(2)	2673(2)	1818(1)	30(1)
O(2W)	3474(2)	-537(2)	1615(1)	29(1)
O(3W)	2075(2)	4796(2)	2726(1)	41(1)
O(4W)	1117(2)	1965(2)	2393(1)	26(1)
O(5W)	4006(2)	1476(2)	2445(1)	24(1)
O(6W)	4597(2)	6923(2)	3198(1)	42(1)

Table S4 continued

O(7W)	6419(2)	10356(2)	3264(1)	26(1)
O(8W)	9894(2)	4913(2)	2388(1)	45(1)
O(9W)	-3057(2)	-2234(2)	2899(1)	45(1)
O(10W)	-897(2)	-2078(2)	2614(1)	39(1)
O(11W)	1947(2)	-3135(2)	2031(1)	30(1)
O(12W)	-1637(2)	-4938(2)	2964(1)	29(1)
O(13W)	-3204(3)	-5457(2)	2020(1)	50(1)
O(14W)	6701(2)	2403(2)	2803(1)	26(1)
O(15W)	5072(2)	-949(2)	2463(1)	23(1)

Table S5: Crystal data and structure refinement of ligand *tr*MCL-3 (**12**).

Empirical formula	$C_{16}H_{32}O_4S_4$	
Formula weight	416.65	
Temperature	173.15 K	
Wavelength	0.71073 Å	
Crystal system	Triclinic	
Space group	P -1	
Unit cell dimensions	a = 9.5948(9) Å	α = 100.741(2)°
	b = 9.6412(9) Å	β = 107.2010(10)°
	c = 12.1268(12) Å	γ = 97.413(2)°
Volume	1032.38(17) $Å^3$	
Z	2	
Density (calculated)	1.340 g/cm^3	
Absorption coefficient	0.477 mm^{-1}	
F(000)	448	
Crystal size	0.774 x 0.212 x 0.196 mm	
Theta range for data collection	1.809 to 31.051°	
Index ranges	-13<=h<=13, -13<=k<=13, 0<=l<=17	
Reflections collected	10217	
Independent reflections	10217	
Completeness to theta = 35.0°	98.3 %	
Absorption correction	semi-empirical from equivalents	
Refinement method	Full-matrix least-squares on F^2	
Data / restraints / parameters	10217 / 73 / 248	
Goodness-of-fit on F^2	1.054	
Final R indices [I>2sigma(I)]	R1 = 0.1009, wR2 = 0.2508	
R indices (all data)	R1 = 0.1150, wR2 = 0.2612	
Extinction coefficient	n/a	
Largest diff. peak and hole	2.342 and –0.789 $e.Å^{-3}$	

Table S6: Atomic coordinates (x 10^4) and equivalent isotropic displacement parameters ($Å^2$x 10^3) for ligand *tr*MCL-3 (**12**). U(eq) is defined as one third of the trace of the orthogonalized U^{ij} tensor.

Atom Label	x	y	z	U(eq)
C(1)	6907(5)	1686(5)	1562(4)	25(1)
C(2)	7010(6)	2953(5)	2576(4)	26(1)
C(3)	8298(6)	3014(6)	3706(4)	32(1)
C(4A)	11387(18)	3176(16)	4803(13)	50(3)
C(4B)	11123(18)	2910(15)	4912(13)	50(3)
C(5A)	11480(20)	1630(15)	4817(17)	51(3)
C(5B)	11150(20)	1348(15)	4844(17)	51(3)
C(6A)	12528(16)	1061(16)	4155(14)	43(2)
C(6B)	12057(16)	797(16)	4054(14)	43(2)
C(7)	13285(7)	-1367(6)	3061(5)	36(1)
C(8)	12804(6)	-2918(6)	2344(4)	31(1)
C(9)	11200(6)	-3247(7)	1489(5)	36(1)
C(10)	8989(6)	-2104(6)	60(5)	31(1)
C(11)	8641(5)	-1126(6)	1044(4)	28(1)
C(12)	6985(5)	-1149(6)	723(4)	28(1)
C(13)	13893(6)	-3158(6)	1657(4)	28(1)
C(14)	12858(7)	-3974(6)	3151(4)	36(1)
C(15)	5558(6)	2780(6)	2876(4)	31(1)
C(16)	7259(6)	4356(6)	2175(4)	33(1)
O(1)	13567(4)	-4589(4)	947(3)	33(1)
O(2)	14286(6)	-3748(5)	4031(3)	49(1)
O(3)	5545(5)	3991(5)	3759(3)	43(1)
O(4)	6080(5)	4385(5)	1138(3)	44(1)
S(1)	6456(2)	-55(2)	1862(1)	33(1)
S(2A)	10103(7)	3434(12)	3484(10)	36(1)
S(2B)	10130(7)	3232(12)	3512(10)	36(1)
S(3A)	12440(4)	-809(5)	4192(3)	33(1)
S(3B)	12040(4)	-1068(5)	3948(3)	33(1)
S(4)	10940(2)	-2169(2)	391(1)	48(1)

Table S7: Crystal data and structure refinement of complex [(*tr*MCL-3)Cu(I)]PF_6•EtOH (**16**)

Empirical formula	$C_{18}H_{38}CuF_6O_5PS_4$	
Formula weight	671.26	
Temperature	110(2)	
Wavelength	0.71073 Å	
Crystal system	Triclinic	
Space group	P -1	
Unit cell dimensions	a = 13.4862(5) Å	α = 71.5710(10)°
	b = 13.6947(4) Å	β = 77.6760(10)°
	c = 15.8096(5) Å	γ = 78.8850(10)°
Volume	2681.45(15) $Å^3$	
Z	4	
Density (calculated)	1.663 g/cm^3	
Absorption coefficient	1.256 mm^{-1}	
F(000)	1392	
Crystal size	0.712 x 0.356 x 0.184 mm	
Theta range for data collection	1.376 to 40.718°	
Index ranges	-24<=h<=24, -24<=k<=25, -28<=l<=28	
Reflections collected	110771	
Independent reflections	33773 [R(int) = 0.1632]	
Completeness to theta = 35.0°	99.5 %	
Absorption correction	semi-empirical from equivalents	
Max. and min. transmission	0.9848 and 0.6912	
Refinement method	Full-matrix least-squares on F^2	
Data / restraints / parameters	33773 / 253 / 683	
Goodness-of-fit on F^2	1.022	
Final R indices [I>2sigma(I)]	R1 = 0.0374, wR2 = 0.0959	
R indices (all data)	R1 = 0.0454, wR2 = 0.1019	
Extinction coefficient	n/a	
Largest diff. peak and hole	1.974 and –0.883 $e.Å^{-3}$	

Table S8: Atomic coordinates (x 10^4) and equivalent isotropic displacement parameters ($Å^2$x 10^3) for complex [(*tr*MCL-3)Cu(I)]PF_6•EtOH (**16**). U(eq) is defined as one third of the trace of the orthogonalized U^{ij} tensor.

Atom Label	x	y	z	U(eq)
Cu(1)	1094(1)	3816(1)	8647(1)	13(1)
Cu(2)	3702(1)	1419(1)	6433(1)	15(1)
S(1)	1085(1)	2729(1)	7834(1)	14(1)
S(2)	-264(1)	5059(1)	8388(1)	13(1)
S(3)	2503(1)	4658(1)	8372(1)	13(1)
S(4)	1217(1)	2881(1)	10129(1)	13(1)
S(5)	4998(1)	78(1)	6650(1)	15(1)
S(6)	3826(1)	2410(1)	7298(1)	16(1)
S(7)	3659(1)	2458(1)	4949(1)	16(1)
S(8)	2274(1)	642(1)	6583(1)	14(1)
C(1)	-185(1)	3017(1)	7519(1)	15(1)
C(2)	-538(1)	4154(1)	7023(1)	13(1)
C(3)	-1029(1)	4822(1)	7669(1)	15(1)
C(4)	235(1)	6259(1)	7688(1)	18(1)
C(5)	1041(1)	6506(1)	8114(1)	18(1)
C(6)	2142(1)	6035(1)	7844(1)	18(1)
C(7)	2553(1)	4682(1)	9506(1)	14(1)
C(8)	3051(1)	3641(1)	10076(1)	12(1)
C(9)	2603(1)	2686(1)	10081(1)	14(1)
C(10)	1051(1)	1566(1)	10190(1)	17(1)
C(11)	1571(1)	1154(1)	9389(1)	18(1)
C(12)	958(1)	1433(1)	8619(1)	19(1)
C(13)	2892(1)	3754(1)	11039(1)	15(1)
C(14)	4196(1)	3436(1)	9706(1)	14(1)
C(15)	315(1)	4649(1)	6300(1)	15(1)
C(16)	-1425(1)	4112(1)	6564(1)	18(1)
C(17)	5834(1)	240(1)	7347(1)	15(1)
C(18)	5434(1)	892(1)	8017(1)	13(1)
C(19)	5129(1)	2052(1)	7541(1)	15(1)
C(20)	4040(1)	3696(1)	6495(1)	16(1)

Table S8 continued

C(20')	3789(2)	3748(2)	6618(2)	16(1)
C(21)	3292(1)	4053(1)	5803(1)	17(1)
C(21')	4266(2)	3912(2)	5647(2)	22(1)
C(22)	3611(1)	3800(1)	4983(1)	19(1)
C(22')	3807(2)	3745(2)	4908(2)	19(1)
C(23)	2308(1)	2558(1)	4877(1)	15(1)
C(24)	2017(1)	1577(1)	4771(1)	13(1)
C(25)	2423(1)	556(1)	5436(1)	15(1)
C(26)	2529(1)	-733(1)	7188(1)	20(1)
C(27)	3601(1)	-1302(1)	6975(1)	19(1)
C(28)	4431(1)	-1070(1)	7381(1)	21(1)
C(29)	2482(1)	1444(1)	3831(1)	15(1)
C(30)	841(1)	1734(1)	4902(1)	17(1)
C(31)	4578(1)	423(1)	8755(1)	14(1)
C(32)	6360(1)	895(1)	8453(1)	16(1)
C(33)	9315(1)	-596(1)	7383(1)	24(1)
C(34)	9255(1)	515(1)	7377(1)	29(1)
C(35)	4924(1)	4234(1)	2494(1)	23(1)
C(36)	4039(1)	5090(1)	2513(1)	33(1)
F(1A)	7916(4)	3586(4)	4427(4)	44(1)
F(1B)	8126(2)	3337(2)	4415(2)	44(1)
F(2A)	6240(3)	2046(3)	5349(3)	45(1)
F(2B)	6530(2)	1708(1)	5316(1)	45(1)
F(3A)	7588(5)	2136(4)	4186(3)	38(1)
F(3B)	7685(2)	2063(2)	4015(1)	38(1)
F(4A)	6607(3)	3462(4)	5578(2)	49(1)
F(4B)	7010(1)	2978(2)	5724(1)	49(1)
F(5A)	6350(4)	3519(5)	4187(4)	44(1)
F(5B)	6482(2)	3331(2)	4353(2)	44(1)
F(6A)	7819(3)	2104(4)	5572(3)	64(1)
F(6B)	8187(2)	1714(2)	5377(1)	64(1)
F(7A)	1461(1)	-3065(1)	10313(1)	28(1)
F(7B)	1647(5)	-3214(6)	10391(6)	28(1)

Table S8 continued

F(8A)	3389(2)	-1804(2)	9710(2)	41(1)
F(8B)	3225(8)	-1566(8)	9657(10)	41(1)
F(9A)	1681(1)	-1380(1)	9590(2)	50(1)
F(9B)	1563(5)	-1505(4)	10081(6)	50(1)
F(10A)	2652(1)	-2649(1)	9041(1)	34(1)
F(10B)	2371(5)	-2342(5)	9059(3)	34(1)
F(11A)	2195(2)	-2187(2)	10956(1)	57(1)
F(11B)	2499(7)	-2597(8)	11094(4)	57(1)
F(12A)	3153(1)	-3494(1)	10387(1)	46(1)
F(12B)	3304(5)	-3428(5)	10044(5)	46(1)
O(1)	3477(1)	2942(1)	11629(1)	17(1)
O(2)	4700(1)	4256(1)	9722(1)	18(1)
O(3)	-107(1)	5647(1)	5809(1)	20(1)
O(4)	-1039(1)	3587(1)	5885(1)	22(1)
O(5)	2074(1)	2265(1)	3122(1)	18(1)
O(6)	515(1)	852(1)	4807(1)	26(1)
O(7)	4291(1)	1027(1)	9375(1)	18(1)
O(8)	6796(1)	-118(1)	8910(1)	18(1)
O(9)	8324(1)	-927(1)	7745(1)	21(1)
O(10)	5054(1)	3866(1)	1720(1)	21(1)
P(1A)	7092(1)	2798(1)	4873(1)	22(1)
P(1B)	7332(1)	2511(1)	4869(1)	22(1)
P(2A)	2414(1)	-2417(1)	9998(1)	19(1)
P(2B)	2475(4)	-2429(4)	10060(3)	19(1)

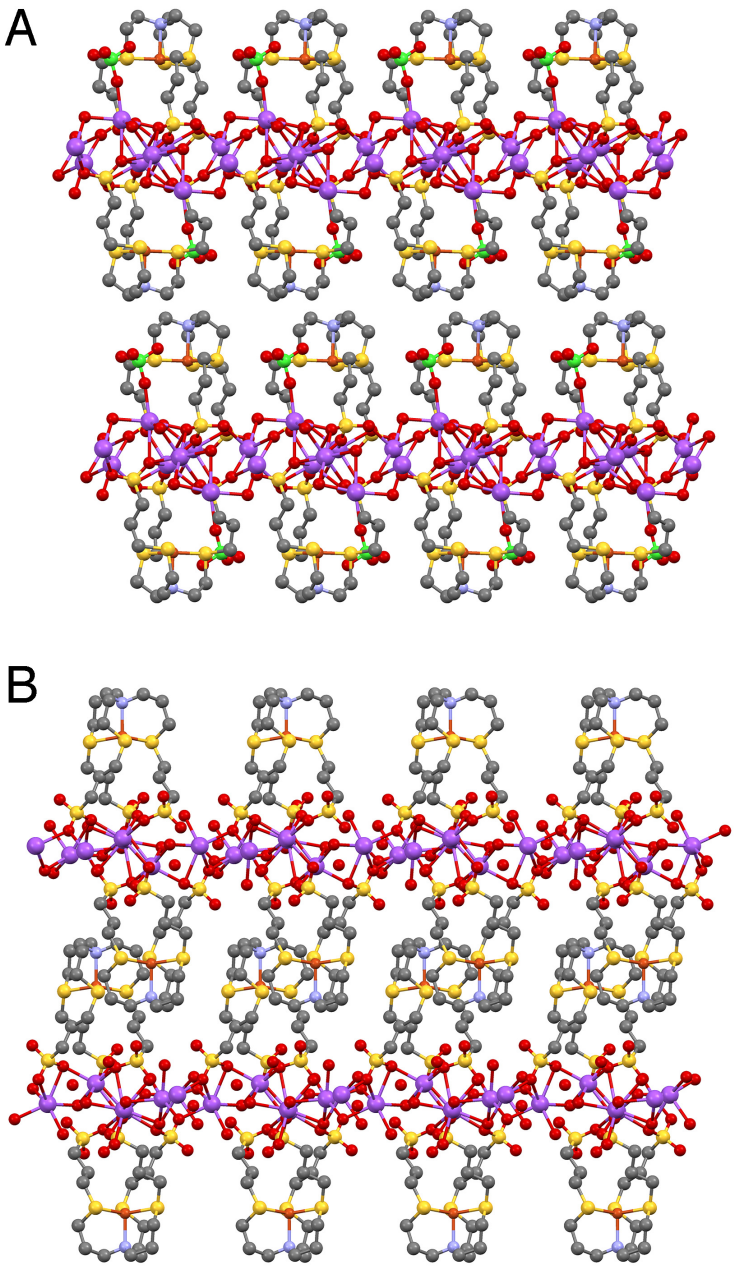

Figure S1: Packing diagram for the x-ray crystal structures of $[Cu(I)\text{-}(MCL\text{-}1)]_2Na_7(ClO_4)_3(H_2O)_3$ **13a** (A) and $[Cu(I)\text{-}(MCL\text{-}2)]_2Na_6(PF_6)_2(H_2O)_{15}$ **14a** (B) illustrating the layered arrangement between the Cu(I) complexes and the sodium counter ions (purple). Both diagrams represent the view along the crystallographic *a* axis.

3. Determination of Protonation Constants

3.1 Mixed-Mode Protonation Constants

The protonation constants listed in Table 3 refer to solution equilibria in which all species are expressed in terms of molar concentrations rather than activities. To convert the concentration-based protonation constants to mixed-mode protonation constants, for which the hydronium ions are expressed in terms of their activities, the tabulated values must be corrected upward by 0.11 as recommended by Martell and Smith.[7] This correction factor can be derived as outlined in the following section.

The activity a_x of a species X is related to its concentration according to equation (1),

$$a_x = \gamma_x \frac{[X]}{[X]_0} \tag{1}$$

where [X] is the molar concentration of species X, $[X]_0$ is the standard concentration (typically 1M), and γ_x is the unitless activity coefficient of species X. The activity coefficient can be estimated based on the extended Debye-Hückel equation (2),[8]

$$-\log \gamma_x = \frac{A z_x^2 \sqrt{I}}{1 + B\alpha_x \sqrt{I}} \tag{2}$$

where z_x is the charge of the species X, α_x is the effective diameter of the hydrated ion X in units of Å, I is the ionic strength of the solution, and A and B are constants that depend on the temperature and dielectric constant of the solvent. In aqueous solution, A and B adopt the values 0.511 and 0.329, respectively.[9] Because the Debye-Hückel theory is strictly valid only for fully dissociated electrolytes, a condition that can only be achieved at infinite dilution, Davies proposed equation (3) for the estimation of the mean ionic activity coefficient of an electrolyte in water at 25°C,[10]

$$-\log \gamma_x = A z_x^2 \left(\frac{\sqrt{I}}{1 + \sqrt{I}} - 0.2I \right) \tag{3}$$

Based on this empirical model, the activity coefficient of the hydronium ion at an ionic strength of 0.1 is $-\log \gamma_x = 0.11$.

For a ligand with N protonation sites, the n^{th} mixed-mode equilibrium constant, K^m_{Hn} (with n = 1,2,3,…N) is defined by

$$K^m_{Hn} = \frac{[H_nL]}{[H_{n-1}L]a_{H_3O^+}} \tag{4}$$

or

$$\log K^m_{Hn} = \log \frac{[H_nL]}{[H_{n-1}L]} - \log a_{H_3O^+} \tag{5}$$

After replacing the hydronium ion activity with the corresponding activity coefficient and concentration according to equation (1), we obtain

$$\log K^m_{Hn} = \log\left(\frac{[H_nL]}{[H_{n-1}L][H_3O^+]}\right) - \log\left(\gamma_{H_3O^+}\right) \tag{6}$$

and hence

$$\log K^m_{Hn} = \log K_{Hn} + 0.11 \tag{7}$$

3.2 Glass Electrode Calibration

All protonation constants were determined as concentration constants ($\log K_H$) based on potentiometric titrations using a combination glass electrode with double junction. The glass electrode was calibrated at 25°C by titration of a strong acid (5 mM HCl, prepared by dilution of a 0.1 M standardized solution, Aldrich) with a strong base (0.1 M KOH, standardized solution, Aldrich) in the presence of 0.1 M KCl as ionic background using a water-jacketed temperature controlled titration vessel (Metrohm). From the experimental emf data, the endpoint, electrode potential and slope were determined using Gran's method as implemented in the GLEE software package (pK_w = 13.78, 0.1 M KCl).[11] The calibration procedure was performed prior to each potentiometric titration, and the experimental electrode potential and slope were derived as the average of the data from three independent titrations.

3.3 Potentiometric Titrations

A 1-5 mM solution of the ligand in 0.1 M KCl was titrated by stepwise addition (motorized burette) of a standardized solution of 0.1 M KOH (Aldrich) using a water-jacketed temperature controlled titration vessel. After addition of each aliquot, the solution was allowed to equilibrate until the electrode potential remained stable. The protonation constants ($\log K_{Hn}$) were determined from the emf data based on non-linear least-square fitting using the Hyperquad software package.[12] In the case of PEMEA and BCA, the protonation constants were derived from spectrophotometric titrations at 25°C. The solution p[H] was directly measured in the UV-vis cuvette using a calibrated combination glass microelectrode with a tip diameter of 6 mm (Microelectrodes Inc., New Hampshire). The UV-vis spectra were analyzed over the entire spectral range by non-linear least squares fitting using the SPECFIT software package.[13]

3.4 Potentiometric Titration Data

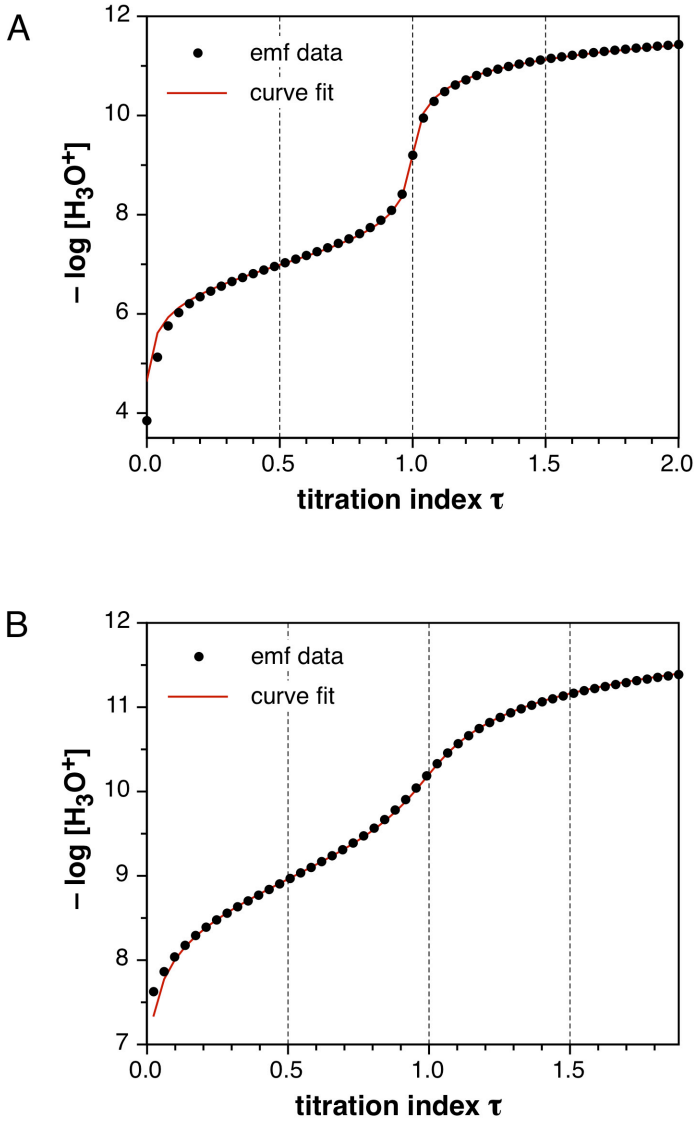

Figure S2: Potentiometric titration curves for (A) MCL-1 and (B) MCL-2 in 0.1 M KCl at 25°C (titration index τ = [KOH]/$[L]_{total}$). Each ligand (5 mM) was first protonated by addition of a stoichiometric amount of aq. HCl and then titrated with a standardized solution of 0.1 M KOH. The emf data were analyzed by non-linear least-square fitting using the Hyperquad software package,[12] to yield the logK_{H1} values of 7.00 ± 0.02 (MCL-1) and 8.98 ± 0.01 (MCL-2).

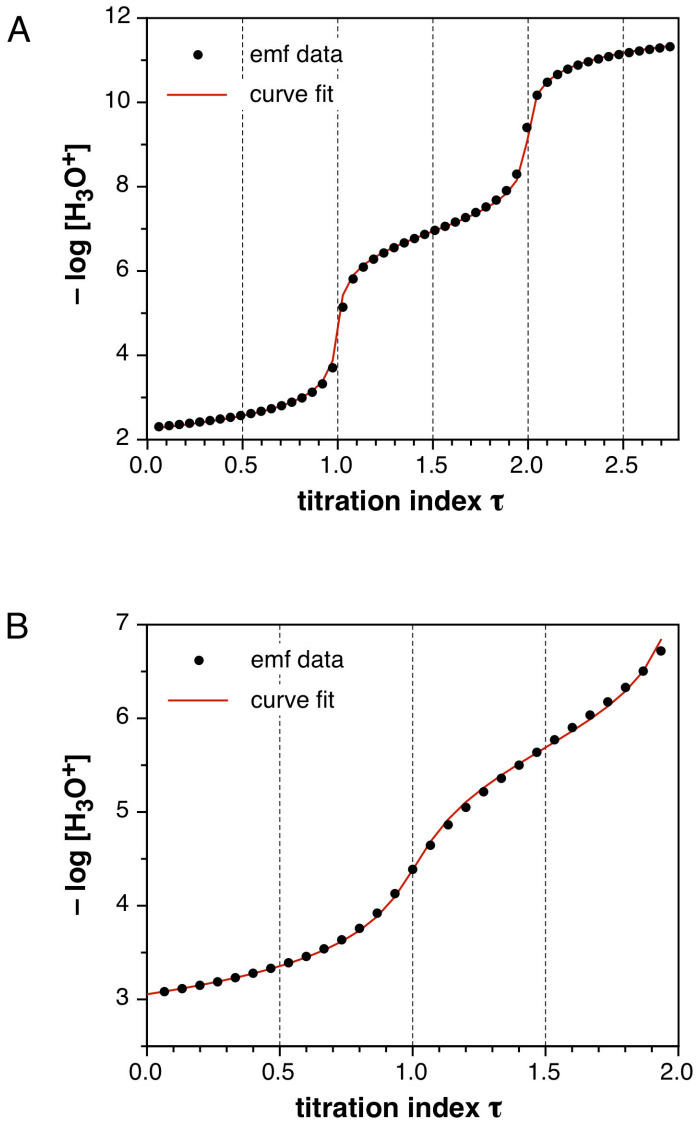

Figure S3: Potentiometric titration curves for (A) DHEAMP (**17**) and (B) BCS in 0.1 M KCl at 25°C (titration index $\tau = [KOH]/[L]_{total}$). The ligands (5 mM for DHEAMP•2HCl and 1 mM for BCS) were titrated with a standardized solution of 0.1 M KOH. In the case of BCS, a stoichiometric amount of aq. HCl was added to protonate the ligand before the titration. The emf data were analyzed by non-linear least-square fitting using the Hyperquad software package,[12] to yield the logK_{H1} values of 6.94 ± 0.01 (DHEAMP) and 5.70 ± 0.02 (BCS).

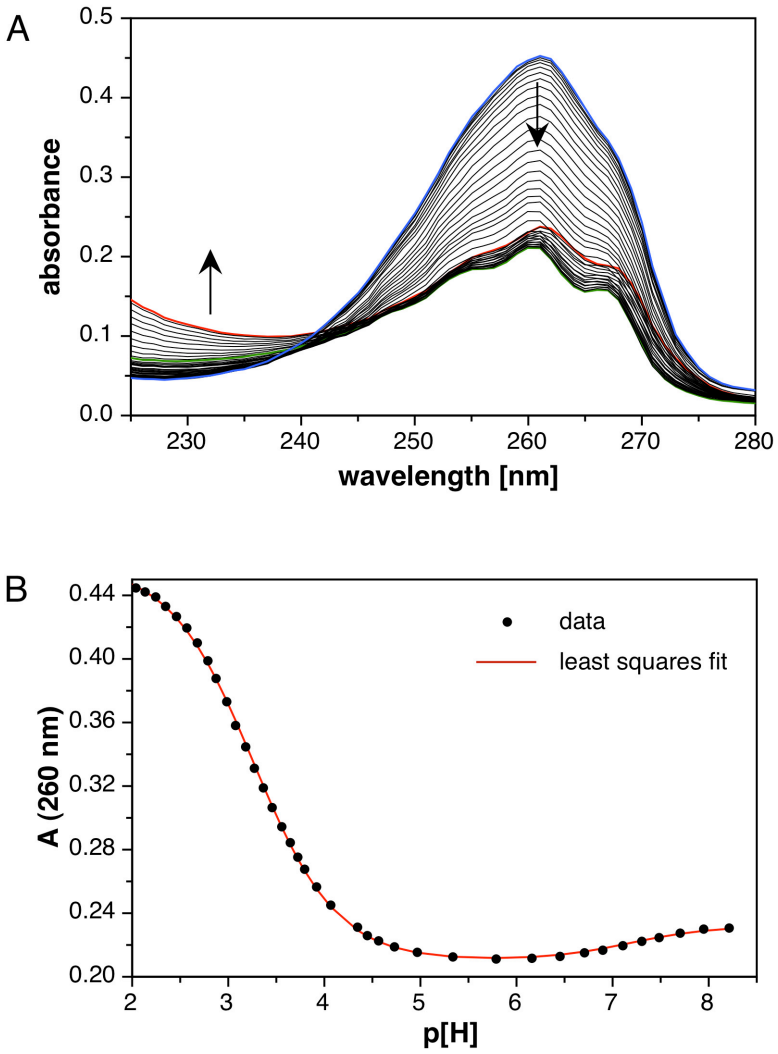

Figure S4: UV-vis spectrophotometric titration to determine the protonation constant of PEMEA. A 50 µM solution of PEMEA in 0.1 M KCl was acidified with aq. HCl to p[H] 1.9 (blue trace) and then titrated by stepwise addition of KOH until p[H] 8.2 was reached (red trace). The green trace corresponds to a p[H] of 5.9. Non-linear least squares fitting of the absorption spectra (A) yielded the protonation constants logK_{H1} of 7.24 ± 0.04 and 3.23 ± 0.04, respectively. Figure B shows the absorbance change and corresponding fit at 260 nm.

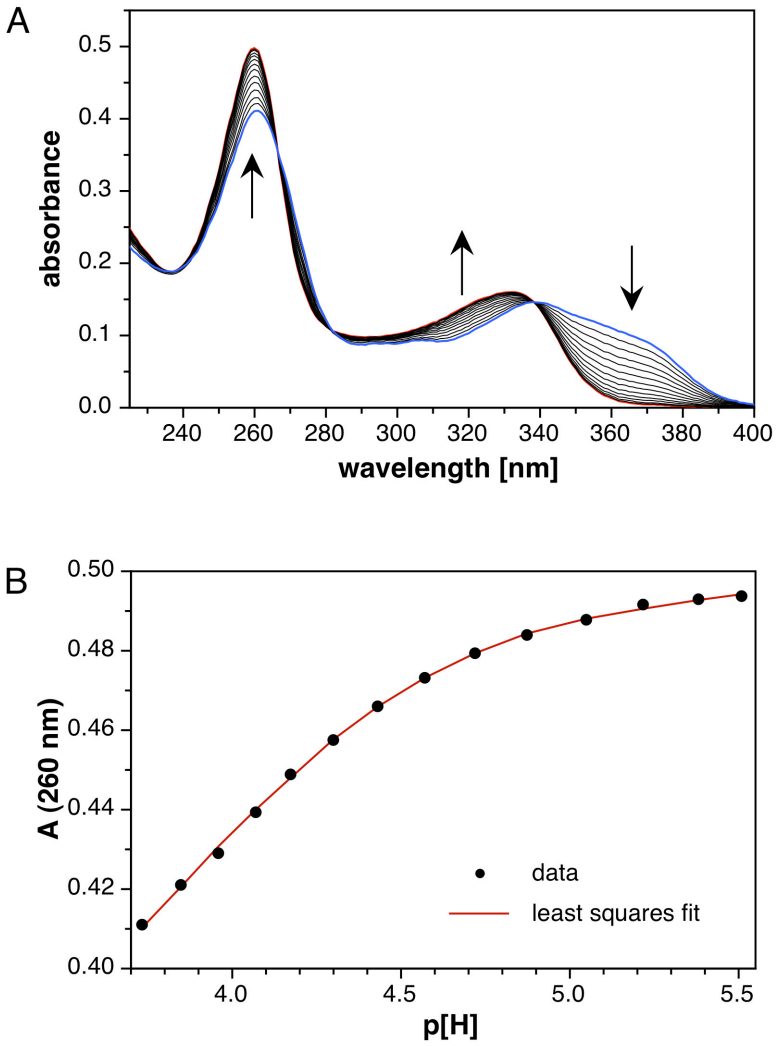

Figure S5: UV-vis spectrophotometric titration to determine the protonation constant of bicinchoninic acid (BCA). A 10 µM solution of BCA in 0.1 M KCl was acidified with aq. HCl to pH 3.7 (blue trace) and then titrated by stepwise addition of KOH until pH 5.5 was reached (red trace). Non-linear least squares fitting of the absorption spectra (A) yielded the protonation constant logK_{H1} of 3.80 ± 0.02. Figure B shows the absorbance change and corresponding fit at 260 nm.

4. Determination of Cu(I) Stability Constants Based on the Nernst Relationship

In cases where the ligand-bound Cu(II/I) couple shows a reversible or quasi-reversible redox reaction, the Cu(I) complex stability constant can be calculated based on the Nernst relationship (8)[14]

$$E^f = E^\circ_{aq} - 2.303\frac{RT}{nF}\log\left(\frac{K_{\mathrm{Cu(II)L}}}{K_{\mathrm{Cu(I)L}}}\right) \qquad (8)$$

where E^f is the formal potential of ligand bound Cu(II/I) couple, E°_{aq} is the reduction potential of the aqueous Cu(II/I) couple expressed in terms of concentrations, F is the Faraday constant, R is universal gas constant, and T is the temperature in units of Kelvin. In practice, the stability constant $K_{\mathrm{Cu(II)/L}}$ and the formal potential E^f are determined in the presence of a background electrolyte to keep the ionic strength constant at a value of I = 0.1; however, according to IUPAC convention[15] the standard reduction potential is defined at I = 0. To take into account the difference in ionic strength, the standard reduction potential of the aqueous Cu(II/I) redox couple ($E°$ = 0.153 V)[16] was adjusted to E°_{aq} = 0.13 V as recommended by Rorabacher and coworkers.[17]

4.1. Cyclic Voltammetry

The formal potentials of the ligand-bound Cu(II/I) couples were determined by slow-scan cyclic voltammetry in buffered solution at a pH of 5.0 (10 mM PIPBS, 0.1 M $KClO_4$) using a CH-Instruments potentiostat (model 600A). The corresponding Cu(II) complexes were formed in situ by addition of excess Cu(II)SO_4 (1 mM) to a 150 μM solution of the ligand. At pH 5, the formation of species arising from Cu(II)-induced hydrolysis is negligible. All measurements were carried out under an atmosphere of argon in a single compartment cell with a glassy carbon working electrode, a Pt counter electrode, and an aqueous Ag/AgCl reference electrode (1 M KCl). The half-wave potentials ($E_{1/2}$) were referenced to ferrocenium (0.40 vs. SHE)[16,18] or ferroin (1.112 vs. SHE)[5,19] as external standards. Measurements were typically performed with a scan rate of 20 - 50 mV/s.

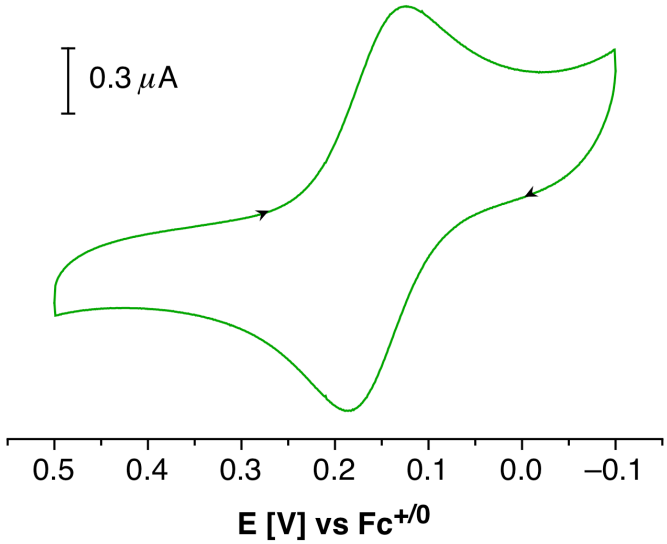

Figure S6: Cyclic voltammogram for a solution of 150 μM PEMEA (**4**) containing 1 mM Cu(II)SO_4 in pH 5.0 buffer (10 mM PIPBS, 0.1 M $KClO_4$, glassy carbon working electrode, Pt counter electrode, aqueous Ag/AgCl/1M KCl reference electrode, scan rate 20 mV/s, direction indicated by black arrows). The voltammogram was referenced against the external $Fc^{+/0}$ potential measured under the same conditions.

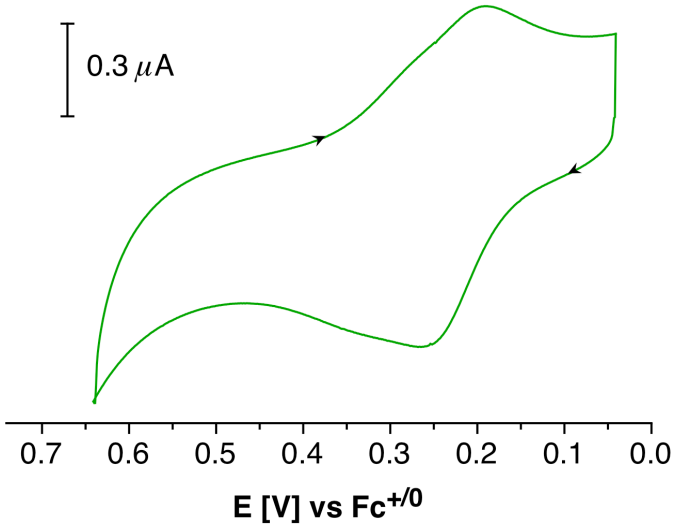

Figure S7: Cyclic voltammogram for a solution of 150 μM bathocuproine disulfonate (BCS, **5**) containing 50 μM [Cu(I)$(CH_3CN)_4$]PF_6 in pH 5.0 buffer (10 mM PIPBS, 0.1 M $KClO_4$, glassy carbon working electrode, Pt counter electrode, aqueous Ag/AgCl/1M KCl reference electrode, scan rate 50 mV/s, direction indicated by black arrows). The voltammogram was referenced against the external $Fc^{+/0}$ potential measured under the same conditions.

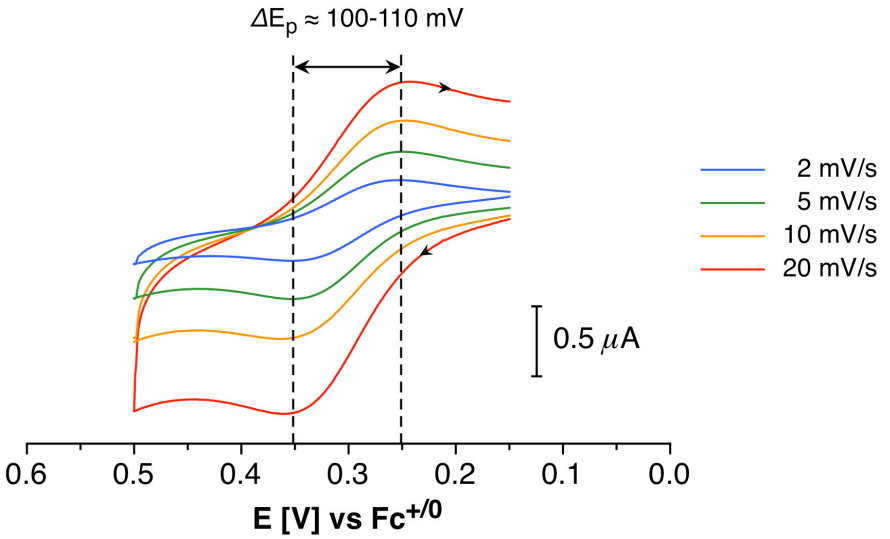

Figure S8: Cyclic voltammograms at varying scan rates for a solution of 150 μM MCL-3 (**3**) in the presence of $CuSO_4$ (1 mM) at pH 5.0 (10 mM PIPBS, 0.1 M $KClO_4$, glassy carbon working electrode, Pt counter electrode, aqueous Ag/AgCl/1M KCl reference electrode, scan direction indicated by black arrows). Each voltammogram was referenced against the external $Fc^{+/0}$ potential measured under the same conditions. With increasing scan rates the peak potential separations increased from 100 mV (2 mV/s) to 110 mV (20 mV/s).

4.2. Determination of Cu(II) Stability Constants

All Cu(II) stability constants were determined as mixed mode constants based on spectrophotometric titrations. As for the cyclic voltammetry measurements, the titrations were conducted under mildly acidic conditions to avoid Cu(II)-induced hydrolysis. The solution pH was precisely adjusted with a pH combination glass electrode, which was calibrated based on commercially available buffer solutions (Fisher). In a typical experiment, a 50-100 μM solution of the ligand in pH 5.0 buffer (10 mM PIPBS, 0.1 M $KClO_4$, 25°C) was titrated in a quartz cuvette with 1 cm pathlength with Cu(II)SO_4 supplied from a 25-50 mM stock solution in water. After addition of each aliquot, the solution was allowed to equilibrate until the UV-vis traces showed no further changes. The corresponding stability constants were obtained from the titration data by non-linear least-squares fitting over the entire spectral range using the SPECFIT software package.[13] Although the titrations were conducted at pH 5.0, we directly determined the pH-independent mixed mode stability constants ($\log\beta_n$) by including the corresponding protonation constant(s) in the equilibrium definition of the non-linear least squares fitting procedure.

Because the solution pH reflects the proton activity, the experimental protonation constants $\log K_H$ were adjusted upward by 0.11 for this purpose (see also section 3.1). In the case of BCS, the Cu(II) stability constant ($\log \beta_2$) was too high to be obtained from a direct molar-ratio titration. For this reason, we used DHEAMP[20] (**17**) as a competitor ligand for the Cu(II) titration of BCS, and also determined the Cu(II) stability constant of DHEAMP under the same conditions.

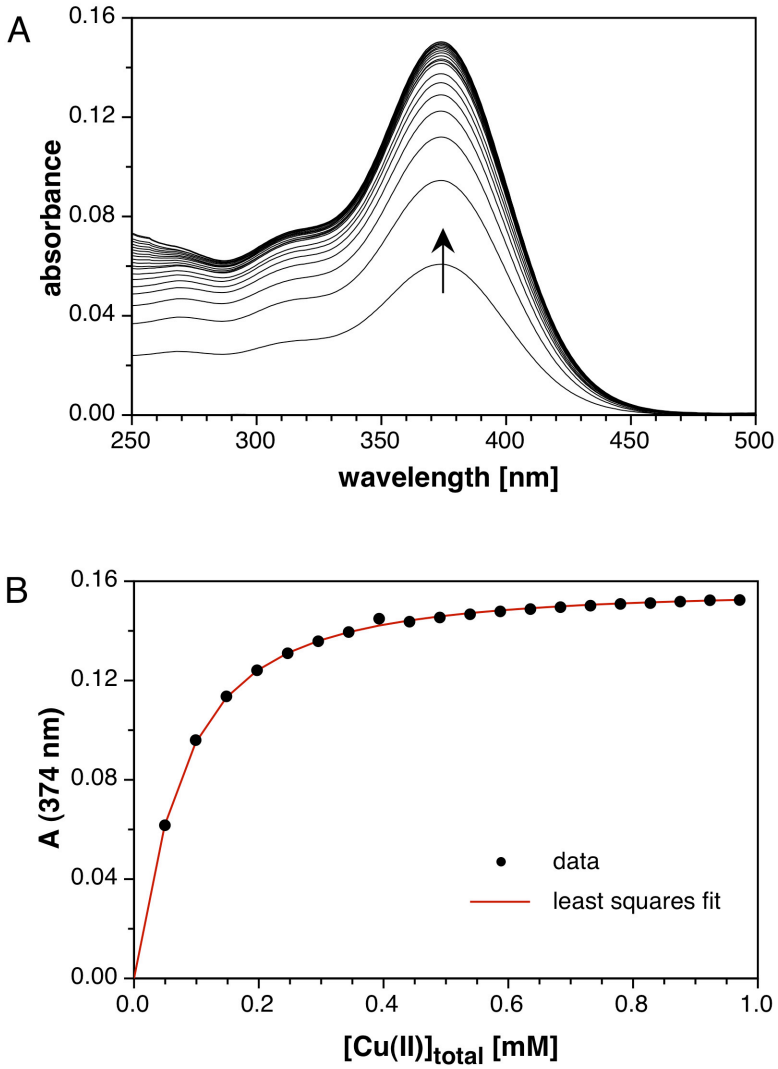

Equilibrium System Definition:

Species	Cu(II)	MCL-1	H	logβ
Cu(II)	1	0	0	0.0
MCL-1	0	1	0	0.0
(MCL-1)H	0	1	1	7.11
Cu(II)(MCL-1)	1	1	0	*6.42 ± 0.02*

Figure S9: Spectrophotometric determination of the Cu(II) stability constant of MCL-1 (**1**). A solution of MCL-1 (50 µM) was titrated with Cu(II)SO_4 at a constant pH of 5.0 (10 mM PIPBS, 0.1 M $KClO_4$, 25°C). The UV-vis traces (A) were analyzed by non-linear least squares fitting over the spectral range of 300-450 nm to yield an average log$K_{Cu(II)L}$ of 6.42 ± 0.02 (n = 3). Figure B shows the absorbance change and corresponding fit at 374 nm.

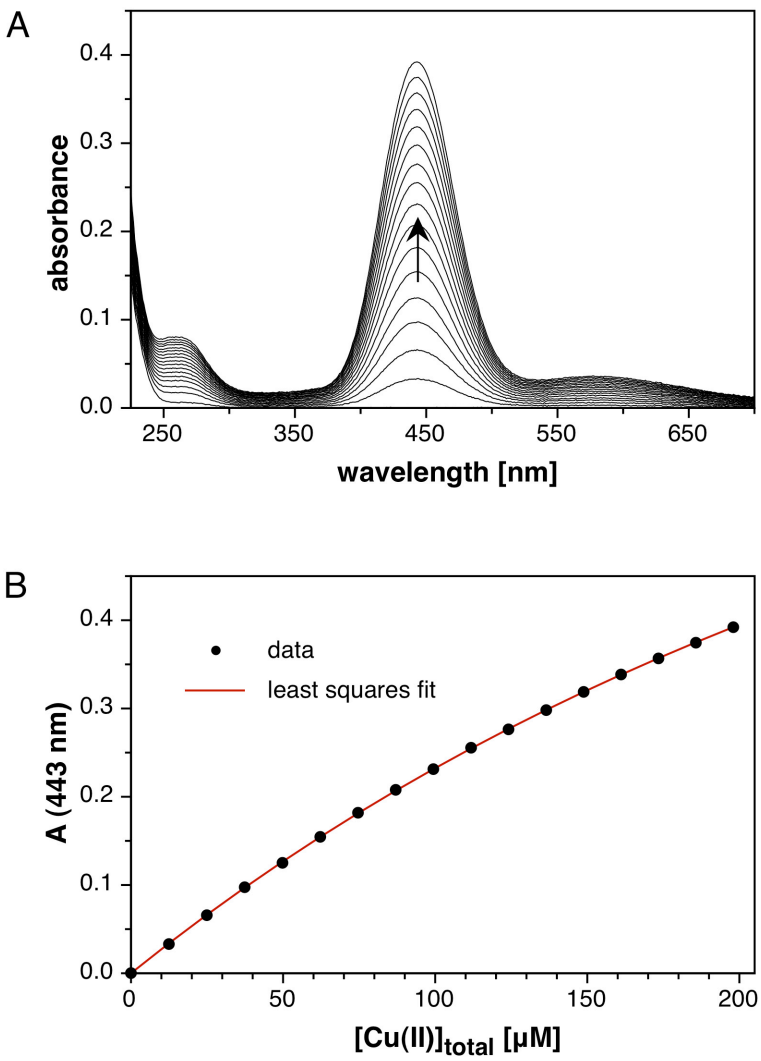

Equilibrium System Definition:

Species	Cu(II)	MCL-3	H	logβ
Cu(II)	1	0	0	0.0
MCL-3	0	1	0	0.0
Cu(II)(MCL-3)	1	1	0	*3.47 ± 0.04*

Figure S10: Spectrophotometric determination of the Cu(II) stability constant of MCL-3 (**3**). A solution of MCL-3 (100 µM) was titrated with Cu(II)SO_4 at a constant pH of 5.0 (10 mM PIPBS, 0.1 M $KClO_4$, 25°C). The UV-vis traces (plot A) were analyzed by non-linear least squares fitting over the spectral range of 300-700 nm to yield an average log$K_{Cu(II)L}$ of 3.47 ± 0.04 (n = 3). Figure B shows the absorbance change and corresponding fit at 443 nm.

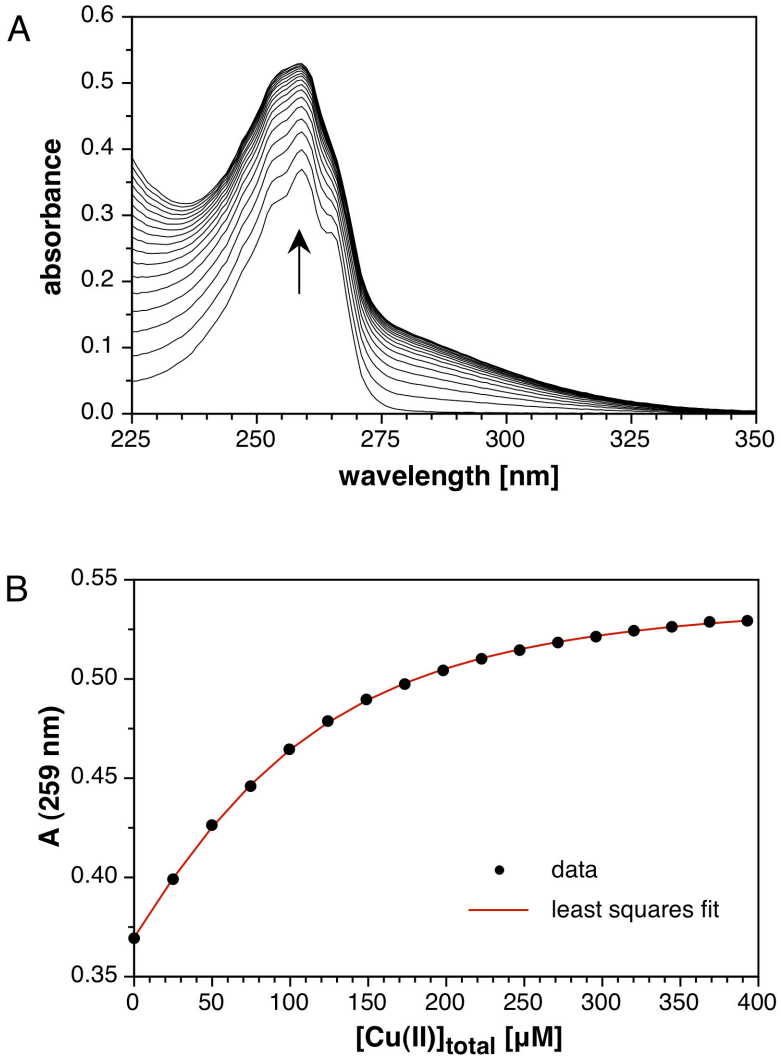

Equilibrium System Definition:

Species	Cu(II)	DHEAMP	H	logβ
Cu(II)	1	0	0	0.0
DHEAMP	0	1	0	0.0
(DHEAMP)H	0	1	1	7.05
Cu(II)(DHEAMP)	1	1	0	*9.21 ± 0.02*

Figure S11: Spectrophotometric determination of the Cu(II) stability constant of DHEAMP[20] (**17**). A solution of DHEAMP (100 µM) was titrated with Cu(II)SO_4 at a constant pH of 2.11 (10 mM $HClO_4$, 0.1 M $KClO_4$, 25°C). The UV-vis traces (A) were analyzed by non-linear least squares fitting over the entire spectral range to yield an average log$K_{Cu(II)L}$ of 9.21 ± 0.02 (n = 3). Figure B shows the absorbance change and corresponding fit at 259 nm.

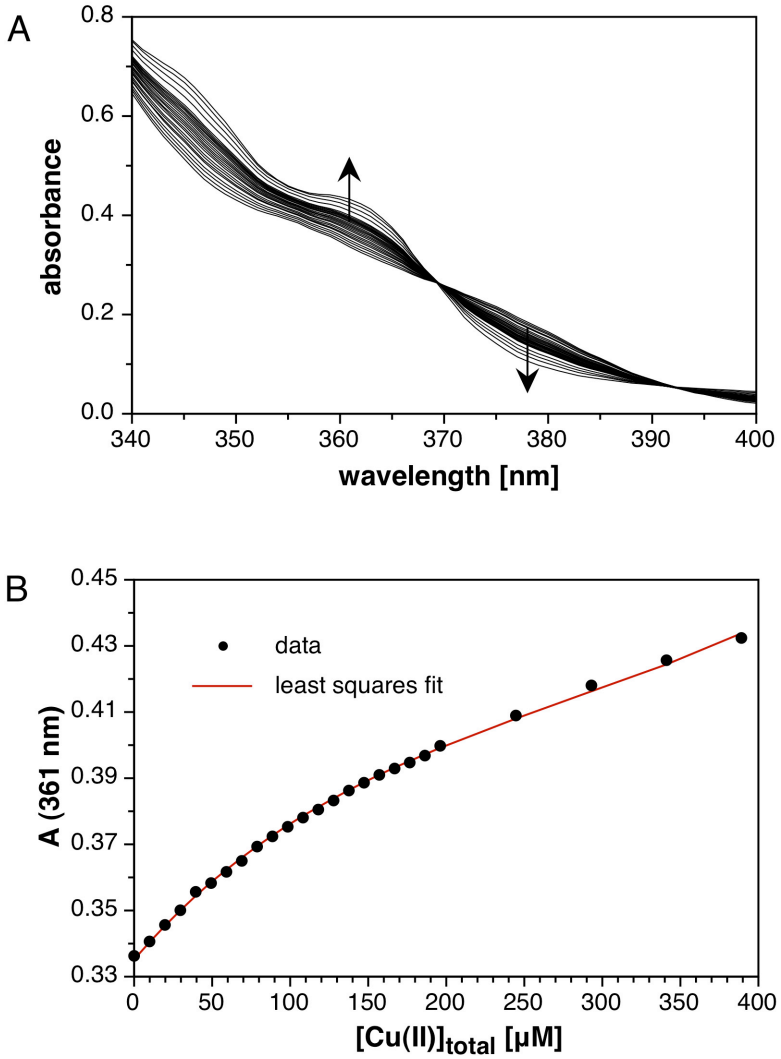

Equilibrium System Definition:

Species	Cu(II)	DHEAMP	BCS	H	logβ
Cu(II)	1	0	0	0	0.0
DHEAMP	0	1	0	0	0.0
BCS	0	0	1	0	0.0
(DHEAMP)H	0	1	0	1	7.05
(BCS)H	0	0	1	1	5.81
Cu(II)(DHEAMP)	1	1	0	0	9.21
Cu(II)$(BCS)_2$	1	0	2	0	*12.42 ± 0.07*

Figure S12: Spectrophotometric determination of the Cu(II) stability constant of bathocuproine disulfonate (BCS, **5**) by competition with DHEAMP[20] (**17**). A solution of BCS (300 µM) was titrated with Cu(II)SO_4 in the presence of DHEAMP (300 µM) at a constant pH of 6.0 (10 mM MES, 0.1 M $KClO_4$, 25°C). The UV-vis traces (A) were analyzed by non-linear least squares fitting over the entire spectral range to yield an average log$K_{Cu(II)L}$ of 12.42 ± 0.07 (n = 3). Figure B shows the absorbance change and corresponding fit at 361 nm.

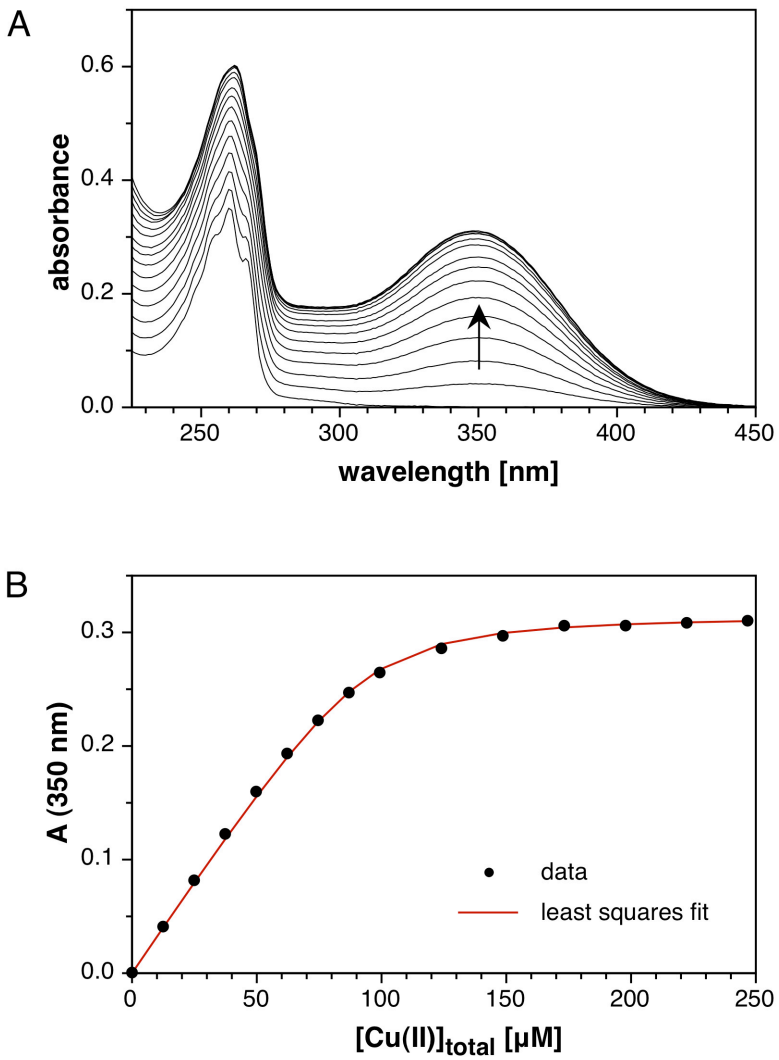

Equilibrium System Definition:

Species	Cu(II)	PEMEA	H	logβ
Cu(II)	1	0	0	0.0
PEMEA	0	1	0	0.0
(PEMEA)H	0	1	1	7.35
(PEMEA)H_2	0	1	2	10.69
Cu(II)(PEMEA)	1	1	0	*7.85 ± 0.08*

Figure S13: Spectrophotometric determination of the Cu(II) stability constant of PEMEA (**4**). A solution of PEMEA (96 µM) was titrated with Cu(II)SO_4 at a constant pH of 5.0 (10 mM PIPBS, 0.1 M $KClO_4$, 25°C). The UV-vis traces (A) were analyzed by non-linear least squares fitting over the spectral range of 300-450 nm to yield an average log$K_{Cu(II)L}$ of 7.85 ± 0.08 (n = 3). Figure B shows the absorbance change and corresponding fit at 350 nm.

5. UV-vis Absorption Spectra of the MCL-Ligands and their Cu(I) Complexes

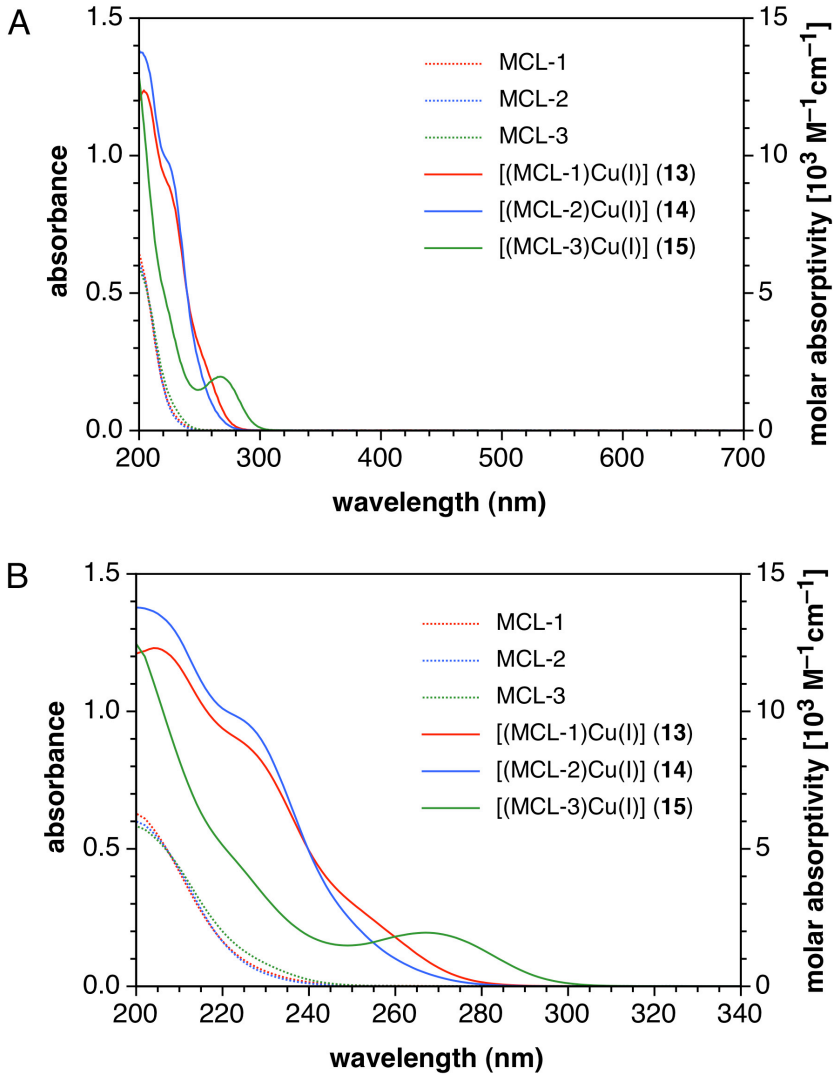

Figure S14: UV-vis absorption spectra of ligands MCL-1 (**1**), MCL-2 (**2**), MCL-3 (**3**), and the Cu(I) complexes [(MCL-1)Cu]Na_3PF_6 (**13**), [(MCL-2)Cu]Na_3PF_6 (**14**), [(MCL-3)Cu]Na_4PF_6 (**15**) in H_2O at 100 µM. A) Full UV-vis spectral range from 200-700 nm. B) UV range from 200-340 nm for the traces shown in graph (A).

6. Determination of Cu(I) Stability Constants Based on Competition Equilibria

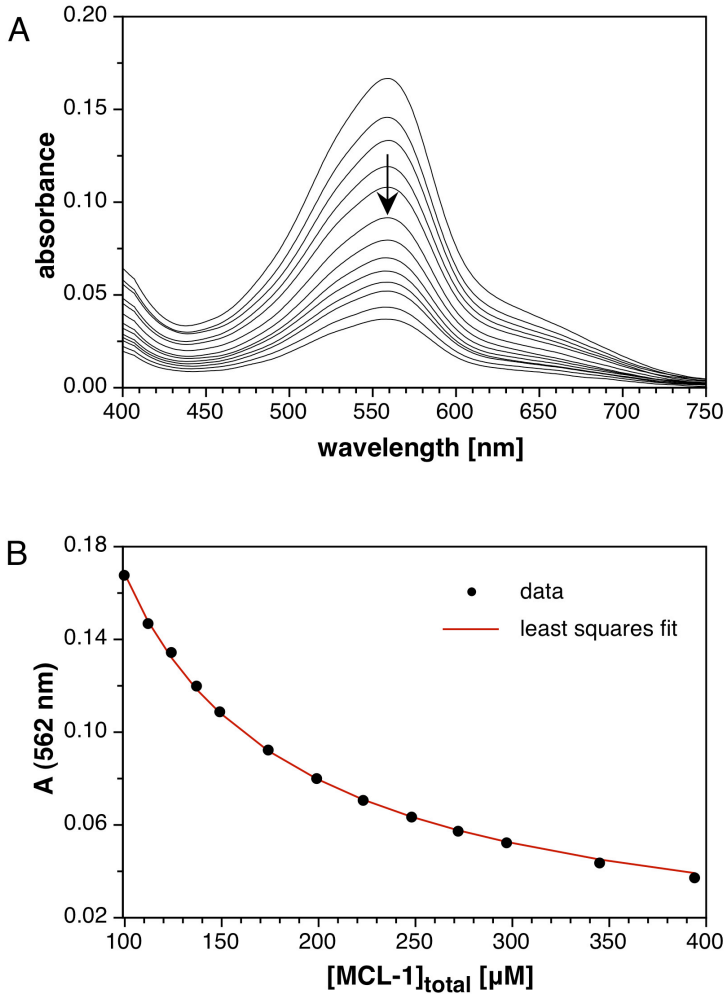

Equilibrium System Definition:

Species	Cu(I)	BCA	MCL-1	H	logβ
Cu(I)	1	0	0	0	0.0
BCA	0	1	0	0	0.0
MCL-1	0	0	1	0	0.0
(BCA)H	0	1	0	1	3.91
(MCL-1)H	0	0	1	1	7.11
Cu(I)(MCL-1)	1	0	1	0	16.33
Cu(I)$(BCA)_2$	1	2	0	0	*17.67 ± 0.03*

Figure S15: Spectrophotometric determination of the Cu(I) stability constant of 2,2'-bicinchoninic acid (BCA, **6**) via competition with MCL-1 (**1**). A solution of $[Na_3(MCL\text{-}1)Cu(I)]PF_6$ (**13**, 100 μM) and BCA (100 μM) was equilibrated at pH 5.0 (10 mM PIPBS, 0.1 M $KClO_4$, 25°C) and then titrated with MCL-1 to a final concentration of 0.4 mM. The UV-vis traces (A) were analyzed by non-linear least squares fitting over the spectral range of 450-700 nm to yield an average log$K_{Cu(I)L}$ of 17.67 ± 0.03 (n = 3). Figure B shows the absorbance change and corresponding fit at 562 nm.

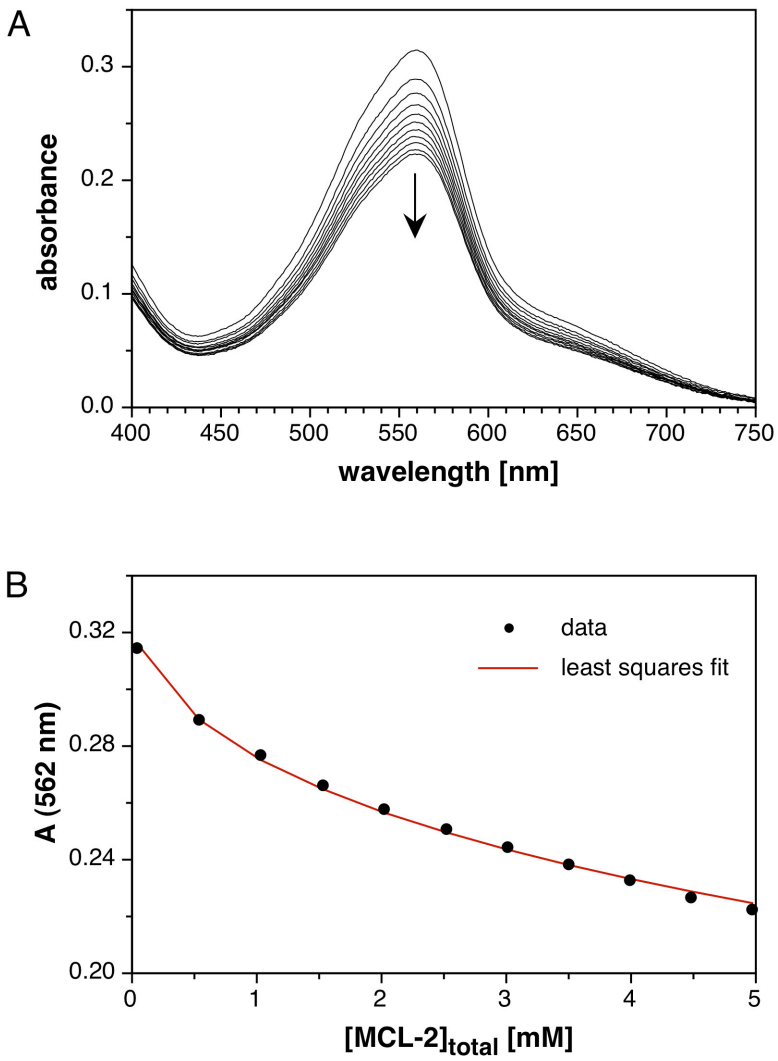

Equilibrium System Definition:

Species	Cu(I)	BCA	MCL-2	H	logβ
Cu(I)	1	0	0	0	0.0
BCA	0	1	0	0	0.0
MCL-2	0	0	1	0	0.0
(BCA)H	0	1	0	1	3.91
(MCL-2)H	0	0	1	1	9.09
Cu(I)$(BCA)_2$	1	2	0	0	17.67
Cu(I)(MCL-2)	1	0	1	0	*13.08 ± 0.13*

Figure S16: Spectrophotometric determination of the Cu(I) stability constant of MCL-2 (**2**) via competition with 2,2'-bicinchoninic acid (BCA, **6**). A solution of $[Na_3(MCL\text{-}2)Cu(I)]PF_6$ (**14**, 40 μM) and BCA (100 μM) was equilibrated at pH 7.0 (50 mM PIPES, 60 mM $KClO_4$, 25°C) and then titrated with MCL-2 to a final concentration of 5 mM. The UV-vis traces (A) were analyzed by non-linear least squares fitting over the spectral range of 450-700 nm to yield an average log$K_{Cu(I)L}$ of 13.08 ± 0.13 (n = 3). Figure B shows the absorbance change and corresponding fit at 562 nm.

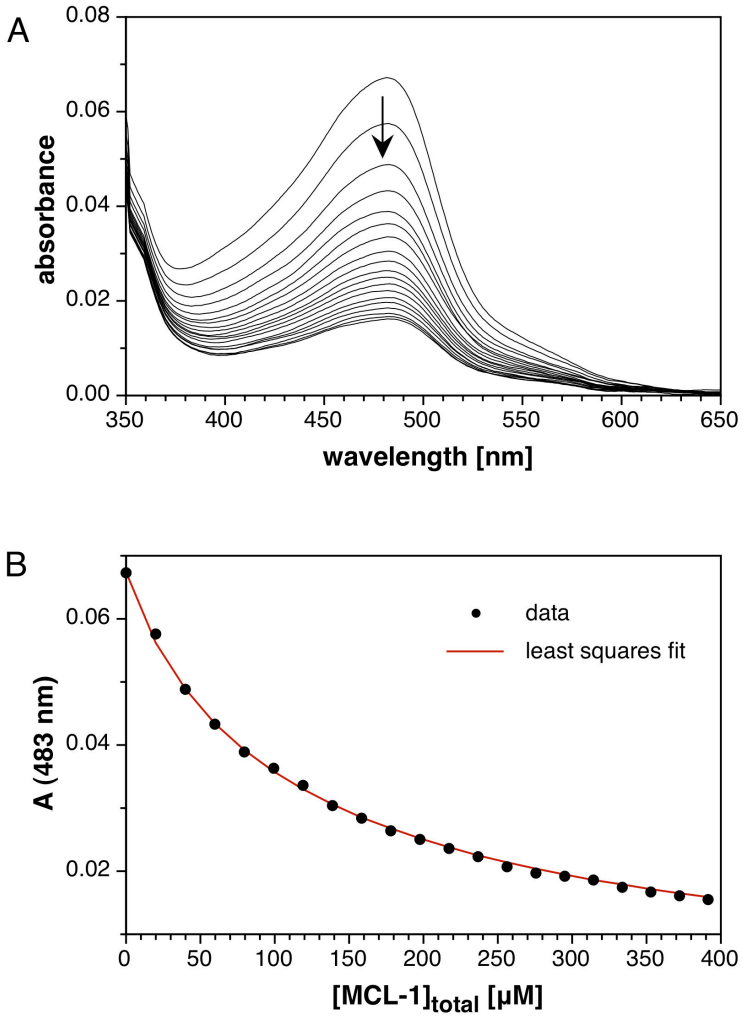

Equilibrium System Definition:

Species	Cu(I)	BCS	MCL-1	H	logβ
Cu(I)[a]	1	0	0	0	0.0
BCS	0	1	0	0	0.0
MCL-1	0	0	1	0	0.0
(BCS)H	0	1	0	1	5.81
(MCL-1)H	0	0	1	1	7.11
Cu(I)(MCL-1)	1	0	1	0	16.33
Cu(I)$(BCS)_2$	1	2	0	0	*20.81 ± 0.04*

[a] $[Na_3(MCL\text{-}2)Cu(I)]PF_6$ (**14**) was used as a source of Cu(I). Because the Cu(I) affinity of MCL-2 is much lower compared to MCL-1, MCL-2 was not included in the equilibrium definition.

Figure S17: Spectrophotometric determination of the Cu(I) stability constant of bathocuproine disulfonate (BCS, **5**) via competition with MCL-1 (**1**). A solution of $[Na_3(MCL\text{-}2)Cu(I)]PF_6$ (**14**, 5 μM) and BCS (50 μM) was equilibrated at pH 7.0 (10 mM PIPES, 0.1 M $KClO_4$, 25°C) and then titrated with MCL-1 to a final concentration of 0.4 mM. The UV-vis traces (A) were analyzed by non-linear least squares fitting over the spectral range of 400-600 nm to yield an average $\log K_{Cu(I)L}$ of 20.81 ± 0.04 (n = 3). Figure B shows the absorbance change and corresponding fit at 483 nm.

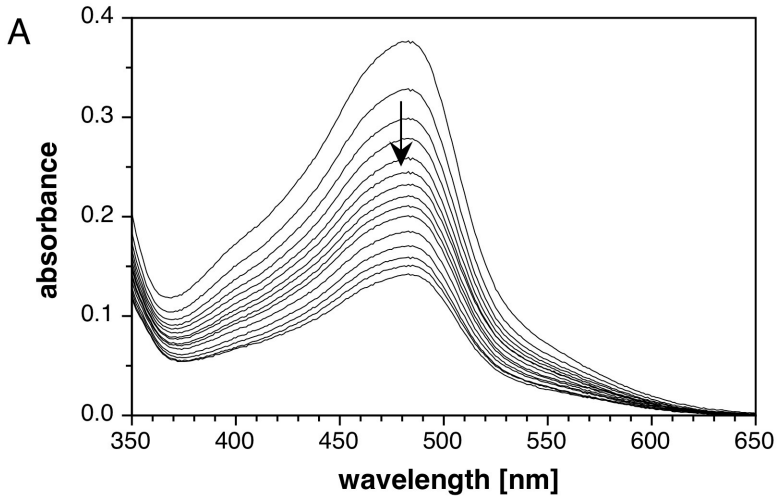

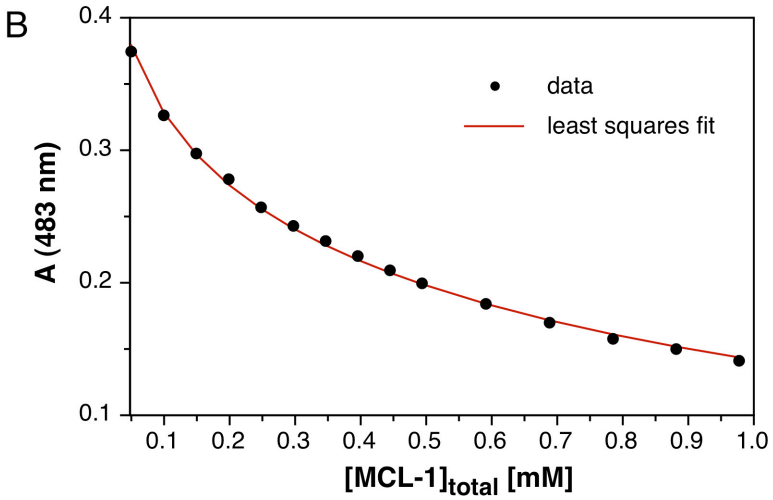

Equilibrium System Definition:

Species	Cu(I)	BCS	MCL-1	H	logβ
Cu(I)	1	0	0	0	0.0
BCS	0	1	0	0	0.0
MCL-1	0	0	1	0	0.0
(BCS)H	0	1	0	1	5.81
(MCL-1)H	0	0	1	1	7.11
Cu(I)(MCL-1)	1	0	1	0	16.33
Cu(I)$(BCS)_2$	1	2	0	0	*20.80 ± 0.03*

Figure S18: Spectrophotometric determination of the Cu(I) stability constant of bathocuproine disulfonate (BCS, **5**) via competition with MCL-1 (**1**). A solution of $[Na_3(MCL\text{-}1)Cu(I)]PF_6$ (**13**, 50 μM) and BCS (100 μM) was equilibrated at pH 7.0 (10 mM PIPES, 0.1 M $KClO_4$, 25°C) and then titrated with MCL-1 to a final concentration of 1 mM. The UV-vis traces (A) were analyzed by non-linear least squares fitting over the spectral range of 400-600 nm to yield an average log$K_{Cu(I)L}$ of 20.80 ± 0.03 (n = 3). Figure B shows the absorbance change and corresponding fit at 483 nm.

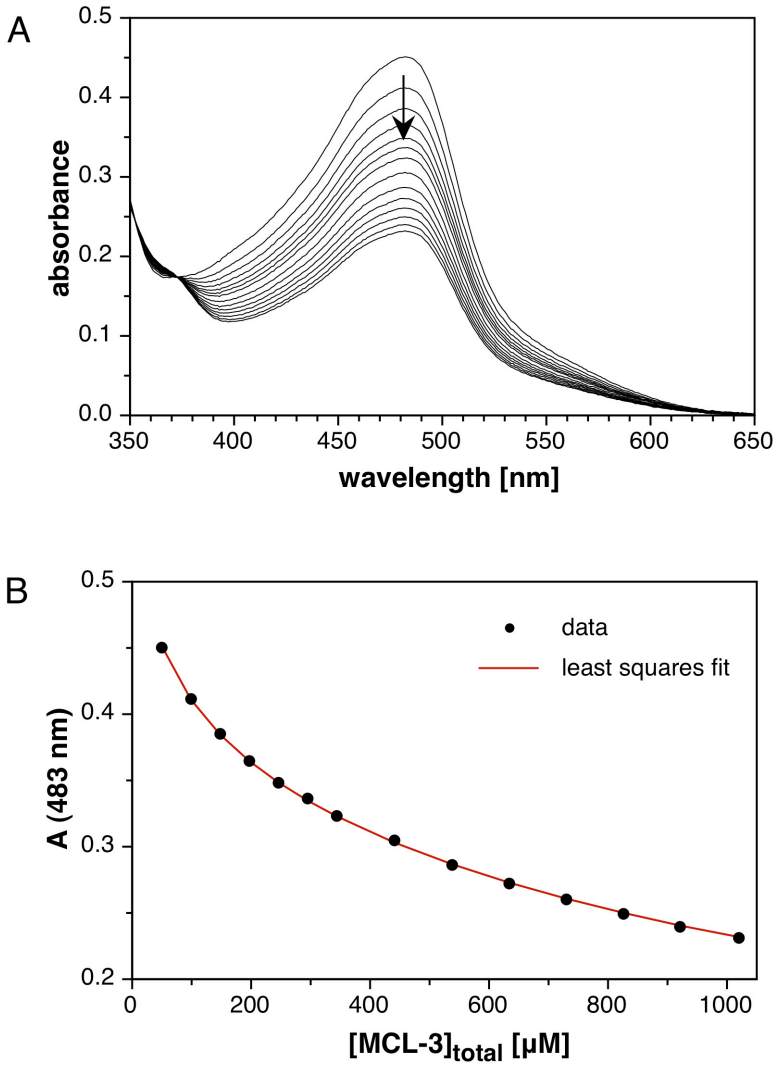

Equilibrium System Definition:

Species	Cu(I)	BCS	MCL-3	H	logβ
Cu(I)	1	0	0	0	0.0
BCS	0	1	0	0	0.0
MCL-3	0	0	1	0	0.0
(BCS)H	0	1	0	1	5.81
Cu(I)$(BCS)_2$	1	2	0	0	20.81
Cu(I)(MCL-3)	1	1	0	0	*13.80 ± 0.04*

Figure S19: Spectrophotometric determination of the Cu(I) stability constant of MCL-3 (**3**) via competition with bathocuproine disulfonate (BCS, **5**). A solution of $[Na_4(MCL\text{-}3)Cu(I)]PF_6$ (**15**, 50 μM) and BCS (100 μM) was equilibrated at pH 5.0 (10 mM PIPBS, 0.1 M $KClO_4$, 25°C) and then titrated with MCL-3 to a final concentration of 1.0 mM. The UV-vis traces (A) were analyzed by non-linear least squares fitting over the spectral range of 400-600 nm to yield an average $\log K_{Cu(I)L}$ of 13.80 ± 0.04 (n = 3). Figure B shows the absorbance change and corresponding fit at 483 nm.

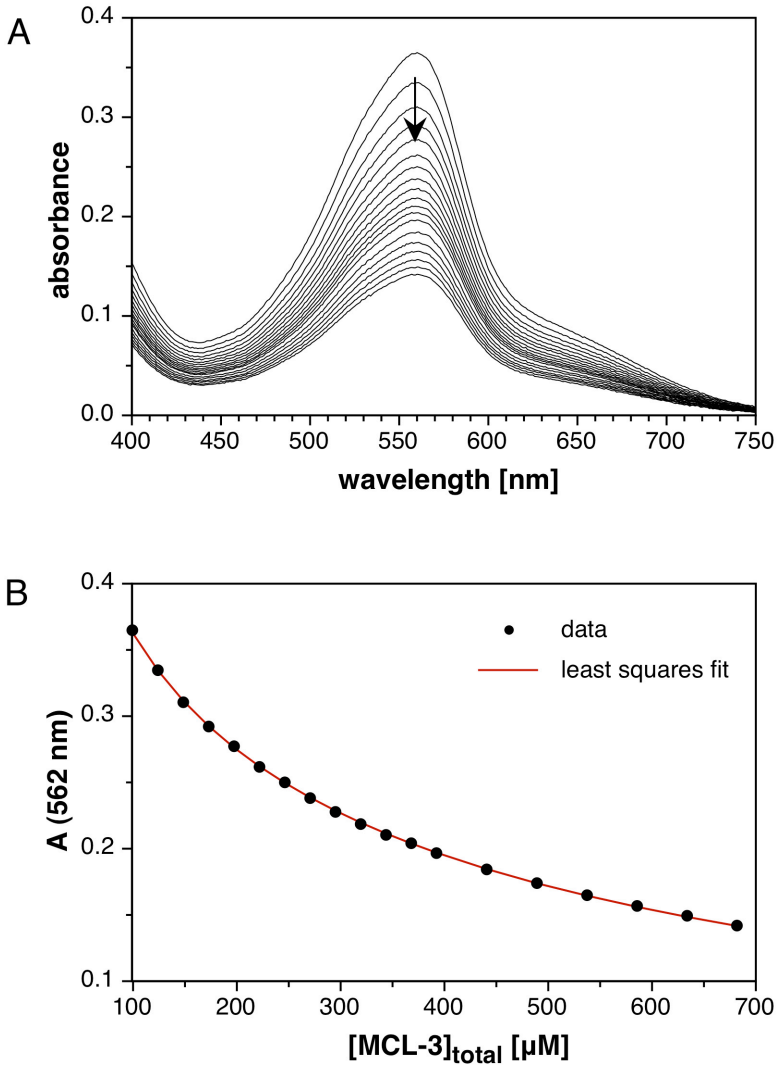

Equilibrium System Definition:

Species	Cu(I)	BCA	MCL-3	H	logβ
Cu(I)	1	0	0	0	0.0
BCA	0	1	0	0	0.0
MCL-3	0	0	1	0	0.0
(BCA)H	0	1	0	1	3.91
Cu(I)(BCA)$_2$	1	2	0	0	17.67
Cu(I)(MCL-3)	1	0	1	0	*13.78 ± 0.06*

Figure S20: Spectrophotometric determination of the Cu(I) stability constant of MCL-3 (**3**) via competition with 2,2'-bicinchoninic acid (BCA, **6**). A solution of [Na$_4$(MCL-3)Cu(I)]PF$_6$ (**15**, 100 μM) and BCA (200 μM) was equilibrated at pH 5.0 (10 mM PIPBS, 0.1 M KClO$_4$, 25°C) and then titrated with MCL-3 to a final concentration of 0.7 mM. The UV-vis traces (A) were analyzed by non-linear least squares fitting over the spectral range of 450-700 nm to yield an average log$K_{Cu(I)L}$ of 13.78 ± 0.06 (n = 3). Figure B shows the absorbance change and corresponding fit at 562 nm.

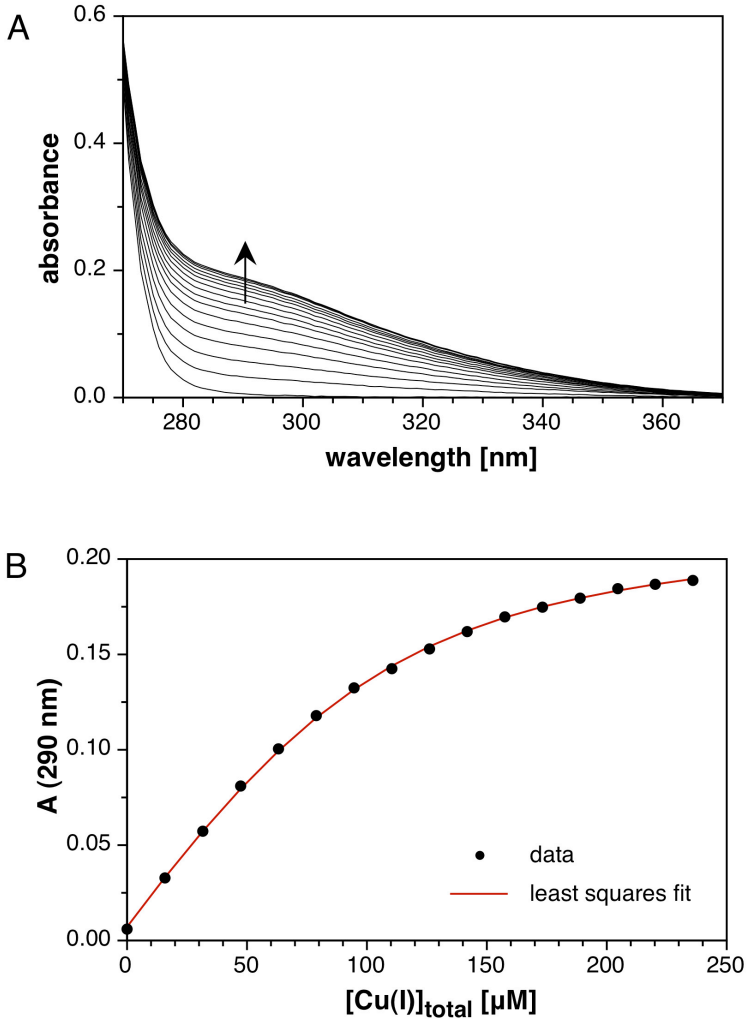

Equilibrium System Definition:

Species	Cu(I)	PEMEA	MeCN	H	logβ
Cu(I)	1	0	0	0	0.0
PEMEA	0	1	0	0	0.0
MeCN	0	0	1	0	0.0
(PEMEA)H	0	1	0	1	7.35
(PEMEA)H_2	0	1	0	2	10.69
Cu(I)(MeCN)	1	0	1	0	2.63
Cu(I)$(MeCN)_2$	1	0	2	0	4.02
Cu(I)$(MeCN)_3$	1	0	3	0	4.29
Cu(I)(PEMEA)	1	1	0	0	*15.75 ± 0.02*

Figure S21: Spectrophotometric determination of the Cu(I) stability constant of PEMEA (**4**) via competition with acetonitrile (MeCN). A solution of PEMEA (100 µM) was titrated with $[Cu(I)(CH_3CN)_4]PF_6$ in the presence of MeCN (958 mM) at pH 2.0 (14 mM $HClO_4$, 100 µM sodium ascorbate, 0.1 M $KClO_4$, 25°C). The UV-vis traces (A) were analyzed by non-linear least squares fitting over the entire spectral range to yield an average log$K_{Cu(I)L}$ of 15.75 ± 0.02 (n = 3). Figure B shows the absorbance change and corresponding fit at 290 nm.

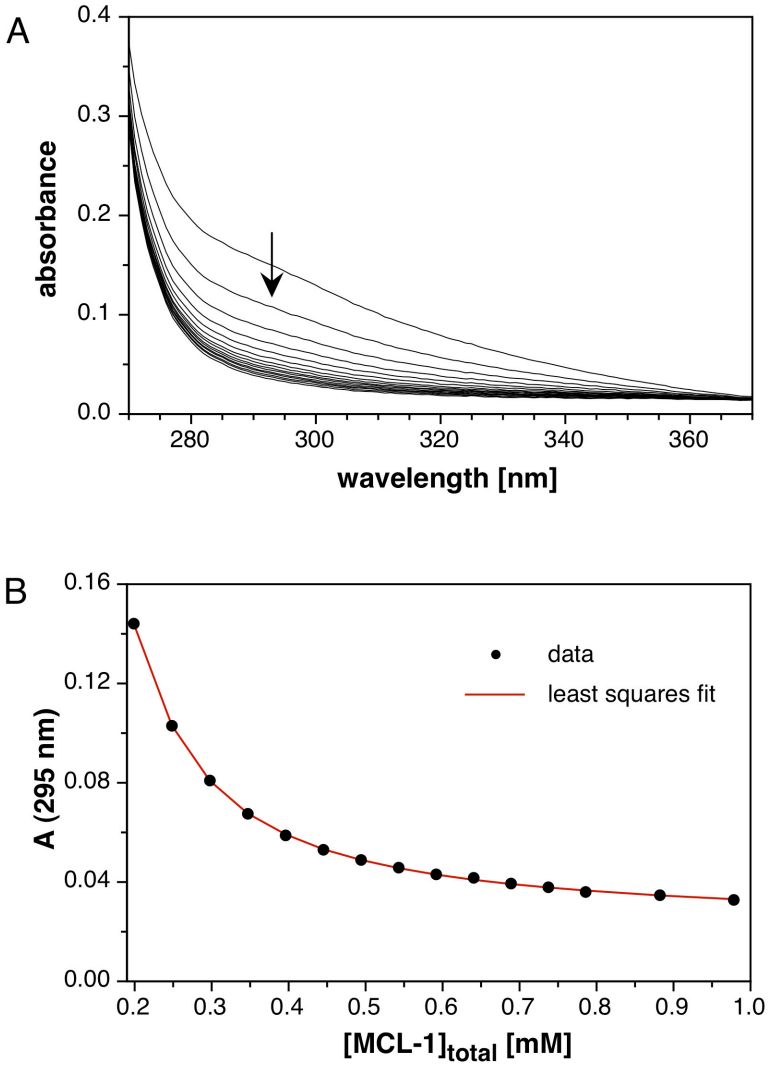

Equilibrium System Definition:

Species	Cu(I)	PEMEA	MCL-1	H	logβ
Cu(I)	1	0	0	0	0.0
PEMEA	0	1	0	0	0.0
MCL-1	0	0	1	0	0.0
(PEMEA)H	0	1	0	1	7.35
(PEMEA)H_2	0	1	0	2	10.69
(MCL-1)H	0	0	1	1	7.11
Cu(I)(PEMEA)	1	1	0	0	15.71
Cu(I)(MCL-1)	1	0	1	0	*16.33 ± 0.07*

Figure S22: Spectrophotometric determination of the Cu(I) stability constant of MCL-1 (**1**) via competition with PEMEA (**4**). A solution of [Na_3(MCL-1)Cu(I)]PF_6 (**13**, 200 µM) and PEMEA (96 µM) was equilibrated at pH 5.0 (10 mM PIPBS, 0.1 M $KClO_4$, 25°C) and then titrated with MCL-1 to a final concentration of 1 mM. The UV-vis traces (plot A) were analyzed by non-linear least squares fitting over the entire spectral range to yield an average log$K_{Cu(I)L}$ of 16.33 ± 0.07 (n = 3). Figure B shows the absorbance change and corresponding fit at 295 nm.

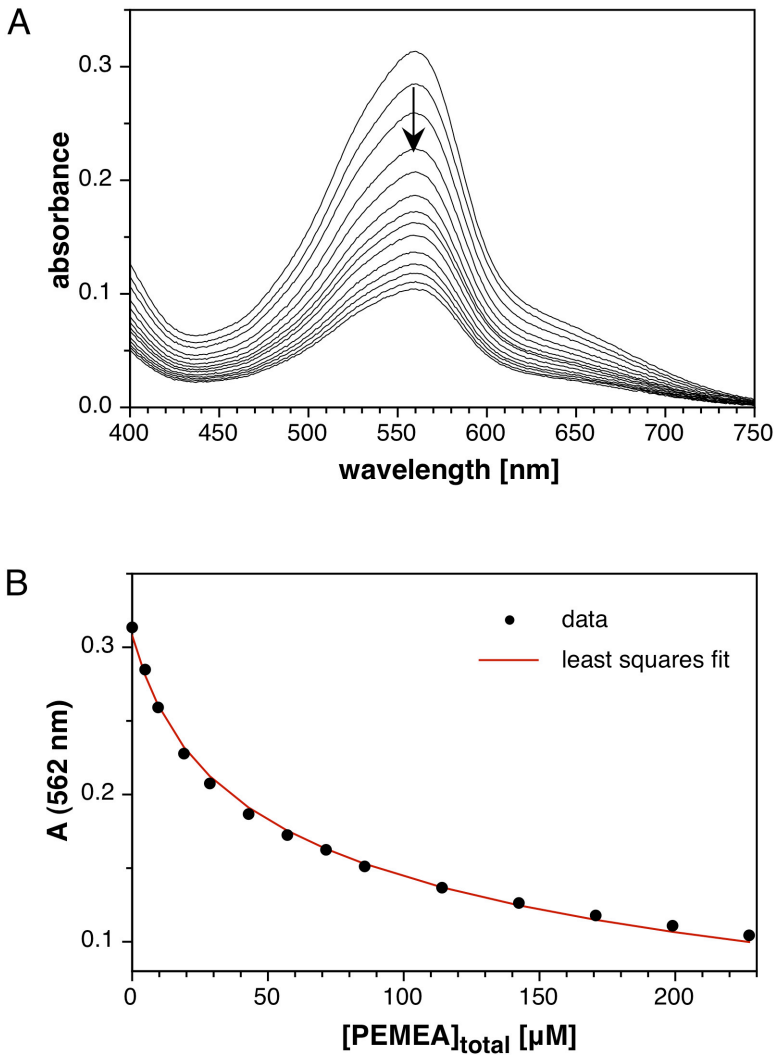

Equilibrium System Definition:

Species	Cu(I)	PEMEA	BCA	H	logβ
Cu(I)	1	0	0	0	0.0
PEMEA	0	1	0	0	0.0
BCA	0	0	1	0	0.0
(PEMEA)H	0	1	0	1	7.35
(PEMEA)H_2	0	1	0	2	10.69
(BCA)H	0	0	1	1	3.91
Cu(I)(PEMEA)	1	1	0	0	15.71
Cu(I)$(BCA)_2$	1	0	2	0	*17.63 ± 0.05*

Figure S23: Spectrophotometric determination of the Cu(I) stability constant of BCA (**6**) via competition with PEMEA (**4**). A solution of $[Cu(I)(CH_3CN)_4]PF_6$ (40 μM) and BCA (100 μM) was equilibrated at pH 5.0 (10 mM PIPBS, 0.1 M $KClO_4$, 25°C) and then titrated with PEMEA to a final concentration of 230 μM. The UV-vis traces (A) were analyzed by non-linear least squares fitting over the spectral range of 450-700 nm to yield an average $\log K_{Cu(I)L}$ of 17.63 ± 0.05 (n = 3). Figure B shows the absorbance change and corresponding fit at 562 nm.

7. Calculation of Apparent Stability Constants and pCu Values

If the ligand and metal ion are engaged in protonation equilibria, the metal ion affinity of the ligand becomes pH dependent. By using a buffer with sufficient capacity, the proton concentration can be kept constant throughout the titration. According to Schwarzenbach, the metal ion affinity of the ligand can then be expressed by the apparent or conditional stability constant *K*',[21,22]

$$K' = \frac{[ML]}{[M'][L']} \tag{13}$$

where [M'] is the total concentration of all metal ion species that are not complexed by the ligand L,

$$[M'] = [M(H_2O)n] + [M(H_2O)_{n-1}(OH)] + \ldots \tag{14}$$

and [L'] is the total concentration of all protonation states of the ligand not complexed to M,

$$[L'] = [L] + [HL] + [H_2L] + \ldots [H_nL] \tag{15}$$

By introducing the coefficients α_M and α_L, the conditional stability constant *K*' can be further related to the stability constant *K*,[22] with

$$K' = K\alpha_M\alpha_L \tag{16}$$

and

$$\alpha_M = \frac{[M(H_2O)_n]}{\{[M(H_2O)_n] + [M(OH)(H_2O)_{n-1}] + \ldots\}} \tag{17a}$$

$$\alpha_L = \frac{[L]}{\{[L] + [HL] + [H_2L]\ldots\}} \tag{17b}$$

After inserting the corresponding pK_a values of the ligand L and the pK_M of the solvated metal ion M, equations 16-17 yield[23]

$$K' = \frac{K}{(1 + 10^{(pH - pK_M)})(1 + 10^{(pK_1 - pH)} + 10^{(pK_2 - 2pH)} + \ldots)} \tag{18}$$

For the calculation of the apparent stability constants compiled in Table 4, the corresponding protonation constants $\log K_{Hn}$ were corrected upward by 0.11 to account for the ionic background of 0.1 M.

The presence of multiple binding equilibria makes it impossible to compare the metal ion affinity of ligands with different metal binding stoichiometries and pK_a's. As a workaround to this problem, Raymond and coworkers introduced pM values to compare the affinity of various iron-binding siderophores.[24] In analogy to p[H], the pM is defined as –log[M], where [M] represents the free aqueous metal ion concentration. As the pM depends on the solution pH as well as the ligand and metal ion concentrations, it must be reported for a defined set of experimental conditions, e.g. at pH 7.4 with $[M]_{tot}$ = 1 μM and $[L]_{tot}$ = 10 μM.[24] In analogy to these conditions, the pCu values compiled in Table 4 were also calculated for a metal ion and ligand concentration of 1 and 10 μM, respectively, however, a pH of 7.0 was assumed for ease of comparison with the CusF data. Similar to the calculation of the apparent stability constants, we used the corresponding ionic strength adjusted pK_a values to derive the pCu values. All calculations were performed with the Hyss software package.[25]

8. Determination of the Cu(I) Stability Constants of CusF

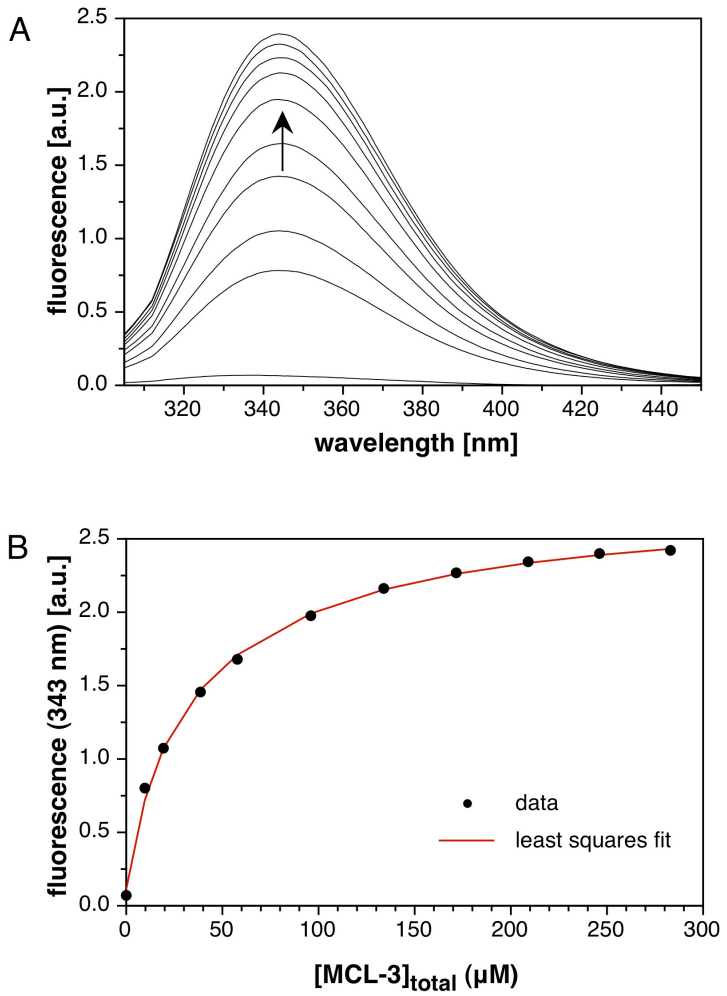

Equilibrium System Definition:

Species	Cu(I)	MCL-3	CusF	H	logβ
Cu(I)	1	0	0	0	0.0
MCL-3	0	1	0	0	0.0
CusF	0	0	1	0	0.0
Cu(I)(MCL-3)	1	1	0	0	13.80
Cu(I)(CusF)	1	0	1	0	*14.29 ± 0.11*

Figure S24: Determination of the Cu(I) stability constant of CusF via competition with MCL-3 (**3**) by fluorescence spectrometry. A solution of holo-CusF (20 μM) in pH 7 buffer (50 mM MOPS, 150 mM NaCl, 25°C) was titrated with MCL-3 to a final concentration of 280 μM. Fluorescence emission spectra were acquired with excitation at 290 nm at each titration step. The fluorescence traces (A) were analyzed by non-linear least squares fitting over the entire spectral range to yield an average log$K_{Cu(I)L}$ of 14.29 ± 0.11 (n = 4). Figure B shows the fluorescence intensity change and corresponding fit at 343 nm.

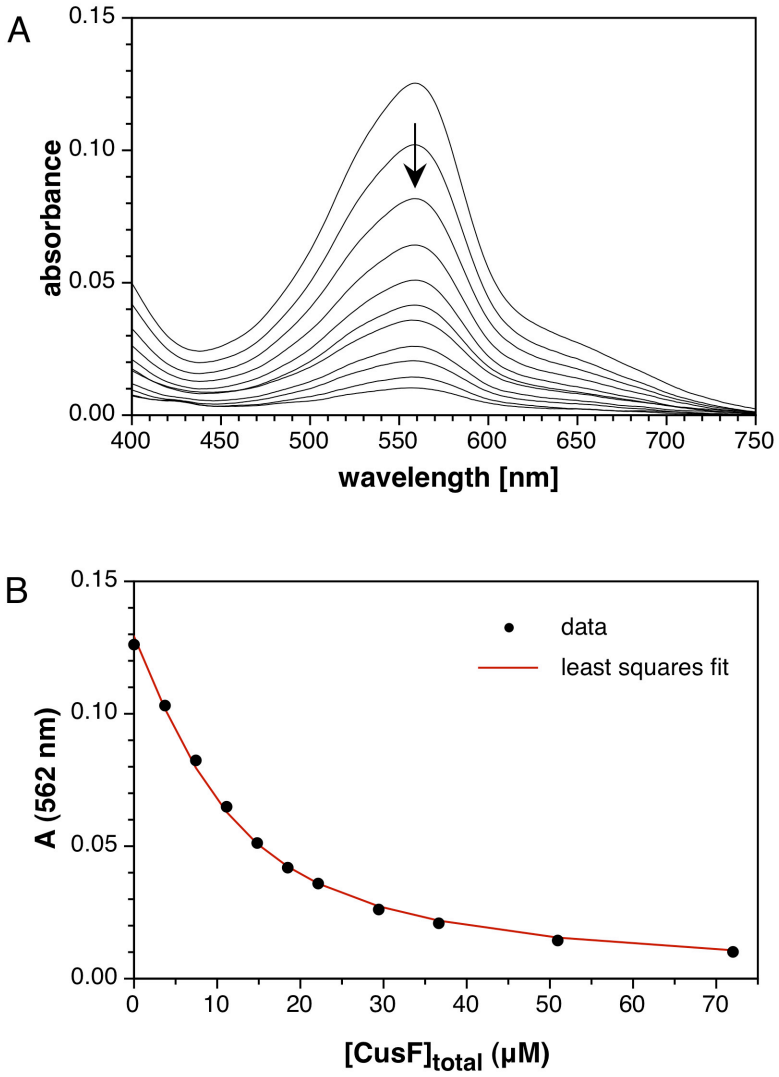

Equilibrium System Definition:

Species	Cu(I)	BCA	CusF	H	logβ
Cu(I)	1	0	0	0	0.0
BCA	0	1	0	0	0.0
CusF	0	0	1	0	0.0
BCA(H)	0	1	0	1	3.91
Cu(I)(BCA)$_2$	1	2	0	0	17.67
Cu(I)(CusF)	1	0	1	0	*14.21 ± 0.01*

Figure S25: Spectrophotometric determination of the Cu(I) stability constant of CusF via competition with BCA (**6**). A solution of [Cu(I)(CH$_3$CN)$_4$]PF$_6$ (16 μM) and BCA (50 μM) was equilibrated at pH 7.0 (50 mM MOPS, 150 mM NaCl, 25°C) and then titrated with apo-CusF to a final concentration of 72 μM. The UV-vis traces (A) were analyzed by non-linear least squares fitting over the spectral range of 450-700 nm to yield an average log$K_{Cu(I)L}$ of 14.21 ± 0.01 (n = 3). Figure B shows the absorbance change and corresponding fit at 562 nm.

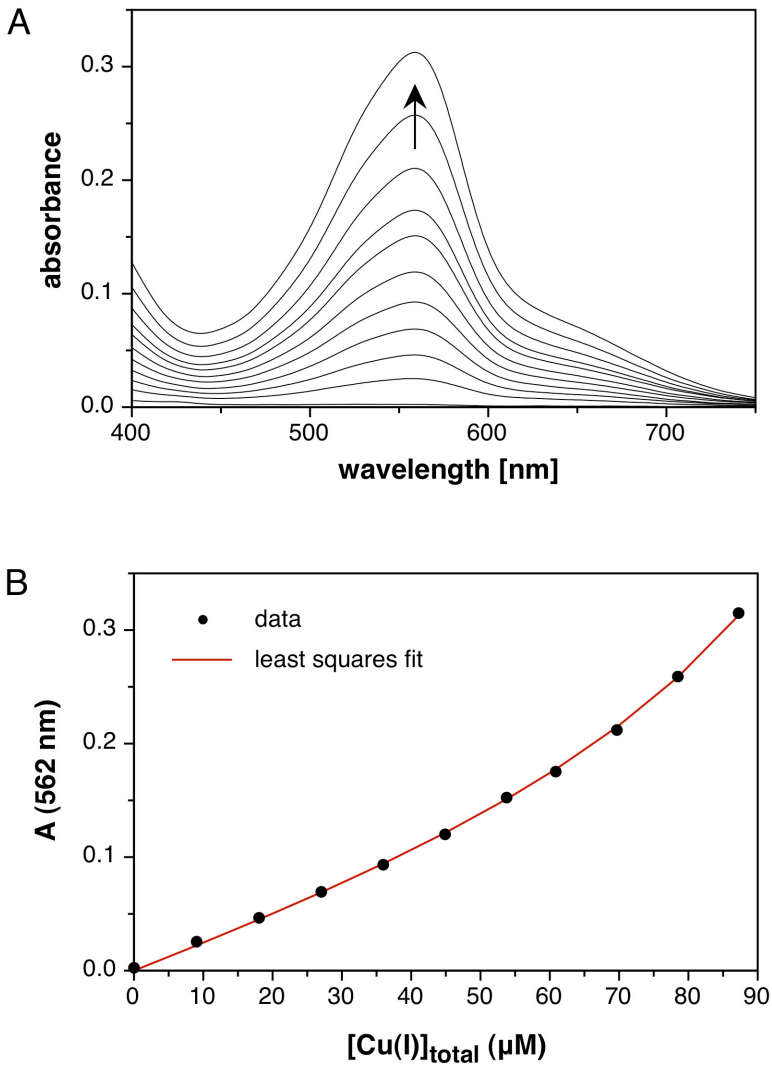

Equilibrium System Definition:

Species	Cu(I)	BCA	CusF	H	logβ
Cu(I)	1	0	0	0	0.0
BCA	0	1	0	0	0.0
CusF	0	0	1	0	0.0
BCA(H)	0	1	0	1	3.91
Cu(I)(BCA)$_2$	1	2	0	0	17.67
Cu(I)(CusF)	1	0	1	0	*14.21 ± 0.01*

Figure S26: Spectrophotometric determination of the Cu(I) stability constant of CusF via competition with BCA (**6**). A solution of apo-CusF (65 μM) and BCA (80 μM) was titrated at pH 7.0 (50 mM MOPS, 150 mM NaCl, 25°C) with $[Cu(I)(CH_3CN)_4]PF_6$ to a final concentration of 87 μM. The UV-vis traces (A) were analyzed by non-linear least squares fitting over the spectral range of 450-700 nm to yield an average log$K_{Cu(I)L}$ of 14.21 ± 0.01 (n = 3). Figure B shows the absorbance change and corresponding fit at 562 nm.

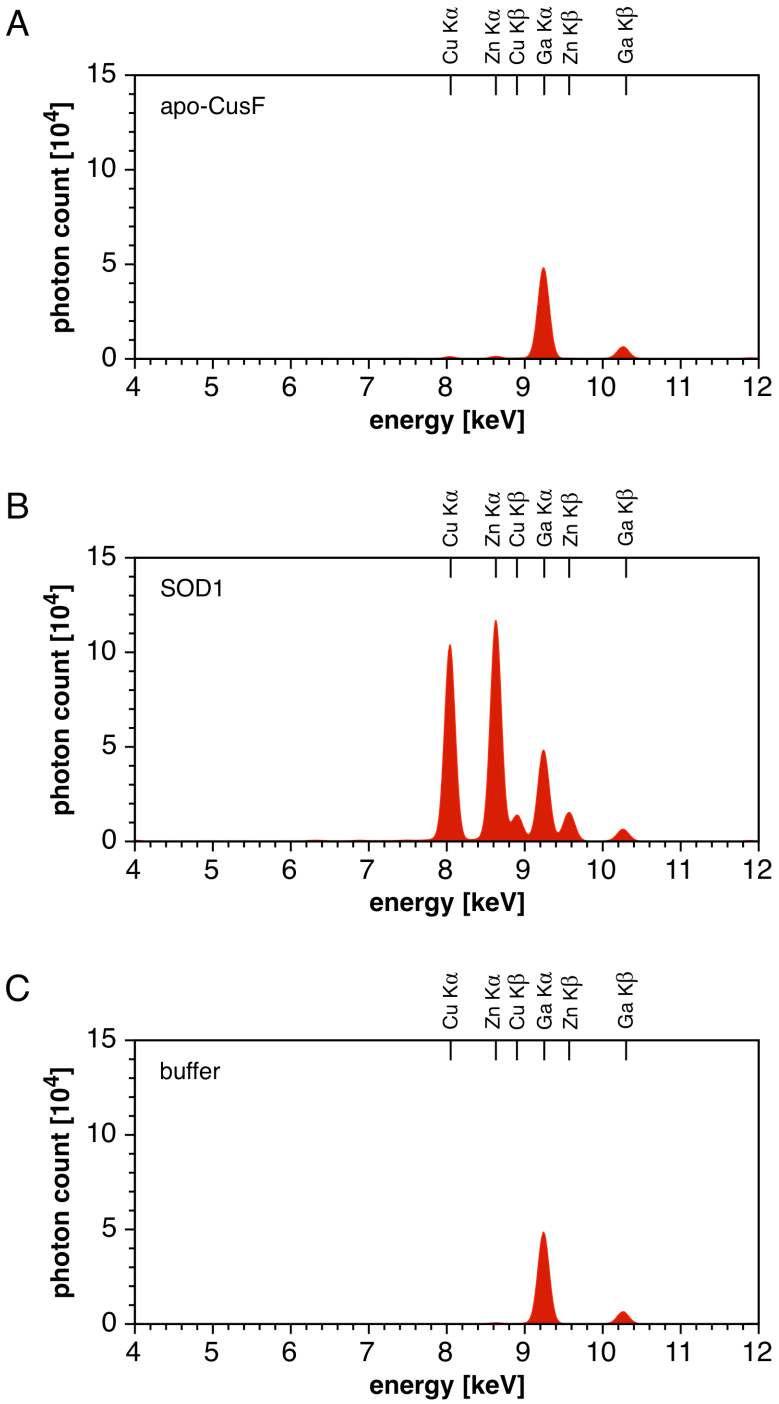

Figure S27: Trace elemetal analysis of the copper and zinc content of purified CusF by TXRF spectroscopy. A) X-ray fluorescence (XRF) spectrum of CusF as isolated after overexpression in *E. coli* and purification by gel filtration. The analysis was performed with 2 µL of a 2 mM protein stock solution in MOPS buffer (50 mM MOPS, 0.15 M NaCl, pH 7.0). B) XRF spectrum of SOD1 (Sigma, from bovine erythrocytes) in MOPS buffer as control sample. C) XRF spectrum of MOPS buffer only. Each sample was referenced to gallium as internal standard. After subtraction of buffer background, the Cu and Zn occupancy of purified CusF was found to be below 1%.

9. References and Notes

(1) Morgan, M. T.; Bagchi, P.; Fahrni, C. J. *J. Am. Chem. Soc.* **2011**, *133*, 15906.
(2) Hahn, F. E.; Rupprecht, S. *Chem. Ber.* **1991**, *124*, 481.
(3) Alternatively, diiodide **10** can be obtained in 73% yield by column chromatography on silica gel (hexanes-MTBE) after reaction for only 4 days at 65 °C.
(4) With chromatographic purification of the starting diiodide **10**, macrocycle **11** was obtained in 75% yield following the above procedure at half scale.
(5) Ambundo, E. A.; Deydier, M. V.; Grall, A. J.; Aguera-Vega, N.; Dressel, L. T.; Cooper, T. H.; Heeg, M. J.; Ochrymowycz, L. A.; Rorabacher, D. B. *Inorg. Chem.* **1999**, *38*, 4233.
(6) Wu, C.-C.; Datta, S.; Wernsdorfer, W.; Lee, G.-H.; Hill, S.; Yang, E.-C. *Dalton Trans.* **2010**, *39*, 10160.
(7) Martell, A. E.; Smith, R. M. *Critical Stability Constants*; Plenum Press: New York, 1974.
(8) Debye, P.; Hückel, E. *Phys. Z.* **1923**, *24*, 185.
(9) Manoc, G. G.; Bates, R. G.; Hamer, W. J.; Acree, S. F. *J. Am. Chem. Soc.* **1943**, *65*, 1765.
(10) Davies, C. W. *J. Chem. Soc.* **1938**, 2093.
(11) Gans, P.; O'Sullivan, B. *Talanta* **2000**, *51*, 33.
(12) Gans, P.; Sabatini, A.; Vacca, A. *Talanta* **1996**, *43*, 1739.
(13) *SPECFIT Global Analysis System*, Spectrum Software Associates, Marlborough MA 01752, 2001
(14) Bernardo, M. M.; Schroeder, R. R.; Rorabacher, D. B. *Inorg. Chem.* **1991**, *30*, 1241.
(15) Cox, J. D. *Pure Appl. Chem.* **1982**, *54*, 1239.
(16) Milazzo, G.; Caroli, S. *Tables of Standard Electrode Potentials*; Wiley: New York, 1978.
(17) Bernardo, M. M.; Heeg, M. J.; Schroeder, R. R.; Ochrymowycz, L. A.; Rorabacher, D. B. *Inorg. Chem.* **1992**, *31*, 191.
(18) Koepp, H.-M.; Wendt, H.; Stkehlow, H. *Z. Elektrochem.* **1960**, *64*, 483.
(19) Yee, E. L.; Cave, R. J.; Guyer, K. L.; Tyma, P. D.; Weaver, M. J. *J. Am. Chem. Soc.* **1979**, *101*, 1131.
(20) Damu, K. V.; Shaikjee, M. S.; Michael, J. P.; Howard, A. S.; Hancock, R. D. *Inorg. Chem.* **1986**, *25*, 3879.
(21) Ringbom, A. *J. Chem. Ed.* **1958**, *35*, 282.
(22) Schwarzenbach, G. *Complexometric Titrations*; Interscience Publisher: New York, 1957.
(23) Tsien, R.; Pozzan, T. *Methods Enzym.* **1989**, *172*, 230.
(24) Harris, W. H.; Raymond, K. N. *J. Am. Chem. Soc.* **1979**, *101*, 6534.
(25) Alderighi, L.; Gans, P.; Ienco, A.; Peters, D.; Sabatini, A.; Vacca, A. *Coord. Chem. Rev.* **1999**, *184*, 311.